

# Cyclase associated protein 2: Roles in heart physiology and wound healing

INAUGURAL-DISSERTATION  
zur  
Erlangung des Doktorgrades  
der Mathematischen-Naturwissenschaftlichen Fakultät  
der Universität zu Köln



vorgelegt von  
**Kosmas Kosmas**  
aus  
Ioannina, Griechenland

Köln, 2014

Referees/Berichterstatter: Prof. Dr. Angelika A. Noegel  
Prof. Dr. Jürgen Dohmen

Date of oral examination: 23/06/2014  
Tag der mündlichen Prüfung

The present research work was carried out under the supervision of Prof. Angelika Noegel and Dr. Vivek Peche, in the Institute of Biochemistry I, Medical Faculty, University of Cologne, Cologne, Germany, from April 2011 to April 2014.

Diese Arbeit wurde von April 2011 bis April 2014 am Institut für Biochemie I der Medizinischen Fakultät der Universität zu Köln unter der Leitung von Prof. Angelika Noegel und Dr. Vivek Peche durchgeführt.

*“Δεν μπορώ να διδάξω σε κανένα τίποτα. Μπορώ μόνο να τον κάνω να σκέφτεται.”*

*Σωκράτης*

*“I cannot teach anybody anything. I can only make them think.”*

*Socrates*

## Acknowledgments

The present thesis was carried out in the research group of Prof. Dr. Angelika A. Noegel in the Institute of Biochemistry I, Medical Faculty, University of Cologne under the supervision of Dr. Vivek Peche.

First of all, I would like to thank my boss, Dr. Vivek Peche, for introducing me to the laboratory methods and the real scientific way of thinking, for supervising my experiments, the nice working conditions in the lab and for making me think and work totally independently.

My thanks also go to the director of the institute Prof. Dr. Angelika A. Noegel for the chance she gave me to work in her institute, for her interest in the development of my work and my skills, and the critical corrections of the manuscripts.

In addition, I would like to thank my 2<sup>nd</sup> referee Prof. Dr. Jürgen Dohmen and the chair of my committee Prof. Dr. Peter Kloppenburg for their time and effort spent on my thesis.

I would also like to thank all the members of the Biochemistry I and II for their useful tips throughout my work, their assistance and the nice moments we had all these years. I will not list the names because I will definitely need 10 pages. I feel grateful for all the people including the professors, the employees, the students, the secretary, the lab assistants, the technical assistants and the animal care takers.

Special thanks to the IGSDHD for the funding, the support and for making the official work easy.

Last but not least, my heartiest gratitude goes to my family and friends for their constant support throughout my studies.

## Abbreviations

aa	amino acids
ATP	Adenosine 5'-triphosphate
bp	base pair(s)
cDNA	complementary DNA
DMEM	Dulbecco's Modified Eagle's Medium
DMSO	Dimethylsulphoxide
DNA	Deoxyribonucleic Acid
DTT	1,4-dithiothreitol
E. coli	Escherichia coli
EDTA	Ethylenediaminetetraacetic acid
EGTA	Ethyleneglycol-bis (2-amino-ethylene)N,N,N,N-tetraacetic acid
ES	Embryonic stem
FITC	Fluorescein-5-isothiocyanate
GAPDH	Glyceraldehyd-3-phosphat Dehydrogenase
GFP	Green Fluorescent Protein
GST	Glutathion-S-Transferase
HEK	Human Embryonic Kidney
IPTG	iso-propylthio-galactopyranoside
M	Molar
MW	Molecular Weight
NP	Nonyl Phenoxypolyethoxyethanol
PAGE	Polyacrylamide Gel Electrophoresis
PBS	Phosphate Buffered Saline
PCR	Polymerase Chain Reaction
PIPES	Piperazine-N,N'-bis [2-ethanesulphonic acid]
PMSF	Phenylmethylsulphonylfluoride
RNA	Ribonucleic Acid
SDS	Sodium Dodecyl Sulphate
Tris	Tris -(hydroxymethyl)-aminomethane
TRITC	Tetramethylrhodamine Isothiocyanate

### Units of Measure

D	Dalton
g	gram
h	hour
l	litre
m	meter
min	minute
s	sec

### Prefixes

k	kilo ( $10^3$ )
c	centi ( $10^{-2}$ )
m	milli ( $10^{-3}$ )
$\mu$	micro ( $10^{-6}$ )
n	nano ( $10^{-9}$ )

# Table of contents

<b>1.</b>	<b>Introduction</b>	<b>1</b>
1.1	The Cytoskeleton	1
1.2	Types of the cytoskeleton	1
1.3	Actin filaments	2
1.4	Acting binding proteins	3
1.5	CAP2	4
1.6	CAP2 and cardiomyopathy	6
1.7	Cell migration and actin cytoskeleton	7
1.8.	Wound healing	10
1.8.1	Phases of wound healing	10
	A. Inflammation	10
	B. Repair	11
	C. Remodeling	12
1.9	Aim of the research	14
<b>2.</b>	<b>Materials and methods</b>	<b>16</b>
2.1	Generation of <i>Cap2<sup>gt/gt</sup></i>	16
2.2	Skin wounding	16
2.3	Preparation of tissue	17
2.4	Immunohistochemistry, antibodies and histology	17
2.5	Cell culture and cell scratch assay	18
2.6	Western blot analyses	18
2.7	Focal adhesion assay	19
2.8	Disruption of actin cytoskeleton and recovery	19
2.9	RNA isolation	19
2.10	Expression of CAP2 domains and in vitro assays	20
2.11	DNA transfection	20
2.12	Recombinant protein expression	20
<b>3.</b>	<b>Results</b>	<b>21</b>
3.1	Generation of a CAP2 knockout mouse	21
3.2	Characterization of CAP2 monoclonal antibodies	23
3.3	CAP2 deletion leads to weight loss and is lethal in postnatal stages of mice	23
3.4	Cardiac and skeletal muscle phenotype of <i>Cap2<sup>gt/gt</sup></i> mice	25
3.4.1	<i>Cap2<sup>gt/gt</sup></i> mice develop dilated cardiomyopathy	25
3.4.2	CAP2 is required for proper sarcomeric organization in cardiac and skeletal muscle	28
3.4.3	CAP2 deletion may lead to sarcopenia	30
3.5	Roles of CAP2 in wound healing	31
3.5.1	Expression of CAP2 in human wounds	31
3.5.2	Loss of CAP2 results in delayed wound repair	33
3.5.3	Histological analysis with Masson's trichrome staining	34
3.5.4	Proliferation is reduced in <i>Cap2<sup>gt/gt</sup></i> mice	35
3.5.5	Delayed wound contraction in <i>Cap2<sup>gt/gt</sup></i> mice	36
3.5.6	<i>Cap2<sup>gt/gt</sup></i> mice show decreased macrophage infiltration	37
3.5.7	Slower neovascularization in <i>Cap2<sup>gt/gt</sup></i> mice	38
3.5.8	Increase in apoptosis in <i>Cap2<sup>gt/gt</sup></i> wounds	39
3.6	Cell migration defects in <i>Cap2<sup>gt/gt</sup></i> fibroblasts	40

3.6.1	<i>Cap2<sup>gt/gt</sup></i> fibroblasts show reduced velocity	40
3.6.2	<i>Cap2<sup>gt/gt</sup></i> fibroblasts develop long filopodia	42
3.6.3	Focal adhesions are altered in <i>Cap2<sup>gt/gt</sup></i> fibroblasts	42
3.6.4	G-/F-actin ratio is altered in <i>Cap2<sup>gt/gt</sup></i> fibroblasts	44
3.6.5	Recovery of the actin cytoskeleton is faster in mutant fibroblasts	45
3.7	Identification of CAP2 interacting partners	46
3.7.1	CAP2 interacts with CPT1B	50
3.8	CAP in cancer	51
<b>4.</b>	<b>Discussion</b>	<b>53</b>
4.1	CAP2 in the cardiovascular system and in skeletal muscle	53
4.2	Role of CAP2 in wound healing	56
	<b>Summary / Zusammenfassung</b>	<b>64</b>
	<b>Bibliography</b>	<b>66</b>
	<b>Erklärung</b>	<b>78</b>
	<b>Curriculum Vitae / Lebenslauf</b>	<b>79</b>

# 1. Introduction

## 1.1 The Cytoskeleton

A vital need for the survival of eukaryotic cells is to adapt to a variety of shapes and to carry out coordinated and directed movements. This is carried out by the cytoskeleton which is a complex network of protein filaments that extends throughout the cytoplasm. This network is a highly dynamic protein mosaic that dynamically coordinates cytoplasmic biochemistry and is reorganized continuously as the cell changes shape, divides and responds to its environment. It is also essential for intracellular transport of vesicles and organelles in the cytoplasm and the segregation of chromosomes at mitosis (Peters, 1929; Alberts *et al.*, 2007, *Molecular Biology of the Cell*, 5<sup>th</sup> Edition).

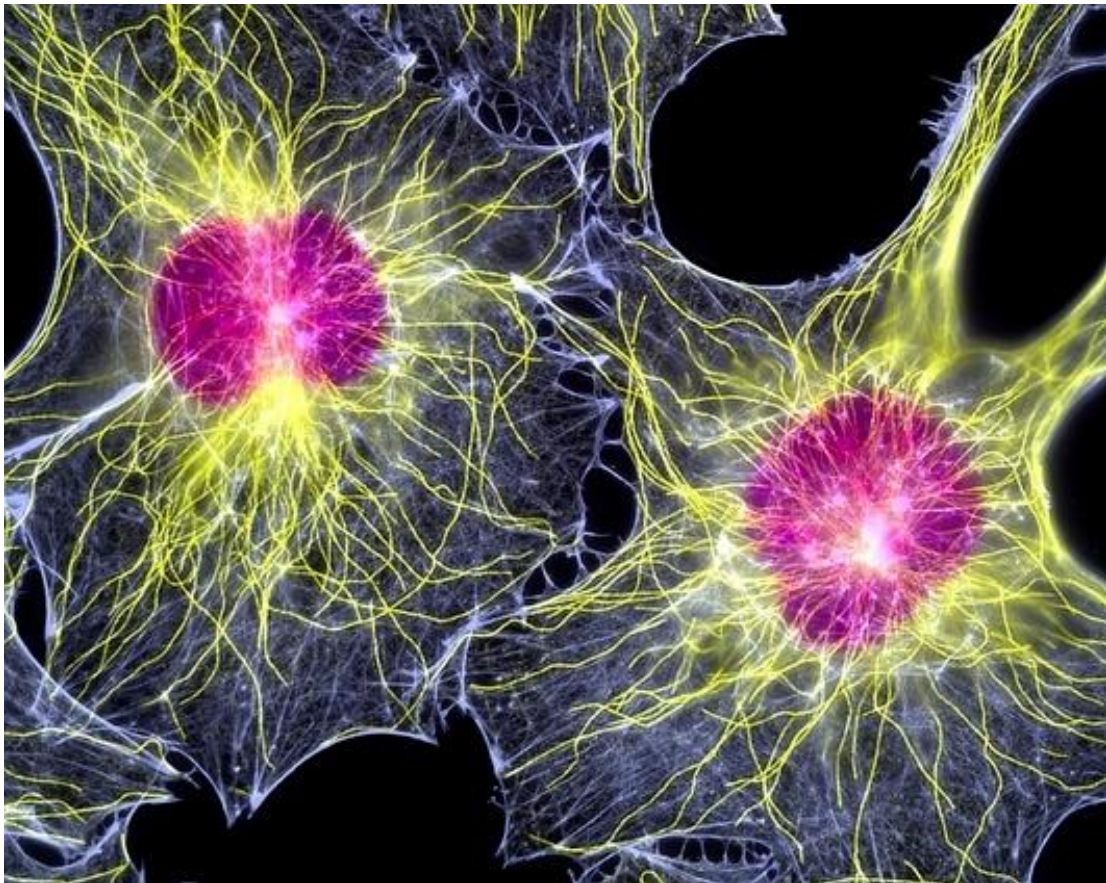


**Figure 1.1:** Fluorescent light micrograph of two fibroblast cells, showing their nuclei (purple) and cytoskeleton. The cytoskeleton is made up of microtubules (yellow) and actin filaments (white) (Image adopted by Google).

## 1.2 Types of the cytoskeleton

The diverse activities of the cytoskeleton depend on three types of protein filaments, actin filaments, microtubules, and intermediate filaments. Each filament type is



formed from a different protein subunit: actin for actin filaments, tubulin for microtubules, and a family of related fibrous proteins, such as vimentin or lamin, for intermediate filaments.

Intermediate filaments have a function in providing cells with mechanical strength. In vertebrate cells they can be grouped into three classes: (1) keratin filaments, (2) vimentin and vimentin-related filaments and (3) neurofilaments, each formed by polymerization of their corresponding subunit proteins (Alberts *et al.*, 2007, Molecular Biology of the Cell, 5<sup>th</sup> Edition).

Microtubules together with actin filaments are the primary organizers of the cytoskeleton. They usually have one end anchored in the centrosome and the other free in the cytoplasm. In many cells microtubules are highly dynamic structures that alternately grow and shrink by the addition and loss of tubulin subunits. Motor proteins move in one direction or the other along microtubules, carrying specific membrane-bound organelles to desired locations in the cell.

Actin filaments are essential for many movements of the cell. They are also dynamic structures, but they normally exist in bundles or networks rather than as single filaments. A layer called the cortex is formed just beneath the plasma membrane from actin filaments and a variety of actin-binding proteins. This actin-rich layer controls the shape and movements of most animal cells (Alberts *et al.*, 2007, Molecular Biology of the Cell, 5<sup>th</sup> Edition).

### 1.3 Actin filaments

All eukaryotic species contain actin. It is the most abundant protein in many eukaryotic cells, often constituting 5% or more of the total cell protein. It exists in a monomeric or G actin state (G for globular) and a polymeric state, F-actin or filamentous actin. Actin filaments can form both stable and labile structures in cells. Stable actin filaments form the core of microvilli and are a crucial component of the contractile apparatus of muscle cells. Cell movements, however, depend on labile structures constructed from actin filaments. Actin filaments appear in electron micrographs as threads about 8 nm wide. They consist of a tight helix of uniformly oriented actin molecules. Like a microtubule, an actin filament is a polar structure, with two structurally and functionally different ends - a relatively inert and slow growing *minus or pointed end* and a faster growing *plus or barbed end*.

Actin is an ATPase. ATP-bound actin is polymerization proficient and is found in newly polymerized filaments. The ATP molecule hydrolyzes and “older” filaments contain ADP actin. ADP actin is released from the pointed end and needs to be recharged with ATP for new polymerization. This ADP/ATP exchange requires several actin-binding proteins like cofilin, profilin and CAP (cyclase associated protein).

#### 1.4 Acting binding proteins

Actin filaments are organized in two general types: bundles and networks that are essential for cell migration, division and intracellular transport. These structures are formed by actin-binding proteins that cross link actin filaments, motor proteins, branching proteins, severing proteins, polymerization factors, and capping proteins. Sets of actin-binding proteins are thought to act cooperatively in generating the movements of cells and inside cells as during endo- and exocytosis or phagocytosis, in cytokinesis and cell locomotion. One family of proteins also called G-actin binding proteins or G-actin sequestering proteins can bind to G-actin and thus is involved in controlling F-actin formation. The binding of these proteins is reversible and through certain extracellular signals they can release G-actin to allow formation of F-actin. Typical members of this family are profilin, cofilin, thymosin and CAP (Carlier and Pantaloni 1994; Gottwald *et al.*, 1996).

Another group is collectively called “capping proteins”. They inhibit further addition of monomers, thus keeping filaments short. By binding to the plus ends of actin filaments, capping proteins slow the rate of filament growth. Even at the minus end the actin filament may be capped by minus end capping proteins. The association of capping proteins with actin filament ends is regulated by various localized intracellular signals. Uncapping of actin filaments makes the plus ends available for elongation, thereby promoting actin filament polymerization near the cell cortex. An example of this category of proteins is the cap32/34 (CapZ) as plus end capping protein that is regulated by PIP<sub>2</sub> (Hartmann *et al.*, 1990; Haus *et al.*, 1991) or tropomodulin as minus end capping protein (Yamashiro *et al.*, 2012). Severing proteins on the other hand fragment F-actin. A representative member of this group is the Ca<sup>2+</sup> activated severin which in addition can also nucleate actin assembly (Eichinger *et al.*, 1991).

The third category of actin binding proteins are the F-actin crosslinking proteins, which can either stabilize the filament itself or crosslink filaments to form bundles as well as three-dimensional networks. Prototypes of this class are tropomyosin, which can stabilize the filament (Lehmann *et al.*, 1994),  $\alpha$ -actinin and filamin, which bundle and crosslink the filaments (Noegel *et al.*, 1987; Stossel *et al.*, 2001).

### 1.5 CAP2

Proteins essential for maintaining the equilibrium between G- and F-actin form the monomer actin binding or G-actin sequestering protein family. CAP belongs to this family and its homologs in yeast and mammals have been shown to sequester G-actin through their C-terminal domain and prevent them from polymerization *in vitro* (Hubberstey and Mottillo, 2002). In addition, recent biochemical studies have revealed new biochemical functions of CAP apart from the actin-monomer-sequestering function involved in actin reorganization (Balcer *et al.*, 2003; Bertling *et al.*, 2004; Freeman and Field, 2000; Peche *et al.*, 2013). It promotes actin filament dynamics closely cooperating with ADF (actin depolymerizing factor)/cofilin *in vitro* and *in vivo* (Moriyama and Yahara, 2002), and self-oligomerization of CAP enhances its activities (Quintero-Monzon *et al.*, 2009). Furthermore, the conservation of CAPs among eukaryotes suggests that CAP is a fundamentally important actin regulator. CAP/Srv2 was originally identified in budding yeast by biochemical means as a protein associated with adenylyl cyclase and also genetically as a suppressor of adenylyl-cyclase in conjunction with hyperactive RAS2(V19), thus explaining the yeast name Srv2 (Field *et al.*, 1990; Fedor-Chaiken *et al.*, 1990). The N-terminal region of Srv2 interacts with adenylyl cyclase; whereas the C-terminal region binds monomeric actin with high affinity (Gerst *et al.*, 1991; Freeman *et al.*, 1995; Mattila *et al.*, 2004). Subsequent studies showed that the ability to interact with actin *in vitro* and regulate actin dynamics *in vivo* are conserved functions of CAPs in all eukaryotes (Hubberstey and Mottillo, 2002). In a screen to identify genes required for *Drosophila* oocyte polarity, a *Drosophila* homologue was found which was allelic to *capulet* and *act up* (Baum *et al.*, 2000; Wills *et al.*, 2002; Benlali *et al.*, 2000). *Caenorhabditis elegans* CAP genes were named *cas-1* and *cas-2*. The amino acid sequence of CAS-1 shows a 37% sequence identity with human CAP1. In addition, CAS-2, a second CAP isoform in *C. elegans*, attenuates the actin-monomer-sequestering effect of ADF/cofilin to increase the steady-state levels of actin filaments in an ATP-dependent

manner (Nomura *et al.*, 2012; Nomura *et al.*, 2013). ASP-56 has been isolated from pig platelets and characterized by actin-binding assays as the first mammalian orthologue of CAP (Gieselmann and Mann, 1992). Furthermore, rat *MCHI* cDNA encodes a protein of 474 amino acids that is 36% identical to *S. cerevisiae* CAP and is capable of suppressing the loss of the COOH-terminal functions of CAP when expressed in yeast. (Zelicof *et al.*, 1993). Except for these, “cyclase-associated protein” or CAP is used as a common name in most of the literature. CAPs play a major role in various cellular activities. Knockout of CAP in *Dictyostelium discoideum* and in yeast has revealed many important functions of CAP like in cell polarity and cell migration (Noegel *et al.*, 2004; Vojtek *et al.*, 1991). Although oocyst development is not considered as an actin-dependent process, inactivation of the CAP homologue from *Plasmodium berghei* demonstrated that this protein is essential for malaria parasite oocyst development in the mosquito midgut. The direct role of CAP in this process needs to be elucidated (Hliscs *et al.*, 2010). Inactivation of CAP in *C. elegans*, *Drosophila*, and plant cells results in severe defects in the organization of the actin cytoskeleton, abnormal accumulation of filamentous actin, and consequently problems in many actin-dependent processes (Nomura *et al.*, 2012; Baum *et al.*, 2000; Benlali *et al.*, 2000; Barrero *et al.*, 2002; Effendi *et al.*, 2013).

Mammals have two CAP genes encoding the related CAP1 and CAP2. CAP1 has been well studied. It is expressed in nearly all cells and organs of the mouse and is highly abundant. At the subcellular level, it is present in regions with high actin dynamics (Bertling *et al.*, 2004). CAP2 shows a more restricted distribution and is significantly expressed only in brain, heart and skeletal muscle, and in skin. CAP2 is found in the nucleus in undifferentiated myoblasts and at the M-line of differentiated myotubes. During myogenesis, CAP2 is mainly a nuclear protein; in the adult muscle it is an M-band protein. In skin-derived cell lines, CAP2 is primarily a nuclear protein, in skin it is a nuclear protein and also present at cell borders (Peche *et al.*, 2007).

A comparison of the CAP1 and CAP2 amino acid sequences shows that mammalian CAP1 and CAP2 are highly related proteins. Mouse CAP2 shares 62 % identity and 76 % similarity with mouse CAP1. CAP1 and CAP2 from various mammalian species are 93 – 96 % (CAP1) and 88 – 93 % (CAP2) identical among each other and are equally distant to CAPs from non-mammalian species showing 33 – 34% identity each to CAP/Srv2 from *S. cerevisiae*. The degree of homology between mouse CAP1

and CAP2 varies within the domains. It is slightly higher in the C-terminal domain than in the proline-rich central domain and the N-terminal domain. Loss of CAP results in defects in cell morphology, migration, endocytosis and development in *S. cerevisiae*, *D. discoideum* and *Drosophila* (Hubberstay and Mottillo, 2002).

In Pam212, a mouse keratinocyte cell line, CAP2 is enriched in the nucleus and less prominent in the cytosol whereas CAP1 localizes to the cytoplasm in these cells. In human skin, CAP2 is present in all living layers of the epidermis where it localizes to the nuclei and the cell periphery. In biochemical studies it was shown that a C-terminal fragment of CAP2 interacted with actin, indicating that CAP2 has the capacity to bind to actin. CAP2 is also strongly enriched in the nucleus in developing cardiomyocytes. It changes its localization in the adult cardiomyocyte and is then observed at the M-band. The M-band is an important element of the sarcomere, the elementary contractile unit of striated muscle. It maintains the thick filament lattice through interactions of the prominent M-band component myomesin, which links the thick filaments (Peche *et al.*, 2007).

CAP2 is up-regulated in hepatocellular carcinoma (HCC) when compared with noncancerous and precancerous lesions. That indicates that CAP2 is up-regulated in human cancers. Since it is possibly related to multistage hepatocarcinogenesis, it has been suggested as a 'potential biomarker' for pathological diagnosis (Shibata *et al.*, 2006).

### **1.6 CAP2 and cardiomyopathy**

Cardiomyopathy is a disease characterized by either thickening or thinning of the heart muscle, and both conditions, hypertrophic cardiomyopathy (HCM) and dilated cardiomyopathy (DCM), lead to inefficient functioning of the heart muscle and can cause sudden cardiac death. DCM is the most common cardiomyopathy and many studies point out the importance of left ventricular pathophysiology in congestive heart diseases, whereas right ventricular DCM, in which the right ventricle is dilated with thinning of the ventricular wall, is less frequently observed than left ventricular cardiomyopathy and is therefore not extensively studied (Jefferies and Towbin, 2010). At the structural level, DCM is associated with a loss of myofibrils and sarcomeric disorganization (Mann *et al.*, 1991; Schaper *et al.*, 1991). The inherited forms of DCM are associated with mutations in genes that generally encode cytoskeletal and sarcomeric proteins (Jefferies and Towbin, 2010; Harvey and Leinwand, 2011).

In sarcomeres, the precise control of actin filament length contributes to the proper function of the contractile apparatus. This control appears to occur at the barbed and pointed ends of the filament as actin is incorporated at the Z-disc and in the middle of the sarcomere (A-band region) where it depends upon effective termination of polymerization by capZ and tropomodulin, respectively (Sussman *et al.*, 1998; Littlefield and Fowler, 2008). Filament growth is also affected by the G-actin/F-actin equilibrium, which is regulated by G-actin sequestering proteins. Recent studies demonstrated that actin filaments in sarcomeres of actively contracting cells undergo rapid turnover in which actin depolymerizing factors cofilin 1 and 2 are involved promoting rapid actin dynamics (Skwarek-Maruszewska *et al.*, 2009). Importantly, the *Cap2* gene is expressed at early to late developmental stages during cardiogenesis of mice embryos (Christoforou *et al.*, 2008).

Although various studies implicate CAPs in the organization of the actin cytoskeleton, a detailed analysis of the *in vivo* function of CAP in mammals is still lacking. We have generated a mouse in which the *Cap2* gene is inactivated by a gene-trap approach. Our results show that ablation of CAP2 leads to severe cardiac defects marked by dilated cardiomyopathy associated with a drastic reduction in basal heart rate and prolongations in atrial as well as ventricular conduction times. Moreover, we found alterations in the mechanical properties of the CAP2-deficient myofibrils with a significantly reduced Hill coefficient and severe changes in the structure of the sarcomere. As the underlying mechanism, we proposed a misregulation of actin filament assembly near the M-line due to the absence of CAP2 (Peché *et al.*, 2013).

### **1.7 Cell migration and actin cytoskeleton**

Cells can sense and respond to environmental signals such as mechanical forces that act as critical regulators of physiological processes including embryogenesis and wound healing (Janmey and McCulloch, 2007; Parsons *et al.*, 2010; Geiger *et al.*, 2009). These mechanical forces have to be transmitted across the cell membrane in both directions through cell adhesions that are coupled by the actin cytoskeleton. Cell adhesions are large macromolecular assemblies that form cell-extracellular matrix contacts (hemidesmosomes and focal adhesions) or cell-cell contacts (adherence junctions) (Geiger *et al.*, 2009; Geiger *et al.*, 2001). Members of this group include vinculin, talin, zyxin, FAK, and paxilin that are organized at the basal surface of adherent cells. Focal adhesions have long been speculated to play a critical role in

many cell functions, in particular, cell migration (Ridley *et al.*, 2003). For example, rapidly moving cells, such as *D. discoideum* and neutrophils exhibit negligible small focal adhesions and seem to glide over the substratum (Nagasaki *et al.*, 2009), while slow-moving cells such as fibroblasts display prominent focal adhesions and seem to crawl over the substratum.

A functional relationship between focal adhesions (surface density, size, shape, number, turnover dynamics, etc.) and cell migration is largely till now missing (Kim and Wirtz, 2013). Cell migration can be easily considered as a highly integrated cyclic process (Lauffenburger and Horwitz, 1996). Initially, cells migrate through polarizing and extending protrusions in the direction of migration. These protrusive structures can be large ruffling veil-like lamellipodia or thin, spike-like filopodia. Lamellipodia are composed of orthogonal arrays of actin filaments with branched actin filaments close to the leading edge of plasma membrane, whereas filopodia consist of parallel bundles of actin filaments (Chhabra and Higgs, 2007). Elongation at the barbed ends of actin in lamellipodia and filopodia is thought to form the protrusive machinery for generating force for leading edge advancement (Pollard and Borisy, 2003; Bugyi and Carlier, 2010).

This membrane protrusion is driven by the polarity of actin filaments through fast-growing “barbed” ends and slow-growing “pointed” ends (Welch and Mullins, 2000). Binding of Arp2/3 complex on the already existing actin filament enables the formation of a new daughter filament that branches off the mother filament. Arp2/3 complex is activated by WASP (Wiskott - Aldrich syndrome Protein)/WAVE (WASP family Verprolin-homologous protein) family members. Actin polymerization is regulated by several actin-binding proteins that affect the pool of available monomers and free ends (Pollard and Borisy, 2003; Dos Remedios, 2003). Profilin, for instance, binds to actin monomers, blocks self-nucleation and also targets monomers to barbed ends. Capping proteins terminate filament elongation, while minimizing polymerization to new filaments close to the plasma membrane. Besides, members of the ADF/cofilin family sever and disassemble already stable filaments at the pointed end, a process that is essential for the replenishment of the actin monomer pool needed for polymerization at the front end. Additional proteins stabilize actin filament like Cortactin, Filamin and  $\alpha$ -actinin (Welch and Mullins, 2000). The pivotal mechanism for the formation of the filopodial protrusion is the filament treadmilling, via which actin filaments elongate at their barbed ends and release actin monomers

from their pointed ends (Welch and Mullins, 2000). Ena/VASP proteins bind at the barbed ends allowing continuous elongation of the actin filaments while antagonizing both capping and branching. Furthermore, stiffness that is required for efficient pushing of the plasma membrane in filopodia is achieved by fascin which is an F-actin bundling protein (Welch and Mullins, 2000).

The formation of lamellipodia and filopodia as well as the adhesion organization are mainly controlled by small guanosine triphosphate (GTP)-binding proteins (GTPases) that belong to the Rho family. In their active form (bound to GTP) these regulators interact with a variety of downstream target proteins including protein kinases, lipid-modifying enzymes and activators of the Arp2/3 complex (Etienne-Manneville and Hall, 2002). Guanine nucleotide exchange factors (GEFs) activate Rho GTPases and GTPase activating proteins (GAPs) terminate the signaling event. The most essential Rho GTPases for the formation of stress fibers, lamellipodia and filopodia are RhoA, Rac and Cdc42 respectively (Ridley et al., 2003; Zhou et al., 2014). Cdc42 and Rac mediate actin polymerization in protrusions via the WASP/WAVE family of Arp2/3 complex activators. Cdc42 stimulates the Arp2/3 complex through binding to WASP proteins in order to induce dendritic actin polymerization (Welch and Mullins, 2000). Besides, Rac stimulates lamellipodial extension by activating WAVE proteins (Gory and Ridley, 2002).

CAP2 contains also a WASP homology (WH2) domain which is responsible for its actin-sequestering activity (Peché *et al.*, 2013). This motif, consisting of 25 amino acids is found in proteins such as WASP, thymosin, Spire, Cordon-bleu, Leiomodin, and JMY. Thymosin mediates sequestration of monomeric actin and inhibition of actin polymerization. On the other hand, Spire, Cordon-bleu, and JMY nucleate actin assembly (Ducka *et al.*, 2010).

The WH2 domain of CAP2 was identified in a comparison with N-WASP and thymosin  $\beta$ 4. It is located at position 247–310 and contains the essential LRHV motif and a N-terminal helix preceding this motif (Chereau *et al.*, 2005). CAP2 influences actin dynamics by binding to G-actin through its WH2 domain, preventing polymerization and can also sever filaments thereby affecting filament stability (Peché *et al.*, 2013). These activities might be vital for the organization of lamellipodia that provide a veil-like structure that is able to push the plasma membrane. The lamellipodium could then grow in a particular direction, providing the basis for directional migration.



## 1.8 Wound healing

Skin is the largest organ in the human body and serves as the interface between the organism and the environment, and protects against infection and excessive water loss. Furthermore, multiple components in the skin, such as the sebaceous and sweat glands, hair follicles, blood capillaries, and nerve endings, confer secondary properties that are essential to everyday function (Almine *et al.*, 2012; Seeley *et al.*, 2005).

Cutaneous trauma disrupts skin architecture and integrity, which elicits a highly regulated localized response that cleans, debrides, and heals the site of injury. Trauma to skin can arise from abrasions, lacerations, and thermal, electrical, or chemical burns (Almine *et al.*, 2012; Trott, 1988).

Cutaneous wound healing is a complex and dynamic process involving soluble mediators, blood cells, extracellular matrix (ECM), and parenchymal cells (Singer and Clark, 1999). This phenomenon is characterized by an attenuated inflammatory response to tissue injury, which involves differential expression of signaling factors, and regeneration of normal skin architecture (Almine *et al.*, 2012). The process of wound healing normally proceeds from coagulation and inflammation through fibroplasia, matrix deposition, angiogenesis, epithelialization, collagen maturation and finally wound contraction (Schäfer and Werner, 2008). These processes compose three different overlapping phases: (1) inflammation, (2) repair, and (3) remodeling (Fig. 2).

### 1.8.1 Phases of wound healing

#### A. Inflammation

Skin injury causes cell damage and injury of blood vessels. A wound must stop bleeding in order to heal and for the injured host to survive. Blood vessels constrict within seconds after injury to prevent blood loss and afterwards platelets are activated by thrombin, they aggregate and clotting occurs (Mahdavian Delavary *et al.*, 2011). Together, these events are responsible for the formation of a haemostatic blood clot, mainly composed of complement cascades which are activated and crosslinked like fibrin, fibronectin, vitronectin, thrombospondin, as well as erythrocytes and platelets (Midwood *et al.*, 2004; Metcalfe and Ferguson, 2007; Krafts, 2010). Immediately after wounding insulin like growth factor  $\alpha$  (IGF- $\alpha$ ), transforming growth factor  $\beta$  (TGF- $\beta$ ), platelet-derived growth factor (PDGF) and vascular endothelial growth

factor (VEGF) are released from the platelets, a process that attracts leukocytes and fibroblasts into the wound area.

Mast cells are migrating first to the wound site assisting the recruitment of neutrophils to protect against infectious agents and initiate the removal of debris from damaged cells and ECM (Egozi *et al.*, 2003). The influx of neutrophils peaks in the first 48 hr after injury. The neutrophils are eventually replaced by monocytes, which will subsequently differentiate into macrophages (Almine *et al.*, 2012).

One of the primary roles of macrophages in the inflammatory stage is to complete the removal of debris and foreign material through their phagocytic function and through their capacity to secrete toxic mediators. In addition they recruit fibroblasts, keratinocytes and endothelial cells through secreting growth factors (Krafts, 2010). Furthermore, macrophages participate in the remodeling of the extracellular matrix for the formation of the scar. Macrophages also assist with the transition of the wound site from inflammation to repair. (Fig. 1.2 A).

## **B. Repair**

The repair stage is characterized by active fibroplasia granulation tissue formation, wound contraction, re-epithelialization, and angiogenesis (Grinnell, 1982). Keratinocytes migrate from the epidermis at the wound edge and express various proteases allowing the degradation of the connective tissue (Martin, 1997). This process is followed by active fibroplasia in which fibroblasts migrate, proliferate and deposit extracellular matrix forming the granulation tissue. Granulation tissue is an amorphous structure composed of blood vessels, extracellular matrix (ECM) (collagen, fibronectin), and fibroblasts, replacing the fibrin eschar (scab) as a scaffold for cell infiltration (Almine *et al.*, 2012).

Some fibroblasts differentiate into myofibroblasts, a contractile cell that expresses  $\alpha$ -smooth muscle actin, and is active in the repair stage of wound healing (Werner *et al.*, 2007). The myofibroblast phenotype is induced by mechanical tension and TGF- $\beta$ . The formation and function of myofibroblasts are essential for drawing the margins of the wound edge together, facilitating the physical closure of the wound site (Tomasek *et al.*, 2002; Hinz and Gabbiani, 2003).

Concurrently, re-epithelialization of the epidermis occurs, where undamaged basal keratinocyte epithelial cells migrate and proliferate to the wound edge providing cover for the formation of the neoepidermis. Epidermal stem cells resting in the hair

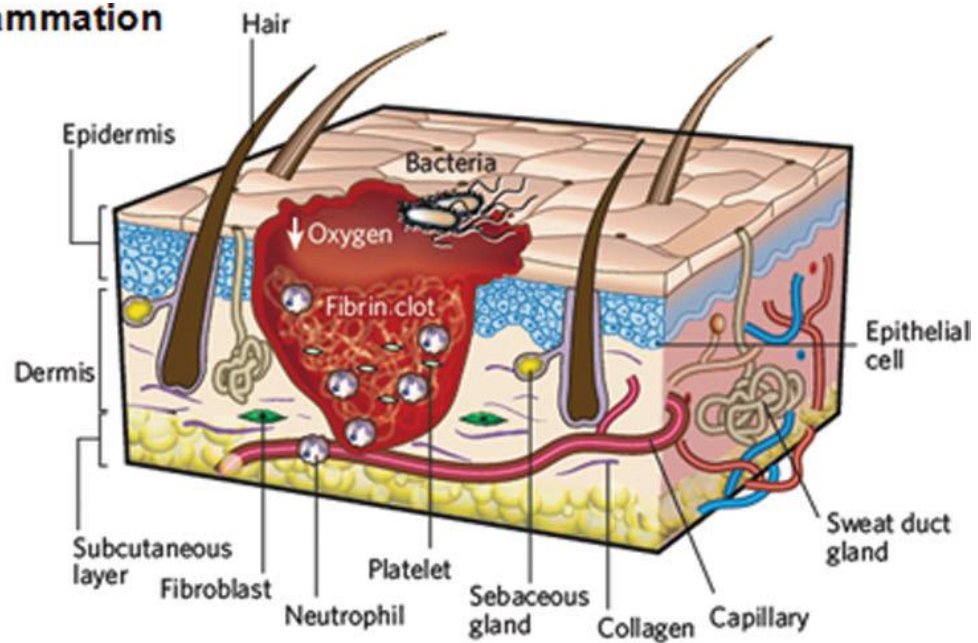
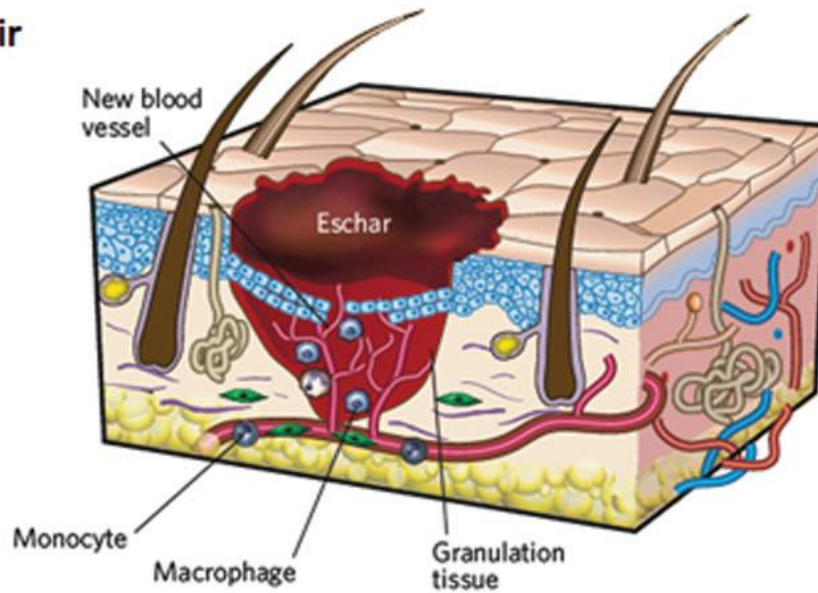
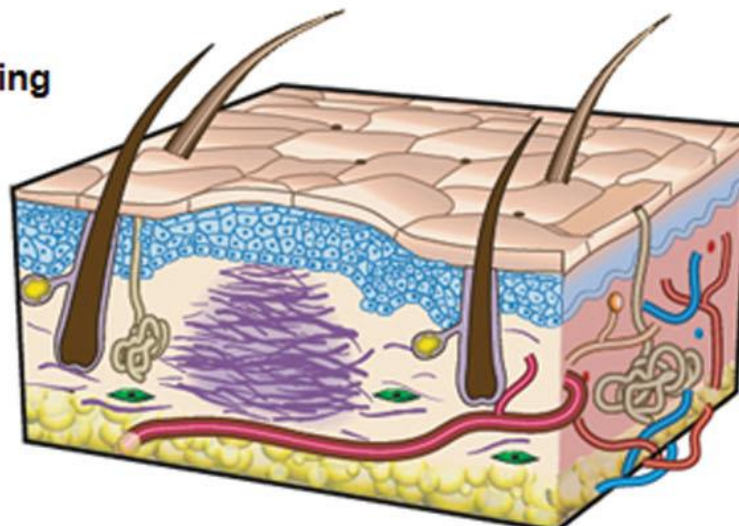
follicle bulge can replenish the pool of proliferative keratinocytes (Gurtner *et al.*, 2008). Consequently, the basement membrane which anchors the epithelium to the dermis underneath through substrate adhesion molecules (SAMs) is re-established by extracellular components secreted and deposited by keratinocytes. This process is also enhanced by fibroblasts. Finally a stratified, keratinized epithelium is formed, due to differentiation of basal keratinocytes caused by contact inhibition (Smola *et al.*, 1993).

In angiogenesis, which is vital for the transport of oxygen, nutrients, and cells, new blood vessels are formed. This step is promoted by the fibrin plug, platelets, and endothelial cells (Singer and Clark, 1999) (Fig. 1.2 B).

### **C. Remodeling**

The remodeling of the mature scar, which is the final and longest stage of wound healing, can last for weeks to months. The acellular, fibrous scar is mainly composed of ECM components (Broughton *et al.*, 2006). During this stage processes like cell proliferation and protein synthesis are slowed down and formation of collagen fibrils takes place (Mahdavian Delavary *et al.*, 2011). The synthesis of collagen I and III increases dramatically to form the central core of the mature scar (Lovvorn *et al.*, 1999). Collagen is remodeled and realigned along tension lines and cells that are no longer needed are removed by apoptosis.

Fibroblasts, macrophages and endothelial cells secrete matrix metalloproteases (MMPs) that contribute in strengthening the repaired tissue (Lovvorn *et al.*, 1999). The collagen-based scar recuperates the rigidity of skin, but exhibits a lower tensile strength, which is due to a deviation in matrix composition and organization compared with uninjured skin (Levenson *et al.*, 1965). Furthermore, the peripheral functions of skin are diminished because skin components, such as hair follicles, sebaceous and sweat glands, are not regenerated (Almine *et al.*, 2012) (Fig. 1.2 C).

**A Inflammation****B Repair****C Remodelling**

**Figure 1.2: The three classical phases in adult skin wound healing.** A) A fibrin clot is formed and inflammatory cells enter the wound site. B) Re-epithelialization and angiogenesis of a provisional matrix occurs. C) Remodeling is the final stage of wound healing. ECM remodeling factors modulate and revise the scar tissue (taken from Gurtner *et al.*, 2008).

### 1.9 Aim of the research

Despite the fact that CAP proteins have been studied for more than 20 years and are present in all organisms, many issues remain to be addressed about CAP function in higher eukaryotes. The role of mammalian CAP2 in actin cytoskeleton organization has not been yet studied extensively. For this aim, we generated a whole body knock-out mouse in which the CAP2 gene was inactivated by a gene-trap approach. Cap2 deletion led to weight loss and here I will study whether it is associated with muscular atrophy or even sarcopenia.

The observation that *Cap2<sup>gt/gt</sup>* mice died earlier and had enlarged hearts in contrast to the WT, prompted us to characterize the cardiac phenotype of the mutant animals, since we already know that CAP2 is highly expressed in the cardiac tissue. The severe cardiac defects can be easily marked by dilated cardiomyopathy (DCM) or hypertrophy. The atrial and ventricular conduction times will also be addressed in order to fully characterize the cardiac defects. At tissue level we will investigate the organization of the sarcomeres.

CAP2 is strongly expressed in skin. We plan to focus on this organ in our further analysis of CAP2 knockout animals. Our major plan is to perform *in vivo* wound healing experiments with which we are going to probe CAP2's role in cell proliferation, differentiation and migration in wound healing, something that is still unknown. The role of CAP2 in regulating wound healing will be characterized by evaluating its effect on neo-epidermis formation, fibroblast myofibroblast transition, and cellular proliferation and apoptosis in the wounds. Additional parameters of wound healing process such as macrophage infiltration and neovascularization will also be extensively investigated.

The formation of filopodia and possible difference in the formation of focal adhesions will come under investigation in terms of cell migration. In addition, analysis of the effect of CAP2 on the subcellular G-/F-actin ratio will take place.

Apart from these, we will also try to further characterize the molecular function of CAP2 through identifying its interacting partners. We will generate and characterize monoclonal antibodies against CAP2.

In addition to this, we will focus on the possible role of CAP proteins in cancer and specifically the role of CAP1 and CAP2 in cancer.

## 2. Materials and methods

### 2.1 Generation of *Cap2*<sup>gt/gt</sup>

Clone D07 was obtained from the EUComm consortium, Helmholtz Zentrum München, Munich, Germany. ES cells were microinjected into blastocysts and chimeras were produced. The generated chimeric males were then intercrossed with C57BL/6N females to generate F1 offspring. The *Cap2*<sup>gt</sup> allele was detected by BamHI digestion of genomic DNA and Southern blotting by using probes generated by using primers pairs;

Forward-probe 5'-GGAAAACCTGTTGAAGGCAG-3' and

Reverse-probe 5'-CCCTGAACTG AGAATGTTCC-3'

PCR primers for genotyping were:

Forward-Cap2: 5'GTGCTTCACTGATGGGCTTG3'

Reverse-Cap2: 5'TCACCCACATTTACGATGG3'

Forward-neo: 5'GCCGCTCCCGATTCGCAG3'

Additionally, heterozygous *Cap2* gene-trap mice were obtained from the EUComm consortium, Helmholtz Zentrum München, Munich, Germany. These mice were maintained in the C57BL/6 background.

All animals (C57BL/6) used in these studies were between E13.5 and 1 year of age; age and sex-matched littermates were used as controls. Animals were housed in specific pathogen-free facilities and all animal protocols were approved by the local veterinary authorities.

### 2.2 Skin wounding

For wounding healing experiments mice were first anesthetized, backs were shaved by a hair shaver, cleaned with ethanol, and four circular wounds of 5 mm diameter were generated at the dorsal site by excising skin, the subcutaneous fat and muscle panniculus carnosus using a punch (pfm medical ag, Köln Germany). 4 mice per genotype per time point were used in these studies. Wounds were left uncovered, digitally photographed at the indicated time points and harvested at days 3, 7 and 10 after wounding. Following tracing, the ImageJ software calculated the open wound area. Animals were housed in specific pathogen-free facilities and all animal protocols were approved by the local veterinary authorities.

### 2.3 Preparation of tissue

Wound exudate was obtained from patients with normally healing cutaneous wounds from Prof. Eming, Institute of Dermatology, Medical Faculty, University of Cologne). For histology, the complete wounds were excised with a small margin of surrounding skin. Tissues were fixed for 2 h in 4% paraformaldehyde before paraffin embedding or frozen unfixed in optimal cutting temperature compound (OCT, Sakura, Torrance, CA). The paraffin embedded and cryopreserved wounds were cut in serial sections from the surrounding wound margin across the center of the wound towards the opposite wound edge in the caudocranial direction.

Cardiac and skeletal muscle tissue was fixed for 2 h in 4 % paraformaldehyde, embedded in paraffin, and sectioned (6-9  $\mu\text{m}$ ).

### 2.4 Immunohistochemistry, antibodies and histology

For general histology, the samples (paraffin sections of 7  $\mu\text{m}$ ) were stained with hematoxylin and eosin (H&E) according to standard procedures. For immunofluorescence, paraffin sections were deparaffinised in 2 changes of xylene and rehydrated through a graded ethanol series, which was then followed by antigen retrieval and antibody incubation. For heart and skeletal muscle incubation was done with primary mouse monoclonal antibodies (mAb) specific for desmin, alpha-actinin, troponin-I, connexin 43, rabbit polyclonal antibodies (pAb) specific for myomesin (all from Sigma), rabbit mAb antibodies against cleaved caspase 3 (Cell Signaling Technology, Beverly, MA, USA). For skin samples incubation was done with rabbit pAbs specific for CAP2, cleaved caspase 3 (Cell signaling), Ki-67 (Abcam), rabbit pAbs specific for CD31 (Abcam), mouse mAbs specific for  $\alpha$ -SMA (Sigma), vinculin (Sigma) and rat mAb F4/80 (Molecular Probes). Appropriate secondary antibodies were conjugated with Alexa Fluor 488 and 568 (Molecular Probes). Nuclei were visualized with 4',6-diamidino-2-phenylindole (DAPI) or propidium iodide (PI). Sections were incubated with primary and secondary antibodies for 1 h at room temperature each and then mounted and imaged with a Leica confocal microscope. Masson's trichrome staining to detect fibrosis was performed according to the manufacturer's protocol (Sigma).

Cultured cells were fixed with paraformaldehyde and processed for immunofluorescence analysis for detecting CAP2 with mAb K82-381-1 which had been generated against bacterially expressed N-terminal domain of CAP2 (aa 1-310).



F-actin was visualized with FITC or TRITC Phalloidin. Nuclei were stained with DAPI. Cells were incubated with primary and secondary antibodies for 1 h at room temperature each.

### 2.5 Cell culture and cell scratch assay

Fibroblasts were isolated from both WT and *Cap2<sup>gt/gt</sup>* mice and were cultured in DMEM medium with 10% fetal bovine serum (FBS), L-Glutamine and antibiotics like Penicillin and Streptomycin in 5% CO<sub>2</sub> in a 37°C incubator. For observing cell spreading and morphology, WT and *Cap2<sup>gt/gt</sup>* fibroblasts were trypsinized with 0.05% trypsin/EDTA for 5 min and centrifuged. The cells were resuspended in medium as mentioned above and placed in a 10 cm petri-dish overnight.

For the cell scratch assays, mouse primary fibroblasts from *Cap2<sup>gt/gt</sup>* and WT were cultured in medium as described above and placed in a 15μ-slide 8 well dish (Ibidi) attached to a culture insert (Ibidi). Fibroblasts were trypsinized with 0.05% trypsin for 5 min, centrifuged, and resuspended in medium as mentioned before.  $25 \times 10^3$  cells were seeded and cultured overnight at 37°C with 5% CO<sub>2</sub>. The next day, the culture insert was removed to create the scratch and cells were rinsed with fresh medium once and fed with culture medium supplemented with 10% FBS. Migration of wild type and mutant fibroblasts after creating the scratch was analyzed by time lapse video microscopy (37°C, 5% CO<sub>2</sub>) using a Leica CTR 7000 HS microscope (LAS AF-AF6000 software) equipped with a Hamamatsu A3472-07 camera and a Plan-Neofluar 10x/0.30 Ph1 objective. For the cell-tracking analysis movies were made for 24 h with frames taken every 15 min and quantification of cell migration speed was done using ImageJ tool.

### 2.6 Western blot analyses

Tissues and cells were homogenized and lysed (1% Triton X-100, 0.1 M NaCl, 0.05 M Tris-HCl, pH 7.5, 0.01 M EDTA, freshly added 1x protease inhibitor cocktail (PIC), 0.5 mM PMSF, 0.01 M DTT) and proteins were resolved on polyacrylamide SDS gels, transferred to nitrocellulose membranes, and then subjected to immunolabeling. Primary antibodies used were rabbit pAb against CAP1 and CAP2 (Peché *et al.*, 2007). Horseradish peroxidase conjugated secondary antibodies were used for detection. mAb against GAPDH conjugated with horseradish peroxidase (Sigma, St. Louis, MO, USA) was used as a loading control. For G/F actin ratio, cells were

washed once in ice-cold PBS and lysed with actin stabilization buffer (0.1 M PIPES, pH 6.9, 30% glycerol, 5% DMSO, 1 mM MgSO<sub>4</sub>, 1 mM EGTA, 1% TX-100, 1 mM ATP, and PIC) on ice for 10 minutes. Cells were dislodged by scraping and centrifuged at 4°C for 75 minutes at 16,000 g. The supernatant (G-actin) and the pellet (F-actin) fraction were resolved on 12% SDS-PAGE gels and then western blotted with monoclonal anti-β-actin antibody (Sigma). Densitometric analysis was done using Image J for estimation of the cellular G/F-actin ratio.

### 2.7 Focal adhesion assay

Focal adhesion assay was carried out as described by Taranum *et al.*, 2012. Briefly, trypsinised cells were seeded on coverslips in culture dishes with an initial cell number of  $1 \times 10^3$  and subjected to immunofluorescence as described above by staining for vinculin. Analysis was carried out with a confocal laser scanning microscope TCS-SP5 (Leica) equipped with TCSNT software. The individual immunofluorescences shown have the same magnification and were taken in the same z-plane so that the spreading of focal adhesions on the surface of the coverslip is comparable. LAS-AF Lite Application Suite software from Leica was used to quantify the spreading area in  $\mu\text{m}^2$ .

### 2.8 Disruption of actin cytoskeleton and recovery

WT and *Cap2<sup>gt/gt</sup>* fibroblasts were plated on coverslips overnight in 24 well plates in normal growth medium. Next day cells were washed three times with PBS and 500  $\mu\text{l}$  of DMEM medium containing latrunculin B at a concentration of 2.5  $\mu\text{M}$  (without FBS and antibiotics) were added. For control, on a separate coverslip medium containing 2.5  $\mu\text{l}$  DMSO was added. After 30 minutes incubation in a humidified chamber (5% CO<sub>2</sub>, 37°C), the medium containing latrunculin B was removed and cells were washed three time with PBS to remove any traces of the drug. Normal growth medium was added for cell recovery. Cells were fixed at various time points (10, 20, 30 and 60 min). After permeabilization cells were stained with TRITC-Phalloidin to visualize F-actin. Nuclei were visualized using DAPI. Coverslips were mounted and processed for confocal microscopy.

### 2.9 RNA isolation

Hearts were dissected from 6 to 8-week-old WT and *Cap2*<sup>gt/gt</sup> mice (n = 5 for each group) and immediately frozen in liquid nitrogen. Tissues were homogenized with an ULTRA TURRAX (IKA Labortechnik, Staufen, Germany) and RNA was isolated using Qiagen RNA isolation kit (Qiagen, Hilden, Germany). Quantity and quality of RNA was analyzed on an Agilent Bioanalyser (Agilent Technologies). Northern blot analysis was done as previously described (Peché *et al.*, 2007).

### 2.10 Expression of CAP2 domains and in vitro assays

N-CAP2-WH2 (aa 1–310) and WH2-C-CAP2 (aa 247–476) encoding sequences were cloned into pGEX 4T-3 expression vector (GE Healthcare), proteins were expressed in *E. coli* BL21, purified and the GST moiety was removed by thrombin cleavage.

### 2.11 DNA transfection

For experiments involving transfection two methods were followed. For immunofluorescence, lipofectamine 2000 (Invitrogen) was used to transfect HEK293 cells in a 24-well plate to overexpress GFP-CAP2 and FLAG-CPT1B, cloned in vectors pEGFP-C1 (Clontech Laboratories) and pCMV-3tag-6 (Agilent Technologies), respectively. Samples were fixed 24 h after transfection.

For pulldown, electroporation (single cuvette electroporator Biorad) was applied to transfect COS7 cells in a 15 cm dish to overexpress FLAG-CPT1B cloned in vector pCMV-3tag-6. Samples were harvested 24 h after transfection and lysates were prepared as mentioned above.

### 2.12 Recombinant protein expression

GST pull-down assays were performed using GST-N-CAP2 and GST-C-CAP2 fusion proteins and GST control, which were extracted from *E. coli* BL21 with Bacterial Protein Extraction Reagent (50 mM Tris-HCl, pH:8.0, 300 mM NaCl, 0.05 % NP40) and then purified using Glutathione Agarose 4B (Protino Macherey Nagel).

### 3. Results

#### 3.1 Generation of a CAP2 knockout mouse (Peché *et al.*, 2013)

To generate mice lacking the *Cap2* gene, we used targeted ES cells (JM8.N4) containing an insertional gene trap, which were obtained from the EUCOMM consortium, Helmholtz Zentrum München, Munich, Germany. ES cell clone D07, which was used in this study, represented a gene-trap that could terminate the transcription of the endogenous gene through altered splicing (Fig. 3.1 A). The gene-trap (gt) cassette was inserted in intron 2 of the mouse *Cap2* gene on chromosome 13. Alternative splicing of the *Cap2<sup>gt</sup>* allele generates a new transcript that is a fusion of exon 2 and the LacZ reporter. The fusion protein encodes the first 40 amino acids of CAP2, which are unlikely to show any function mediated by full-length CAP2. We confirmed clones carrying the homologous recombination event with Southern blot analysis in which we detected an additional band of 8 kb representing the mutant allele (Fig. 3.1 B).

We obtained *Cap2<sup>gt/gt</sup>* mice by mating *Cap2<sup>+/gt</sup>* male and *Cap2<sup>+/gt</sup>* female from clone D07. Additionally, we also obtained *Cap2<sup>+/gt</sup>* male and *Cap2<sup>+/gt</sup>* female, which were generated from a different gene-trap clone (B08) at EUCOMM, Munich, Germany. PCR on genomic DNA from tail biopsies was performed with animals, which confirmed the genotype of *Cap2<sup>gt/gt</sup>* mice showing a single band of 800 bp (Fig. 3.1 C). All phenotypes were confirmed with both mouse lines obtained from the two independent clones. We also carried out Northern blot analysis to confirm the mutant and to rule out any possibility of generation of aberrant transcripts. An N-terminal probe (1–671 bp of *Cap2* cDNA) showed the expected transcripts at 3.6 and 3.2 kb in WT as previously reported (Peché *et al.*, 2007). The amounts were reduced in *Cap2<sup>gt/+</sup>* mice and no transcripts were observed in *Cap2<sup>gt/gt</sup>* mice (Fig. 3.1 D). The successful inactivation of the *Cap2* gene was confirmed by Western blot analysis where we probed heart and brain lysates obtained from *Cap2<sup>gt/gt</sup>* mice and their wild-type (WT) littermates with CAP2-specific polyclonal antibodies (Peché *et al.*, 2007). In lysates from WT brain and heart, a signal at ~56 kDa was detected; no protein was seen in lysates from *Cap2<sup>gt/gt</sup>* mice (Fig. 3.1 E). When we probed the blot for expression of CAP1, we did not detect significant up-regulation upon loss of CAP2 excluding the possibility that CAP1 compensates for the deficiency (data not shown) (Peché *et al.*, 2013).

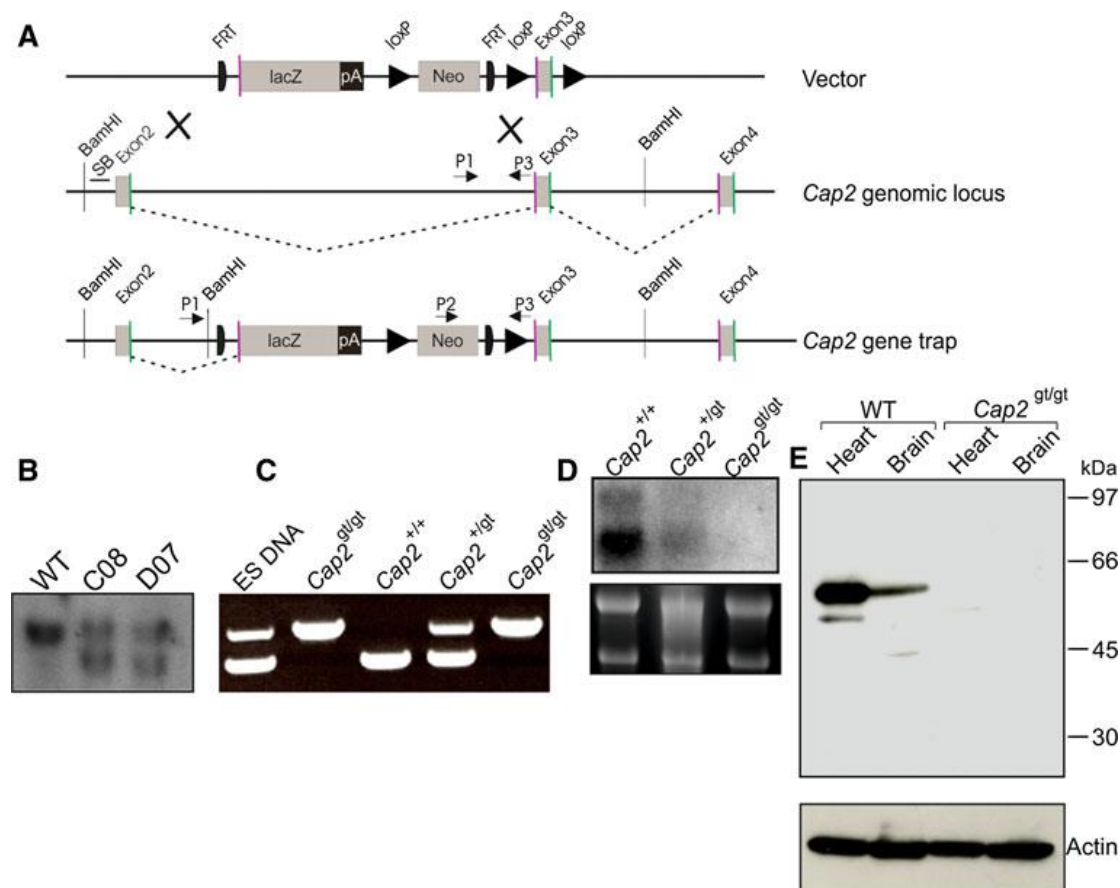


**Figure 3.1: Targeting strategy for  $Cap2^{gt/gt}$  generation.** Schematic representation of CAP2 targeting. A) The knockout vector consists of the lacZ gene as a reporter and the neomycin phosphotransferase gene. Genomic locus of the Cap2 gene depicting exon 2, 3, and 4. Transcripts initiated at the endogenous promoter are spliced from the splice donor (green) of an endogenous exon (exon 2 and exon 3) to the splice acceptor (purple) of endogenous exons (exon 3 and exon 4). Homologous recombination gave rise to a gene trap of CAP2 (3' LoxP missed). Transcripts shown as gray dotted line initiated at the endogenous promoter are spliced from the splice donor of endogenous exon 2 and the splice acceptor of lacZ cassette (diagram not drawn to scale). P1, P2, and P3 are the primers used for genotyping of mice. B) Southern blot analysis of Bam HI digested genomic DNA. Hybridization of radioactively labeled CAP2 probe results in detection of the 10-kb fragment of the WT genomic locus. After the homologous recombination event, restriction with Bam HI enzyme gave rise to an additional fragment of 8 kb. C) PCR analysis for genotyping. PCR was performed using primers mentioned in the Materials and methods section for genotyping the animals. The WT allele gave a product of ~550 bp (P1 and P3) while the mutant allele gave a product of ~800 bp (P2 and P3). D) Northern blot analysis. 10  $\mu$ g of RNA from hearts of WT,  $Cap2^{gt/+}$  and  $Cap2^{gt/gt}$  was separated on a 1% agarose gel in the presence of formaldehyde (6%). The resulting blot was probed with a probe corresponding to nucleotides 1–671 of the mouse CAP2 cDNA. E) Western blot analysis using WT and  $Cap2^{gt/gt}$  heart and brain lysates. Proteins of heart and brain lysates were separated on SDS-PAGE (10% acrylamide) and transferred onto a nitrocellulose membrane. The blots were probed with anti-CAP2 polyclonal antibodies. No protein was detected in  $Cap2^{gt/gt}$ , whereas in WT lysates the protein was detected at ~56 kDa. Actin was used as a control (taken from Peche *et al.*, 2013).

### 3.2 Characterization of CAP2 monoclonal antibodies

For a further analysis of CAP2 distribution at the protein level, apart from the polyclonal antibodies that we have previously used, we generated monoclonal antibodies using a bacterially expressed polypeptide corresponding to the N-terminal domain of CAP2 (amino acids 1-310) as an antigen (Fig. 3.2 A). mAb K82-381-1 detected the protein in immunofluorescence analysis in nuclei of HaCaT cells and as an ~56 kDa protein in western blots (Fig. 3.2 B,C). This part of work was done with Dr. med. dent, Ali Eskandarnaz and Arya B Khorsandi.

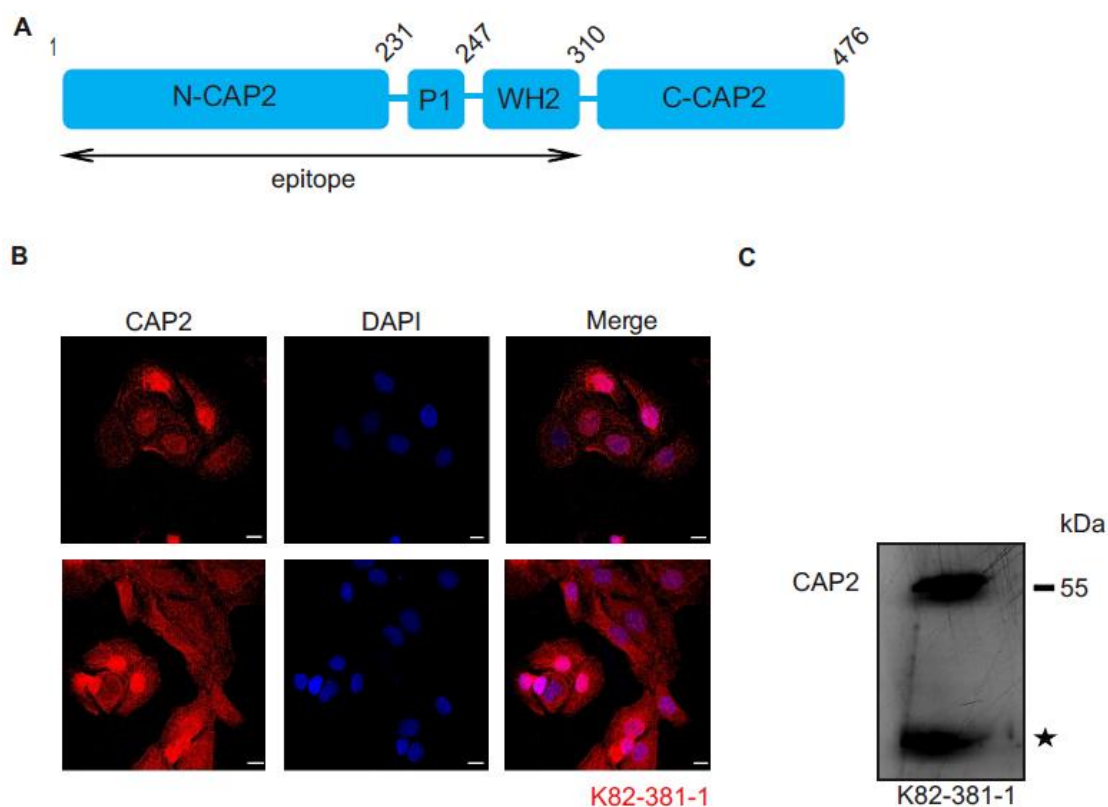


**Figure 3.2: Characterization of CAP2 monoclonal antibody K82-381-1.** A) Schematic representation of CAP2 protein domains depicting the polypeptide against which monoclonal antibody K82-381-1 was raised. B) HaCaT cells were stained with mAb K82-381-1, which recognizes nuclear and cytosolic CAP2. Nuclei were stained with DAPI. Scale bars, 10  $\mu$ m. C) Homogenate of adult mouse heart muscle was separated by SDS-PAGE (10% acrylamide) and the blot probed for CAP2 presence with K82-381-1. The asterisk indicates a degradation product.

### 3.3 CAP2 deletion leads to weight loss and is lethal in postnatal stages of mice

The notion that the size of *Cap2*<sup>gt/gt</sup> mice at birth appeared smaller prompted us to follow the body weight. An average weight reduction of approximately 30–40% was consistently observed in mutant females (Fig. 3.3 A, B). CAP2 deficiency appeared to manifest shortly after birth, as during development there was no significant difference

in the size of the embryos (data not shown). For male mice, we also noted a lower body weight with an average weight reduction of 40–45% compared to their WT littermates (Fig. 3.3 C, 40 days of age,  $n = 8$ ). The survival rates in the  $Cap2^{gt/gt}$  mice differed from the one in WT mice and  $Cap2^{gt/gt}$  died earlier. This phenotype was more drastic in males compared to females as 25 out of 40  $Cap2^{gt/gt}$  males died between 1 and 70 days after birth. The remaining 15 animals were still alive after 70 days (Fig. 3.3 D). Analyses of  $Cap2^{gt/gt}$  embryonic stages revealed that mutant mice did not die during embryogenesis. This was also underlined by the Mendelian ratio in which the animals were born (25% WT, 50%  $Cap2^{+gt}$ , 25%  $Cap2^{gt/gt}$ ) (Peche *et al.*, 2013).

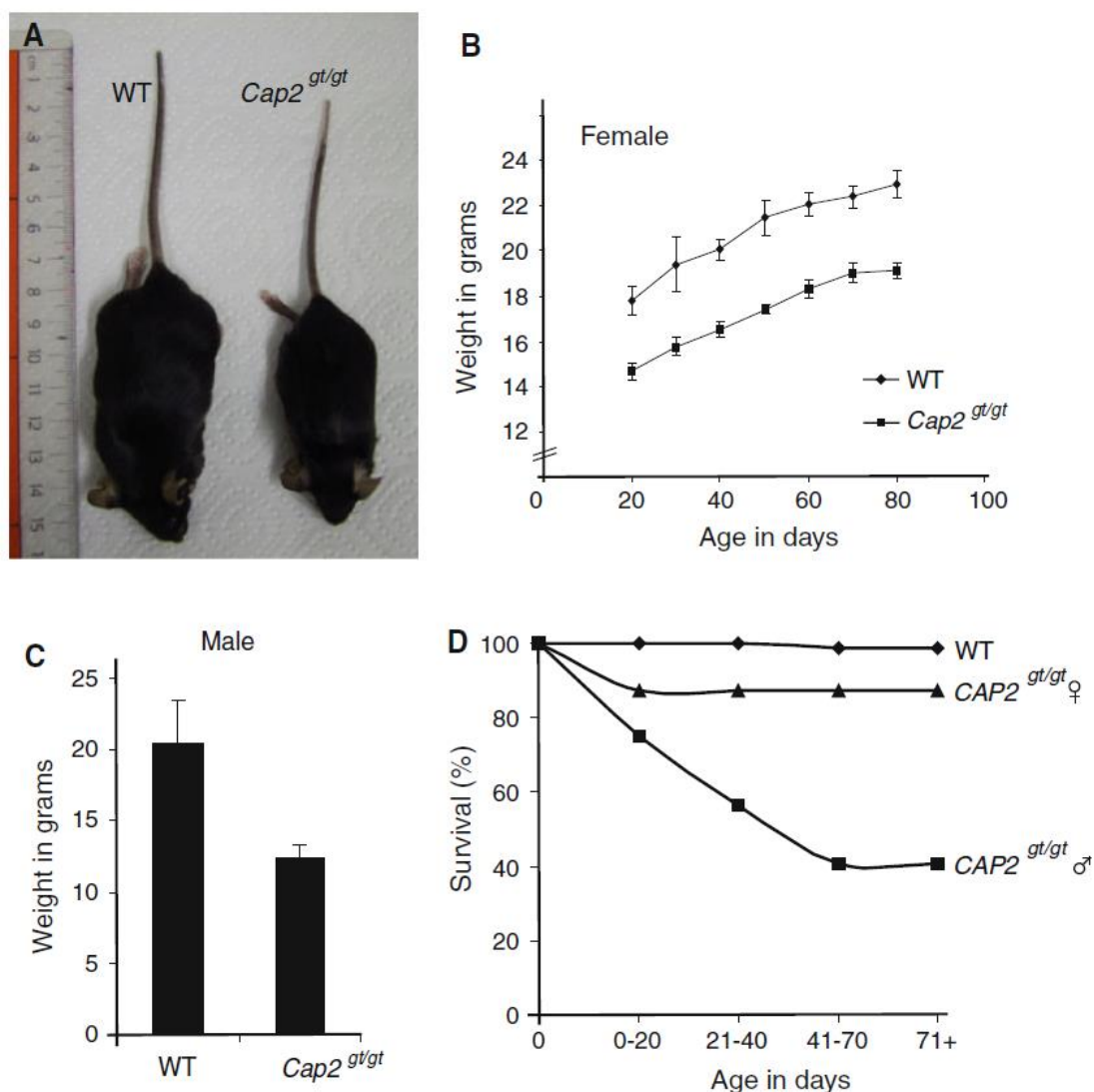


**Figure 3.3: Inactivation of  $Cap2$  leads to weight loss and reduced survival.** A) Overall appearance of WT and  $Cap2^{gt/gt}$  mice aged 40 days. Reduced body length and leanness can be seen in  $Cap2^{gt/gt}$  mice. B, C) Body weight of mice of different genotypes and gender shows a reduction for  $Cap2^{gt/gt}$  mice (WT/ $Cap2^{gt/gt}$  females:  $n = 5/8$ , WT/ $Cap2^{gt/gt}$  males:  $n = 7/7$ ). D) Percent survival versus age in days for WT (male + female,  $n = 86$ ) versus  $Cap2^{gt/gt}$  female ( $n = 47$ ) and  $Cap2^{gt/gt}$  male ( $n = 32$ )

mice. 70+ days survival was monitored in *Cap2<sup>gt/gt</sup>* female and *Cap2<sup>gt/gt</sup>* male. Only 40 % *Cap2<sup>gt/gt</sup>* male and 87 % of *Cap2<sup>gt/gt</sup>* female survived over 70 days in comparison to WT animals (99% survival) (from Peche *et al.*, 2013).

### 3.4 Cardiac and skeletal muscle phenotype of *Cap2<sup>gt/gt</sup>* mice

#### 3.4.1 *Cap2<sup>gt/gt</sup>* mice develop dilated cardiomyopathy

In the following we examined the consequences of the deletion of CAP2 in detail. This work was done with Dr. Vivek Peche. For both sexes, we observed a reduction in weight at any given time point. The animals were fertile and female mice showed a life span up to 12–14 months (n = 24) after which survival decreased rapidly. Autopsy revealed gross morphological differences between *Cap2<sup>gt/gt</sup>* and their control littermates. *Cap2<sup>gt/gt</sup>* male and female hearts were characterized by drastic enlargement of ventricles, which was consistently observed in all mice from 40 days onwards. Interestingly, all of the *Cap2<sup>gt/gt</sup>* mice that died between P1 and P70 also showed an enlarged right and left ventricle. H & E staining, a two-stage stain for cells in which hematoxylin is followed by a counterstain of red eosin so that the nuclei stain a deep blue-black and the cytoplasm stains pink, was applied in cardiac sections and confirmed the dilation of the ventricles (Fig. 3.4 A-D; Table 3.1). Consequently, the total area of the right ventricular chamber was also increased significantly in *Cap2<sup>gt/gt</sup>* mice (Fig. 3.4 E). In addition, we noticed a thinning of the ventricular myocardium compared to the total area (Fig. 3.4 F). Dilated cardiomyopathy is often associated with abnormalities in electrical conductivity of the heart. To check conductivities in mutant hearts, we performed surface electrocardiography (Table 3.2). Nine WT (five male, four female) and eight mutant (four male, four female) animals were used in surface ECG recordings. The surface ECG showed a significantly decreased heart rate in *Cap2<sup>gt/gt</sup>*. With decelerated heart rate, we also observed a significantly prolonged PQ interval at equal P-wave length in *Cap2<sup>gt/gt</sup>* mice, which can be attributed to negative dromotropic effects correlated with slower heart rate. In the *Cap2<sup>gt/gt</sup>* mice, the parameters for atrio-ventricular conduction time (PQ time) as well as intraventricular conduction times (QRS time and QT time) showed marked prolongations compared to WT (Table 3.2; Fig. 3.4 G). After correction for the heart rate, the QTc did not differ between the groups.

Proliferation of interstitial fibroblasts and biosynthesis of extracellular matrix components in the heart are defined as cardiac fibrosis. It is a consequence of remodeling processes initiated by pathologic events associated with a variety of



cardiovascular disorders, which leads to abnormal myocardial stiffness and, ultimately, ventricular dysfunction (Tamura *et al.*, 2000). Staining with Masson's trichrome on transverse cardiac sections of 2-month-old mice revealed no symptoms of fibrosis in *Cap2<sup>gt/gt</sup>* mice (data not shown), but at the age of 6 months we could clearly observe fibrosis in the ventricles of *Cap2<sup>gt/gt</sup>* mice whereas this was not the case in their WT littermates (Fig. 3.4 H). As an increase in fibrosis might be associated with increased apoptosis, we performed caspase 3 staining on cardiac sections (three male, one female; 2–6 months old) and found that mutant myocardium had significantly higher numbers of apoptotic cells than WT (WT, 0.12% cells; *Cap2<sup>gt/gt</sup>*, 0.94% cells;  $p < 0.0005$ ). Also, caspase 3-positive cells were not restricted to any particular region of the myocardium (Fig. 3.4 K). In general, apoptosis was more prominent in failing hearts.

To investigate embryonal heart development and the possibility of development of cardiomyopathy/cardiac defects during embryogenesis, embryos between E11-E15 were studied. Whole-mount analysis revealed that embryos did not show obvious external abnormalities. Similar to their WT littermates, at E13.5 cardiac chamber formation was observed in *Cap2<sup>gt/gt</sup>* mice (Fig. 3.4 I). The cardiac ventricular walls of the *Cap2<sup>gt/gt</sup>* were slightly thinner than those of the control embryos; the ventricular myocardium of control and *Cap2<sup>gt/gt</sup>* appeared normal (Fig. 3.4 I). Thus, overall heart development appeared to be not severely affected during embryogenesis of *Cap2<sup>gt/gt</sup>* mice. At age P4, mutant hearts exhibited dilated atria and mildly dilated ventricles (Fig. 3.4 J). This underlines our previous finding that CAP2 is expressed in all four chambers and is responsible for physiological functioning of the atria and ventricles, which ultimately govern the heart performance (Peché *et al.*, 2013).

**Table 3.1: Gross morphological cardiac defects observed in *Cap2<sup>gt/gt</sup>* mice.**

	Male	Female
Ventricular dilatation (VD)	31	17
Atrial dilatation (AD) with mild VD	3	1
Severe VD and AD	6	4
Total number of mice	40	22
Sudden cardiac death	32	8

**Table 3.2: Surface ECG parameters.**

	WT (n = 9)	Cap2 <sup>gt/gt</sup> (n = 8)
Heart rate (bpm)	445.3 ± 33.0	403.5 ± 39.1*
P (ms)	14.3 ± 1.4	15.4 ± 1.9
PQ (ms)	39.0 ± 6.3	45.4 ± 3.6*
QRS (ms)	12.7 ± 1.5	15.0 ± 1.7**
QT (ms)	30.7 ± 3.0	35.3 ± 3.9*
QTc (ms)	26.4 ± 2.6	28.9 ± 3.4

QTc rate corrected QT time

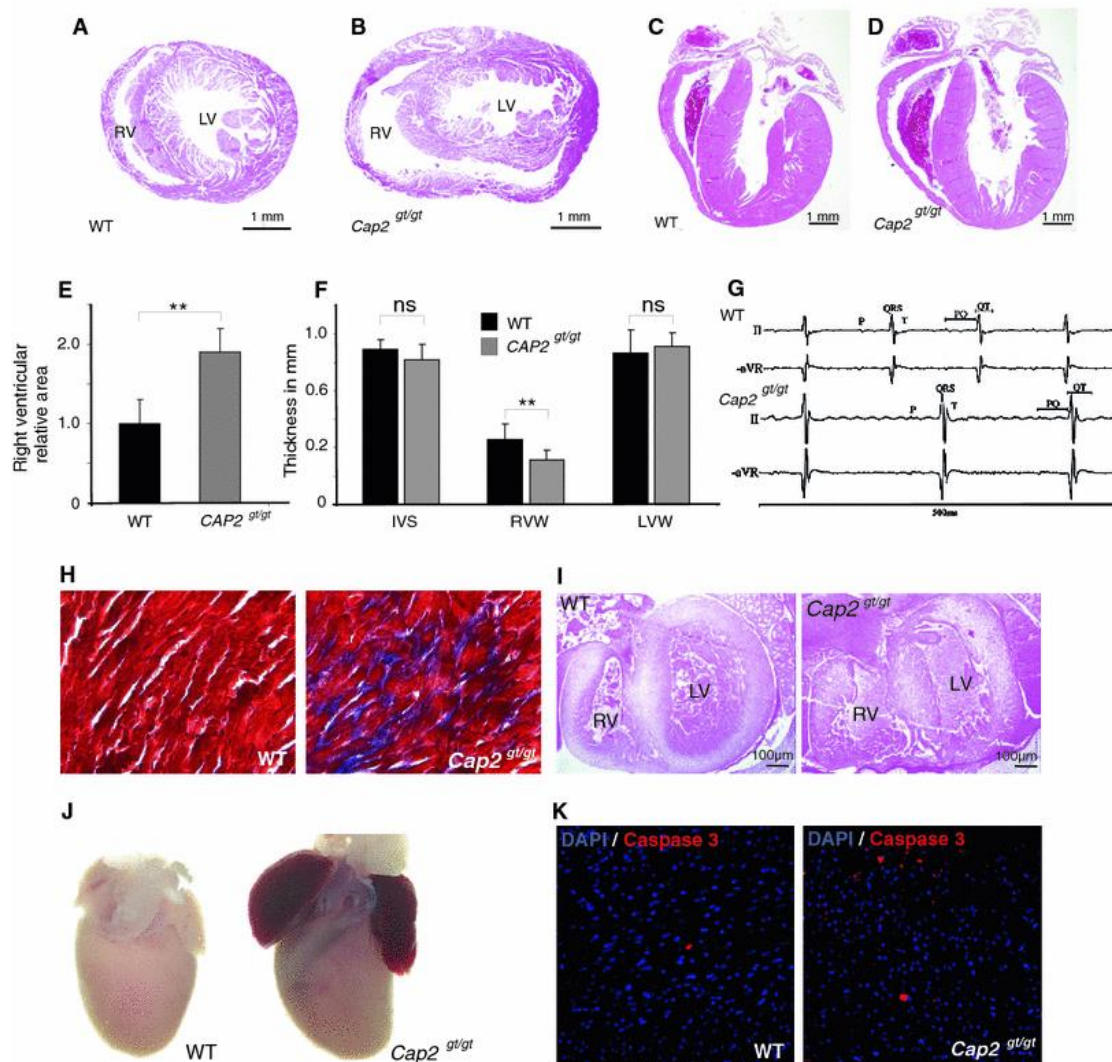


**Figure 3.4: Characterization of cardiac phenotypes of *Cap2*<sup>gt/gt</sup> mice.** Histological analyses of 2-month-old mice. Representative images of transverse (A,B) and longitudinal (C,D) sections of WT and *Cap2*<sup>gt/gt</sup> mice stained with H&E. The mutant exhibited an enlarged ventricular chamber. Scale bars, 1 mm. E) The relative right ventricular area was also increased in *Cap2*<sup>gt/gt</sup> mice as compared to their WT

littermates. F) Mean parameters for both genotypes were compared from respective longitudinal sections (IVS, inter-ventricular septum; RVW, right ventricular free wall; LVW, left ventricular wall). Each bar represents the mean  $\pm$  SEM from four to five animals. G) A representative surface ECG showing recordings from 3-month-old WT and *Cap2<sup>gt/gt</sup>* mice. H) *Cap2<sup>gt/gt</sup>* mice have increased myocardial fibrosis. Masson trichrome-stained sections from *Cap2<sup>gt/gt</sup>* hearts revealed increased fibrosis (blue) in comparison to WT hearts. I) H&E staining of transverse sections through the heart at E13.5 shows no major defects in mutant embryos. J) Mutant mice at P4 showed severe dilation of atria and mild dilation of ventricle. K). Increased apoptosis in mutant mice visualized by immunofluorescence analysis for cleaved caspase 3. Nuclei were stained with DAPI (from Peche *et al.*, 2013).

### 3.4.2 CAP2 is required for proper sarcomeric organization in cardiac and skeletal muscle

Our group previously showed that CAP2 is primarily located at the M-band of the sarcomere accompanied by fine striations on either side of the M-band (Peche *et al.*, 2007). We performed immunofluorescence studies to investigate the effect of CAP2 inactivation on sarcomeric organization. In wild-type cardiac tissue, we observed well-formed regular sarcomeres, whereas for cardiac sections derived from *Cap2<sup>gt/gt</sup>* animals, we observed a mixed sarcomeric organization. Some areas in the ventricles and atrium had well-formed sarcomeres, in other areas the sarcomeric organization was disarrayed. Ventricles and atria appeared equally affected. Double immunofluorescence using desmin (Z-band) and myomesin (M-band) antibodies revealed elongated and well-organized sarcomeres in WT mice, whereas in *Cap2<sup>gt/gt</sup>* mice the M-line was severely disturbed as we could not observe a well-formed M-line as detected by myomesin in many areas of the cardiac sections (Fig. 3.5 A). In heart specimens from the mutant we also saw a striated staining pattern for desmin, alpha-actinin, and troponin-I, however, it was frequently irregular, and in addition we detected areas with deposition of desmin aggregates as observed in desminopathies (Fischer *et al.*, 2006) Aggregate-like structures were also seen when we stained for troponin-I. Consistent with this, we also noted disorganized sarcomeres in mutant skeletal muscle stained with antibodies against desmin and troponin-T when compared to WT (Fig. 3.5 C). The intercalated discs as visualized by connexin 43 labeling appeared not to be dramatically altered at this level of resolution (Fig. 3.5 B).

Consistent with our confocal analysis, examination by electron microscopy revealed severe disarray of sarcomeres in the ventricular myocardium of *Cap2<sup>gt/gt</sup>*. In WT ventricular myocardium, the sarcomeres showed clearly defined A- and I-bands and Z-

discs and M-lines. In *Cap2<sup>gt/gt</sup>* mice, the length of the sarcomeres appeared reduced with the M-lines and I-bands almost indistinguishable. The overview at lower magnification illustrates the reduced number of myofibrils in heart muscle cells as well as the missing of the dark zone and the narrowed banding pattern (Fig. 3.5 D) (Peché *et al.*, 2013).

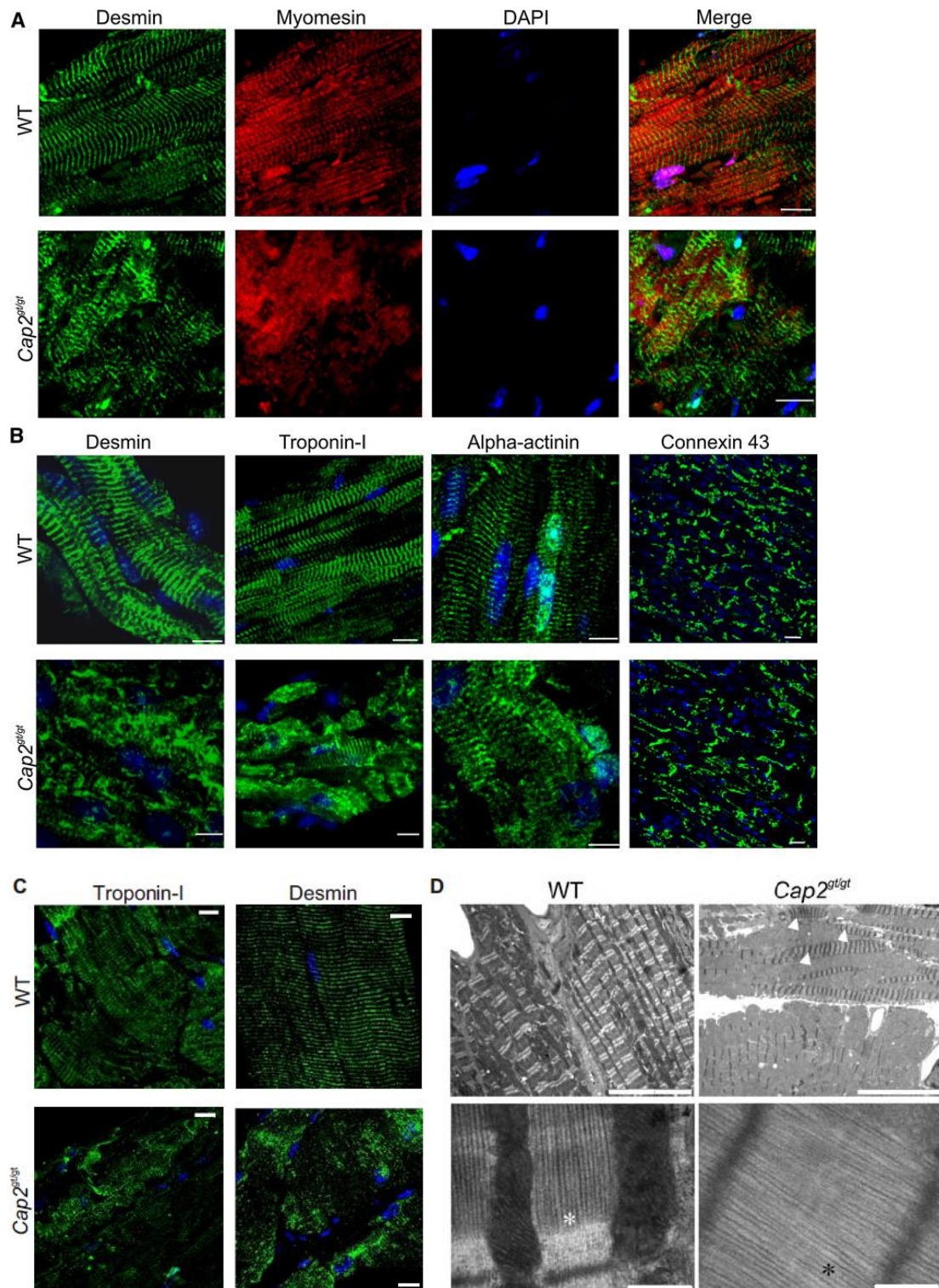


**Figure 3.5: Disarray of sarcomeric organization in *Cap2<sup>gt/gt</sup>* mice.** A) Paraffin-embedded sections of heart muscle stained with desmin (Z-disc) and myomesin (M-line) specific antibodies showing a compromised and disorganized sarcomeric organization in *Cap2<sup>gt/gt</sup>* mice compared to its WT littermate. B) Staining for desmin, alpha-actinin, cardiac troponin-I, and connexin 43 with monoclonal antibodies revealed chaotic organization with fewer striations in *Cap2<sup>gt/gt</sup>* mice when compared to WT. Bar, 10  $\mu\text{m}$  for A, B (connexin 43 panel, bar, 20  $\mu\text{m}$ ). C) Paraffin-embedded sections of skeletal muscle stained with desmin (Z-disc) and troponin T (sarcomere) specific antibodies showing sarcomeric disorganization in *Cap2<sup>gt/gt</sup>* mice compared to WT littermates. D) Electron micrographs of the right ventricular myocardium showing the aberrations in sarcomere organization in mutant animals. The overview at lower magnification (upper panels) illustrates the reduced number of myofibrils, missing of the dark zone and the narrowed Z-line-banding pattern in the sarcomeres (marked with arrows). Higher magnification revealed disarrangement in sarcomere structure. In mutants, there is only one nearly uniformly structured space between the two Z-lines (bottom row, marked with black asterisk) instead of a dark zone (overlapping actin and myosin, marked with white asterisk) flanked by two light zones of solely actin which is evident in WT. Half of a sarcomere is shown for WT reflecting the size differences. Bar, 10  $\mu\text{m}$ , upper panel; 0.5  $\mu\text{m}$ , lower panel (from Peche *et al.*, 2013).

### 3.4.3 CAP2 deletion may lead to sarcopenia

The enlarged hearts and the reduced body weight of the *Cap2<sup>gt/gt</sup>* mice led us to investigate further phenotypic characteristics of this mice. For this reason, we performed H & E staining in paraffin embedded skin sections including the adipose tissue of the hypodermis and the muscle layer below. Interestingly in the 1 year old mice, we found that the muscle was decreased and the adipose tissue was enlarged. These 2 characteristics combined with the age of the mice (1 year) indicate the development of sarcopenia. (Fig. 3.6) Sarcopenia is characterized first by a muscle atrophy (a decrease in the size of the muscle) along with a reduction in muscle tissue "quality," caused by such factors as replacement of muscle fibers with fat, an increase in fibrosis, changes in muscle metabolism, oxidative stress, and degeneration of the neuromuscular junction (Ryall *et al.*, 2008). These changes apparently led to progressive loss of muscle function and frailty with increasing age. Further investigation by staining with different markers like heat shock protein 72, C-terminal agrin fragment, active caspase 3, Cytochrome C Oxidase (COX) sections from mice from different ages from 3 months to 1 year will address this issue.

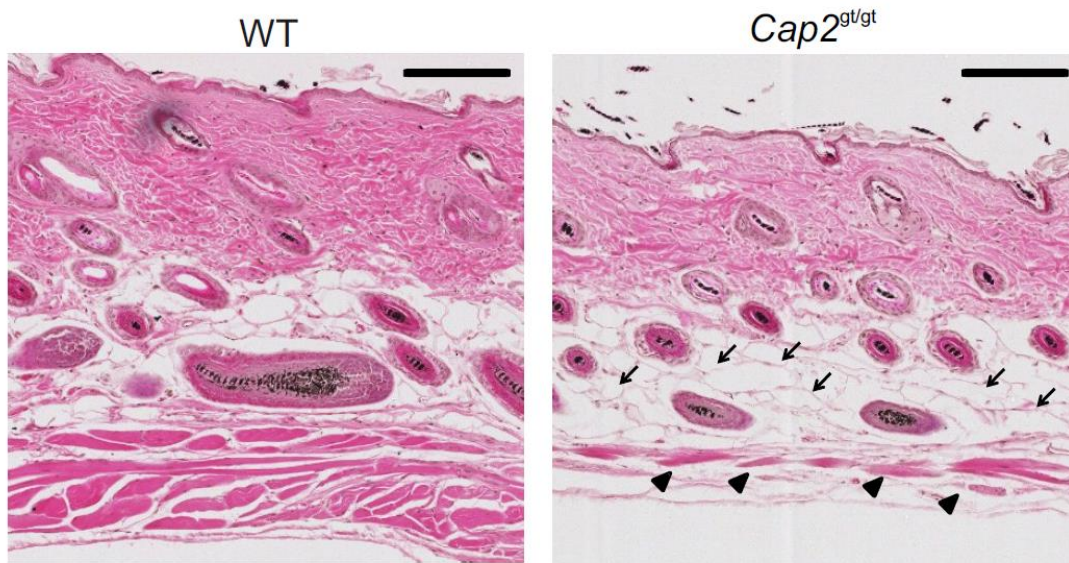


**Figure 3.6: Loss of CAP2 indicates sarcopenia.** 1 year old skin paraffin sections from *Cap2<sup>g<sup>t</sup>/g<sup>t</sup></sup>* and WT mice were stained with H & E. The muscle tissue (arrowheads) is mostly replaced by the adipose tissue (arrows) in the mutant. Scale bar, 200  $\mu$ m.

### 3.5 Roles of CAP2 in wound healing

#### 3.5.1 Expression of CAP2 in human wounds

Earlier we have reported that CAP2 is present in murine skin and also in human skin where it localizes to the nucleus, the cytosol and also to the cell periphery (Peché *et al.*, 2007). It remained however unclear whether CAP2 has any role in human skin repair processes such as wound healing. To study this we performed immunohistochemistry on unwounded human skin and human wounds obtained from patients. In accordance with earlier studies (Peché *et al.*, 2007), in unwounded human skin, we observed expression of CAP2 in all living layers of the epidermis where it was found at the cell periphery and in the nucleus. Interestingly, in human wounds, CAP2 was also expressed in hyperproliferative epidermis and at the migrating tongue (Fig. 3.7 A, upper two panels). In hyperproliferative epidermis in wounds at day 5 and day 20, we detected CAP2 in basal cells which undergo proliferation. Interestingly, the protein exhibited a more cytosolic localization whereas in the stratum spinosum where keratinization begins it was also present at the cell periphery (Fig. 3.7 A, middle two panels). When we quantified the expression of CAP2 in human wounds by intensity per unit area, we found a significant upregulation of CAP2 at day 5 (Fig. 3.7 B) (CAP2 intensity per unit area, unwounded skin  $46.97 \pm 5.68$ , Day 5 post wounding  $61.68 \pm 6.3$ ,  $p = 0.000065823$ ). Based on the notion that CAP2 is upregulated at day 5 post

injury, its presence in hyperproliferative epidermis and its association with the actin network and its regulation, it appears to have an important role in wound healing. This prompted us to study the *in vivo* wound healing further.

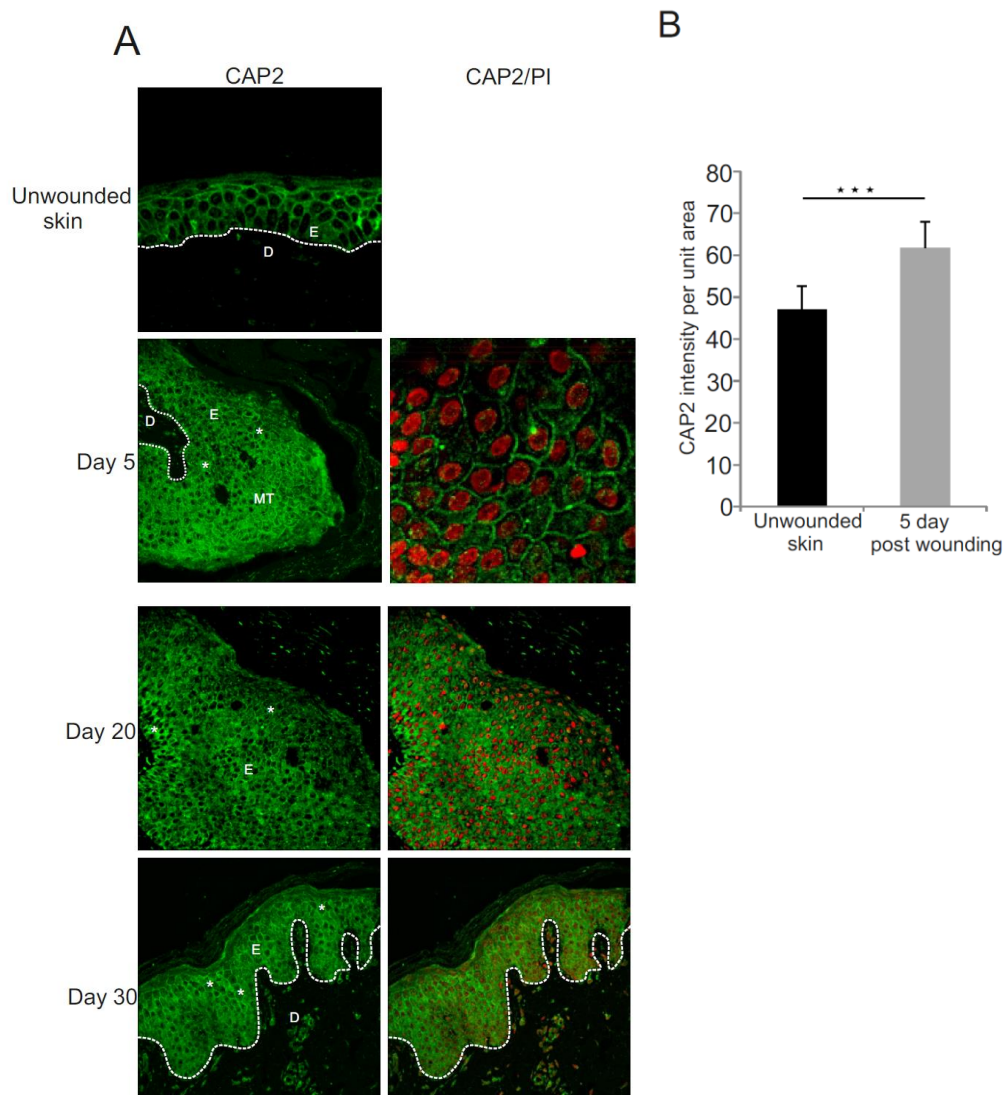


**Figure 3.7: CAP2 is expressed in human wounds.** A) Unwounded skin and human wound paraffin sections were stained with CAP2 specific polyclonal antibodies at day 5, 20 and 30 post injury. In unwounded skin CAP2 is found in all living layers of epidermis (upper panel). Note that, CAP2 is present in the cells of the stratum basale, stratum spinosum and also in the migrating tongue of the wound. Cells marked with asterisk indicate cytosolic CAP2 staining (stratum basale) and also in keratinizing cells (stratum spinosum) at the cell periphery (higher magnification, day 5). Nuclei were stained with propidium iodide. E, Epidermis; D, Dermis; MT, Migrating tongue. B) Quantification of CAP2 intensity per unit area in normal skin versus skin at day 5 post injury showing significant increase of CAP2 upon injury (\*\*\*)  $p < 0.001$ .

### 3.5.2 Loss of CAP2 results in delayed wound repair

CAP2 was detected in homogenates from brain, heart, testis, skeletal muscle and skin. In addition, PAM212 cells, a mouse keratinocyte cell line, showed a strong signal for CAP2 and also a nuclear localization of CAP2 was observed as in primary keratinocytes. In skin CAP2 antibodies revealed strong staining in the cell periphery and inside the nucleus in all living layers of the epidermis (Peche *et al.*, 2007).

To test the response of the mutant skin to an injury we used *Cap2<sup>gt/gt</sup>* mice and their WT littermates at the age of 3 months. Full thickness wounds of 5 mm were generated by circular excision on the shaved back of WT and *Cap2<sup>gt/gt</sup>* mice and the closure followed over a period of ten days. Macroscopic inspection of *Cap2<sup>gt/gt</sup>* wounds revealed a delayed wound closure. On day 7 after wounding, we observed epithelialization of the wounds for WT animals whereas in the mutant animals we observed delayed epithelialization and a bigger scab than in the WT animals (Fig. 3.8 A). Planimetric analysis of surface wound area showed delayed healing in *Cap2<sup>gt/gt</sup>* mice with significantly larger wounds observed when compared to wild-type (Fig. 3.8 C) (open wound area, Day 0, WT 19.63 mm<sup>2</sup>, *Cap2<sup>gt/gt</sup>* 19.63 mm<sup>2</sup>; Day 3, WT 13.22 ± 1.22 mm<sup>2</sup>, *Cap2<sup>gt/gt</sup>* 15.26 ± 1.86 mm<sup>2</sup>, p = 0.04976901 ; Day 7, WT 1.85 ± 0.57 mm<sup>2</sup>, *Cap2<sup>gt/gt</sup>* 2.54 ± 1.01 mm<sup>2</sup>, p = 0.047096663). To confirm the macroscopic observations, we performed H&E stainings on wounds at different stages and observed that the wound healing was slowed down in *Cap2<sup>gt/gt</sup>* mice (Fig. 3.8 B). At day 3, 7 and 10 the distance between the wound margins was greater in sections from *Cap2<sup>gt/gt</sup>* mice compared with WT sections Statistical analysis showed a significant difference in WT and mutant wounds at day 10. (Fig. 3.8 D) (distance between wound ends, Day 0, WT 5000 µm, *Cap2<sup>gt/gt</sup>* 5000 µm; Day 3, WT 2728 ± 588 µm, *Cap2<sup>gt/gt</sup>* 2958 ± 295 µm; Day 7, WT 1475 ± 449 µm, *Cap2<sup>gt/gt</sup>* 1606 ± 372 µm; Day 10, WT 802 ± 247 µm, *Cap2<sup>gt/gt</sup>* 1376 ± 243 µm Day 10, p = 0.,033068501).



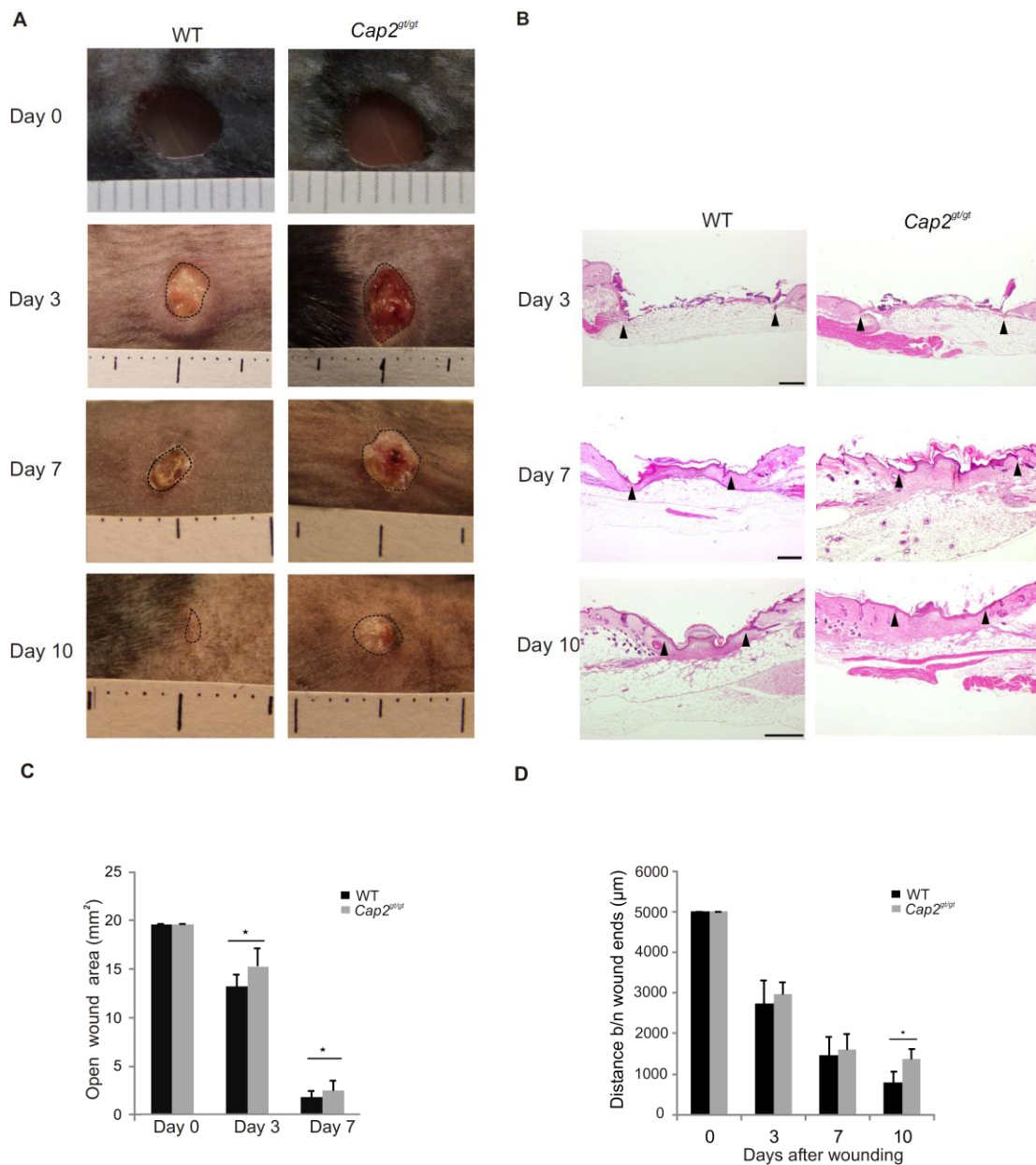


**Figure 3.8: Wound healing is altered in *Cap2*<sup>gt/gt</sup> mice.** A) Macroscopic photos of wounds from WT and *Cap2*<sup>gt/gt</sup> mice at day 0, 3, 7 and 10. The dotted black line indicates the wound area left open at each day. B) Skin sections of WT and *Cap2*<sup>gt/gt</sup> were stained with HE (day 3, 7 and 10). The position of the wound margins are indicated by arrows. In *Cap2*<sup>gt/gt</sup> mice, the wound closure was affected in contrast to WT. Scale bar, 250 µm. C) Graph showing progress in wound closure in WT and *Cap2*<sup>gt/gt</sup> mice. At each time point wounds from WT and *Cap2*<sup>gt/gt</sup> mice were analyzed and the open wound area was calculated from macroscopic observation. D) The distance between the wound margins during wound healing was measured. At day 10 the distance differs significantly in WT and *Cap2*<sup>gt/gt</sup> (4 mice per group and 3-6 sections per wound; \*p < 0.05).

### 3.5.3 Histological analysis with Masson's trichrome staining

The dermal architecture in mutant and in control mice was assessed by Masson's trichrome staining. Masson's staining dyes collagen fibers blue and keratin and muscle fibers red. We wanted to investigate the relation between the wound healing process and the deposition of dermal collagen at day 3, 7 and 10 post wounding. No significant difference was observed in collagen content (blue staining). Nevertheless, the hyperproliferative epithelium (red staining) was thinner and its formation was delayed in *Cap2<sup>gt/gt</sup>* mice (Fig. 3.9).

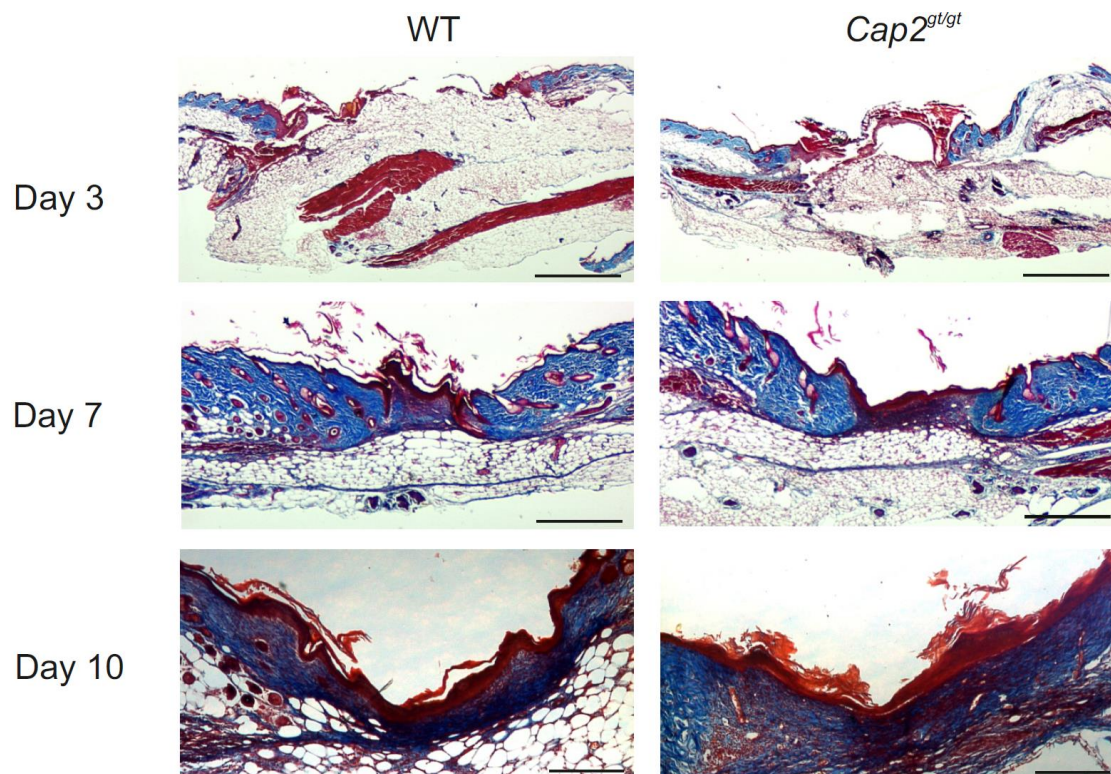


**Figure 3.9:** Masson's trichrome staining of the wounds revealed no significant difference in collagen content (blue) in mutant animals after wounding. Scale bars, 500 μm (day 3), 250 μm (day 7, 10).

#### 3.5.4 Proliferation is reduced in *Cap2<sup>gt/gt</sup>* mice

Keratinocyte migration and proliferation are crucial events for re-epithelialization of the wound and alterations in these processes might cause the delay in wound closure (Rashmi *et al.*, 2012). We assessed keratinocyte proliferation with the cell proliferation marker Ki-67. The Ki-67 antigen is a large nuclear protein (360 kDa) preferentially expressed during all active phases of the cell cycle ( $G_1$ , S,  $G_2$  and M phases), but absent in resting cells ( $G_0$ ) cells. More specifically, Ki-67 antigen is predominantly localized in the nucleolar cortex and in the dense fibrillar components of the nucleolus during interphase, whereas during mitosis it is relocated to the surface of chromosomes

(Isola *et al.*, 1990; Verheijen *et al.*, 1989). Quantification of data revealed a significant decrease in Ki-67 positive cells in *Cap2<sup>gt/gt</sup>* wounds compared to the WT wounds (Fig. 3.10 A, B) (Day 3, ratio Ki-67 positive / normal cells, WT  $0.622 \pm 0.1178$ , *Cap2<sup>gt/gt</sup>*  $0.369 \pm 0.1031$ , Day 3,  $p = 0.004463492$ ).

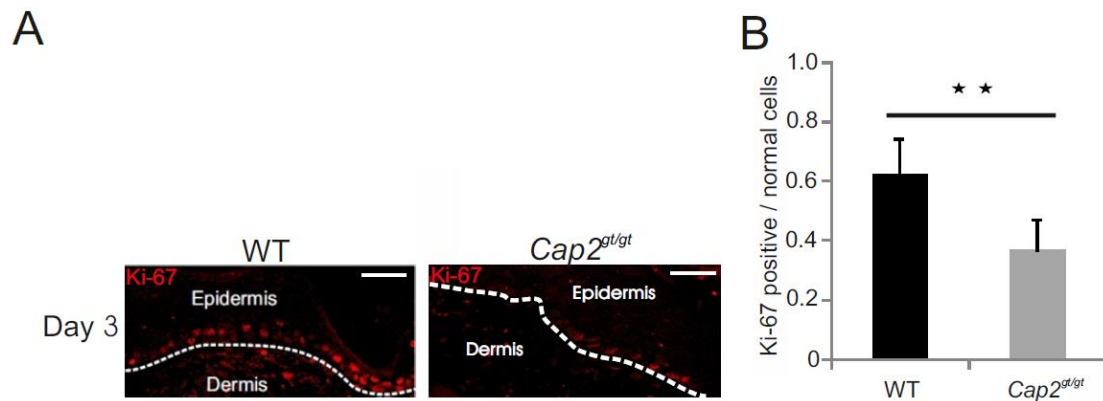


**Figure 3.10:** A) Sections from WT and *Cap2<sup>gt/gt</sup>* wounds were stained with a Ki-67 specific antibody as marker for keratinocyte proliferation. B) Quantification of the number of proliferating cells in *Cap2<sup>gt/gt</sup>* wounds showed reduced proliferation during wound re-epithelialization at day 3. Scale bar, 50  $\mu\text{m}$ ; \*\* $p < 0.01$ .

### 3.5.5 Delayed wound contraction in *Cap2<sup>gt/gt</sup>* mice

Restoration of the dermal matrix requires the migration and proliferation of fibroblasts and overlaps with re-epithelialization. Fibroblasts in the dermis synthesize extracellular matrix to strengthen the damaged tissue and subsequently to contract the granulation tissue. For wound contraction, the fibroblasts differentiate into specialized cells called myofibroblasts which are characterized by stress fibers containing  $\alpha$  smooth muscle actin ( $\alpha$ -SMA) (Hinz *et al.*, 2007; Blumbach *et al.*, 2010). In mammalian cells there are six actin isoforms: two cytoplasmic actin isoforms that are ubiquitously and highly expressed in non-muscle cells,  $\beta$ -actin and  $\gamma$ -actin, and four muscle actin isoforms that are named for their primary localization smooth muscle  $\alpha$ -actin ( $\alpha$ -SMA), smooth muscle  $\gamma$ -actin ( $\gamma$ -SMA), skeletal muscle  $\alpha$ -actin and cardiac muscle  $\alpha$ -actin (Herman, 1993). Increased expression of  $\alpha$ -SMA by itself is sufficient to increase stress fiber and focal adhesion assembly and increase generation of contractile force (Tomasek *et al.*, 2002; Hinz *et al.*, 2001). Furthermore, it makes up approximately 20% of the total actin found in myofibroblasts (Mitchell *et al.*, 1993).  $\alpha$ -SMA is commonly used as a marker of myofibroblast formation (Nagamoto *et al.*, 2000). When we investigated the expression of  $\alpha$ -SMA in the wounds of WT and *Cap2<sup>gt/gt</sup>* mice by immunofluorescence

analysis from day 7 onwards, a significantly lower intensity of  $\alpha$ -SMA staining per unit wound area in  $Cap2^{gt/gt}$  samples was observed indicating that fewer fibroblasts had differentiated into myofibroblasts than in WT which resulted in delayed wound contraction (Fig. 3.11 A, B) ( $\alpha$ -SMA intensity per unit area Day 7, WT  $59.67 \pm 17.25$ ,  $Cap2^{gt/gt}$   $33.54 \pm 14.54$ ,  $p=0.001868$ ).

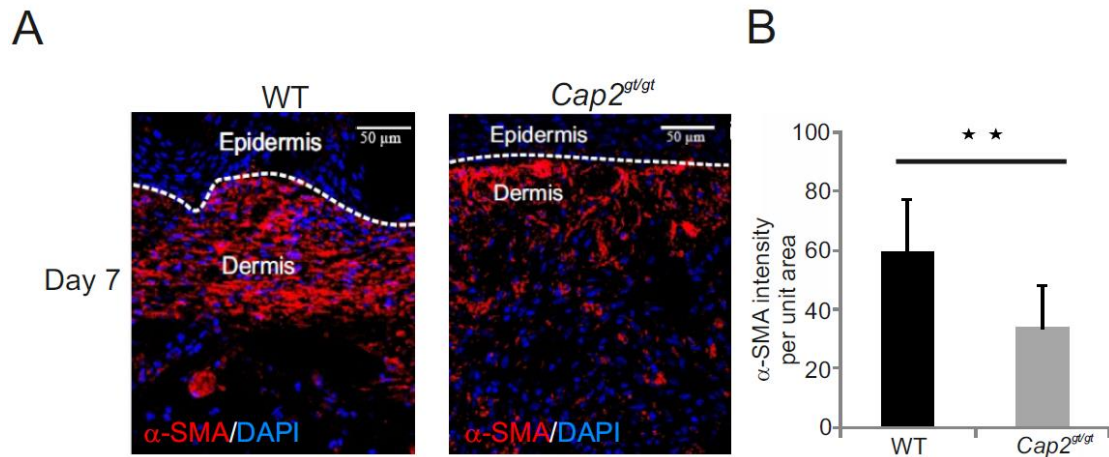


**Figure 3.11:** A) In WT and  $Cap2^{gt/gt}$  mice, differentiated myofibroblasts were identified by staining for  $\alpha$ -smooth muscle actin ( $\alpha$ -SMA) at day 7. B) Differentiation of fibroblasts into myofibroblasts appeared reduced during the wound healing process in  $Cap2^{gt/gt}$  mice. Scale bar, 50  $\mu$ m; \*\* $p < 0.01$ .

### 3.5.6 $Cap2^{gt/gt}$ mice show decreased macrophage infiltration

An important phase of the wound healing process is inflammation, which is followed by re-epithelialization. Once newly recruited monocytes migrate through the vessel wall, they release enzymes that fragment ECM proteins, which creates space for monocytes to migrate into the wound bed. Subsequently, in reaction to the micro-environment, monocytes differentiate into macrophages (Mahdavian Delavary *et al.*, 2011). Macrophage numbers increase during the phase of inflammation, peak during the phase of granulation tissue formation and decline during the maturation phase (Martin and Leibovich, 2005). Macrophages involved in clearance of cells or dead tissue undergo apoptosis. Macrophages that survive and do not undergo apoptosis, remain in the wound bed area and exert other functions that influence the wound healing process, like stimulation of collagen production, angiogenesis and re-epithelialization (Baum and Arpey, 2005). In case of pathogen spreading in the wound bed, macrophages phagocytose these pathogens and present antigens to T-cells. For all these tasks macrophages play a pivotal role in the transition of the inflammatory phase to the proliferative phase in which they coordinate and sustain the wound healing

events (Singer and Clark 1999). To investigate whether the infiltration of wounds by macrophages is affected by CAP2 deficiency, we analyzed macrophage infiltration by F4/80 staining. F4/80 is an extensively referenced membrane protein that is the best known marker for mature mouse macrophages and blood monocytes. We found less macrophage infiltration at day 3 relative to the WT wounds (Fig. 3.12). Scale bar, 50  $\mu\text{m}$ ; \*\* $p < 0.01$ . A, B) (F4/80 intensity per unit area, WT  $21.6 \pm 7.899$ ,  $Cap2^{gt/gt}$   $13.1 \pm 5.462$ , Day 3,  $p = 0.044839061$ ). Although at day 7 we observed a slight increase in macrophage infiltration in  $Cap2^{gt/gt}$  wounds, it was not significant.

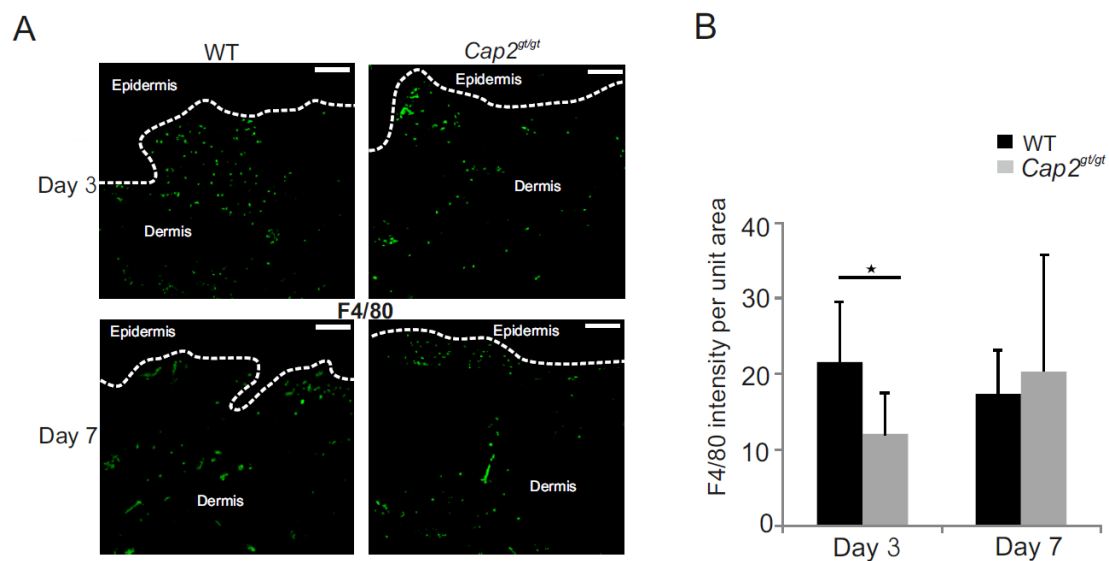


**Figure 3.12:** A) Analysis of macrophage infiltration using F4/80 antibody, a macrophage specific marker. B) Significant reduction in F4/80 positive macrophages in mutant animals infiltrating during wound healing process at day 3. Scale bar, 50  $\mu\text{m}$ ; \* $p < 0.05$ .

### 3.5.7 Slower neovascularization in $Cap2^{gt/gt}$ mice

During the proliferative phase, macrophages stimulate proliferation of connective, epithelial and endothelial tissue directly and indirectly. Especially fibroblasts, keratinocytes and endothelial cells are stimulated by macrophages during this phase to induce and complete ECM formation, reepithelialization and neovascularization (Mahdavian Delavary *et al.*, 2011) Neovascularization is a key event during wound healing in which the functional microvascular networks develop. During this phase, angiogenic capillary sprouts invade the fibrin/ fibronectin/ vitronectin-rich wound clot and within a few days organize into a microvascular network throughout the granulation tissue. As collagen accumulates in the granulation tissue to produce the scar, the density of blood vessels diminishes. A dynamic interaction occurs among endothelial cells, angiogenic cytokines, such as FGF, VEGF, TGF- $\beta$ , angiopoietin, and

mast cell tryptase, and the extracellular matrix (ECM) environment (Tonnesen *et al.*, 2000). Since it has been previously reported that actin and actin binding proteins can play a key role in the morphogenesis and migration of endothelial cells in wounded blood vessels (Nowak *et al.*, 2009), sections were stained with anti CD31 antibody, a specific marker for endothelial cells, to evaluate neovascularization upon CAP2 loss in wounds. Cluster of differentiation 31 (CD31) also known as platelet endothelial cell adhesion molecule (PECAM-1) is a cell adhesion molecule that is required for leukocyte transendothelial migration (TEM) under most inflammatory conditions. Besides, CD31 is expressed on platelets and leukocytes and is primarily concentrated at the borders between endothelial cells. We found that at day 3 there were less CD31 positive cells which could contribute to neovascularization while at day 7 we did not find any significant difference between mutant and WT wounds. (Fig. 3.13 A, B) (CD31 intensity per unit area, Day 3, WT  $32.134 \pm 11.565$ ,  $Cap2^{gt/gt}$   $17.576 \pm 2.607$ ; Day 7, WT  $36.73 \pm 14.562$ ,  $Cap2^{gt/gt}$   $38.35 \pm 17.171$  Day 3,  $p = 0,0000910011$ ).

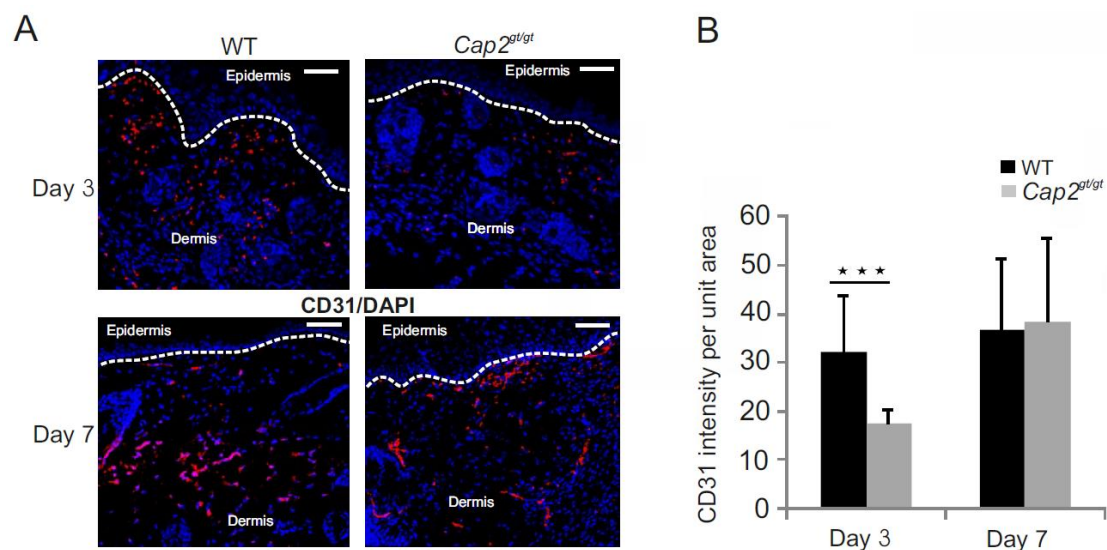


**Figure 3.13:** A) Immunofluorescence analysis with CD31, an endothelial cell specific marker, revealed reduction in the number of positive cells at day 3 post wounding in  $Cap2^{gt/gt}$ . B) Graph depicting the CD31 intensity per unit area at day 3 and 7 post wounding in  $Cap2^{gt/gt}$  and WT wounds. Scale bar, 50  $\mu$ m; \*\*\* $p < 0.001$ .

### 3.5.8 Increase in apoptosis in $Cap2^{gt/gt}$ wounds

Specific cell populations are rapidly increased during the wound healing process that contribute to repair, deposition of new matrices and, finally, maturation of the wound. Upon completing their tasks, prior to the progression to the next phase of healing, these specific cell types must be eliminated from the wound (Greenhalgh, 1998). There is ample evidence that apoptosis is involved in the resolution of the various phases of

tissue repair. The most logical method of cellular down-regulation is through apoptosis. Apoptosis allows for the eliminations of entire cell populations without causing an excessive inflammatory response. In the inflammatory phase of tissue repair, inflammatory cells undergo apoptosis 12 h after wounding (Brown *et al.*, 1997). We also analyzed apoptosis in *Cap2<sup>gt/gt</sup>* wounds with Caspase 3 antibodies. Caspase 3 is the most extensively studied apoptotic protein. It is synthesized as an inactive proenzyme (32 kDa) that is processed in cells undergoing apoptosis by autoproteolysis and/or cleavage by other upstream proteases like caspases 8, 9, and 10. The processed form of caspase 3 consists of large (17 kDa) and small (12 kDa) subunits which associate to form an active enzyme. The active caspase 3 proteolytically cleaves and activates caspases 6 and 7. We found that there was an increase in apoptosis in mutant wounds when compared with WT wounds at day 3 and day 7, (Fig. 3.14 A, B) (ratio apoptotic / no apoptotic cells per unit area, Day 3, WT  $0.0102 \pm 0.00507$ , *Cap2<sup>gt/gt</sup>*  $0.0245 \pm 0.00907$ ; Day 7, WT  $0.0054 \pm 0.00181$ , *Cap2<sup>gt/gt</sup>*  $0.0172 \pm 0.003701$  Day 3,  $p = 0.044347932$ ; Day 7,  $p = 0.000772651$ ).

From these observations it is clear that lack of CAP2 has an effect on macrophage infiltration, neovascularization and apoptosis during wound healing.

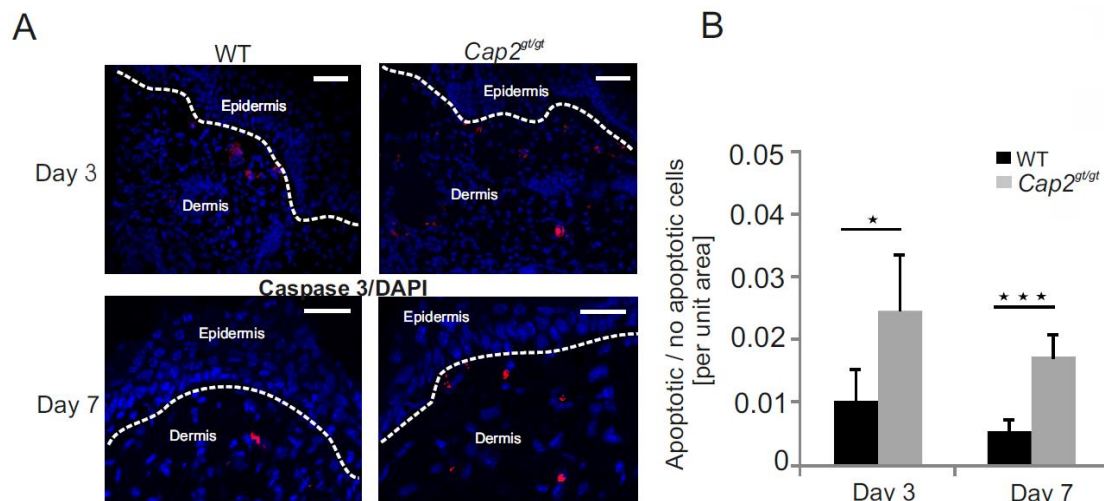


**Figure 3.14:** A) Increased apoptosis in mutant mice visualized by cleaved caspase 3 immunofluorescence at day 3 and 7 post wounding. B) Ratio of apoptotic / no apoptotic cells per unit area at day 3 and 7 post wounding. Scale bar, 50  $\mu\text{m}$ ; \* $p < 0.05$ , \*\*\* $p < 0.001$ .

### 3.6 Cell migration defects in *Cap2<sup>gt/gt</sup>* fibroblasts

#### 3.6.1 *Cap2<sup>gt/gt</sup>* fibroblasts show reduced velocity

To ask whether altered fibroblast migration contributed to the wound healing defect we analyzed the migratory behavior of primary fibroblasts. WT and *Cap2<sup>gt/gt</sup>* fibroblasts were isolated and cultured. Immunocytochemistry and western blot analysis were performed to ensure the loss of CAP2 (Fig. 3.15 A, B).

To monitor the speed and migratory properties of primary fibroblasts from mutant animals we performed scratch assays using monolayers of WT and *Cap2<sup>gt/gt</sup>* fibroblasts. Pictures were taken at different time points using time lapse video microscopy. We found that the gap in WT cells had closed completely 20 hours after it was introduced, whereas the one in the *Cap2<sup>gt/gt</sup>* had closed only marginally after the same time (Fig. 3.15 C) Also, *Cap2<sup>gt/gt</sup>* cells had a significantly decreased cell speed compared to control cells as revealed by quantification of the speed of migration (Fig. 3.15 D) (WT  $0.35 \pm 0.05 \mu\text{m}/\text{min}$ , *Cap2<sup>gt/gt</sup>*  $0.29 \pm 0.03 \mu\text{m}/\text{min}$ ;  $p = 0.004438$ ).

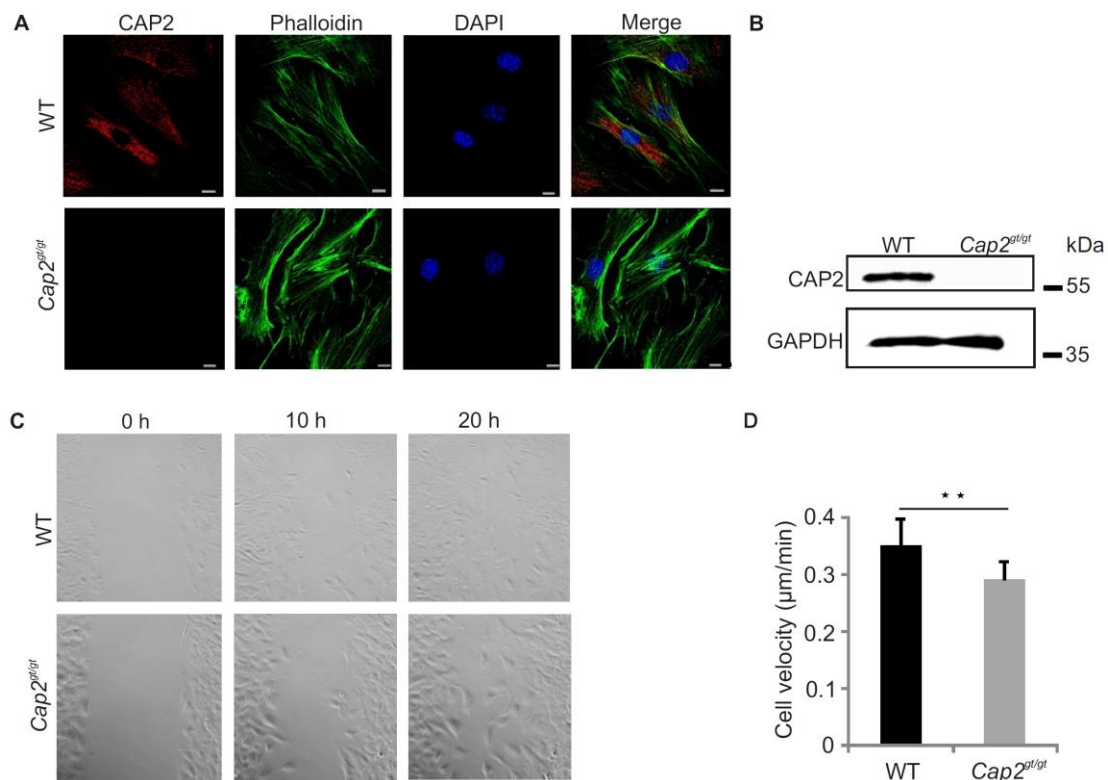


**Figure 3.15: Analysis of primary *Cap2<sup>gt/gt</sup>* and WT fibroblasts.** A) Fibroblasts were fixed and stained with mAb K82–381-1 for detection of CAP2. Mutant fibroblasts showed no CAP2 staining. FITC Phalloidin was used to visualize F-actin, DAPI for nuclei. Scale bar, 10  $\mu\text{m}$ . B) Complete deletion of CAP2 was also confirmed by western blot analysis using polyclonal CAP2 antibodies. GAPDH was used as a loading control. C) Scratch assays revealed a migration defect in *Cap2<sup>gt/gt</sup>* primary fibroblasts. Wound closure was followed by live cell microscopy (0 to 20 h after scratching). D) Speed of migration for WT and *Cap2<sup>gt/gt</sup>* fibroblasts was determined in  $\mu\text{m}/\text{min}$  (\*\* $p < 0.01$ ;  $n = 100$  cells, per cell type).



### 3.6.2 *Cap2<sup>gt/gt</sup>* fibroblasts develop long filopodia

Actin rearrangement plays an important role in cell polarity, migration, and differentiation. The determining factor for these processes is the dynamic rearrangement of the actin cytoskeleton. Motility is initiated by formation of an F-actin-dependent protrusion at the leading edge. These protrusive structures called lamellipodia and filopodia contain actin filaments, which are elongated at the plasma membrane near site (Mattila and Lappalainen, 2008). To analyze this, we performed phalloidin staining on primary fibroblasts (Fig. 3.16 A). Although the fibroblasts of both WT and *Cap2<sup>gt/gt</sup>* genotypes showed a flat morphology with protrusive edges, we observed a higher number of cells that had long extensions (arrow in Fig. 3.16 A) in cells lacking CAP2 as compared to wild type fibroblasts (Fig. 3.16 B) (WT 85.5%  $\pm$  0.5%, *Cap2<sup>gt/gt</sup>* 79%  $\pm$  2%;  $p = 0.024515$ ).

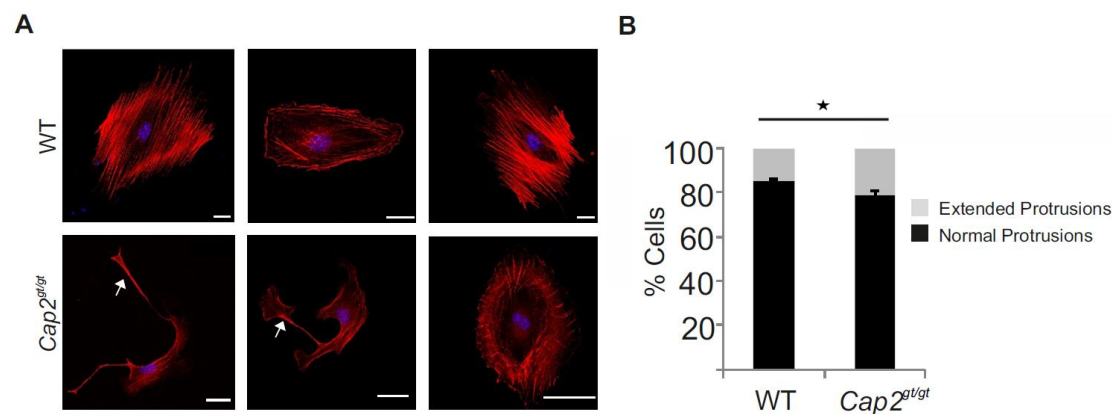


**Figure 3.16:** A) Fibroblasts were fixed, permeabilized and incubated with TRITC-Phalloidin to stain F-actin. Increased numbers of extended protrusions (indicated by arrows) were observed in *Cap2<sup>gt/gt</sup>* cells. B) The graph depicts the percentage of extended protrusions as visualized by F-actin staining in WT and *Cap2<sup>gt/gt</sup>* fibroblasts (n= 185 cells per cell type, \* $p < 0.05$ ). Scale bars, WT, 20  $\mu\text{m}$ ; *Cap2<sup>gt/gt</sup>*, 50  $\mu\text{m}$ .

### 3.6.3 Focal adhesions are altered in *Cap2<sup>gt/gt</sup>* fibroblast

Since altered cell migration is often associated with altered cell adhesion properties, we investigated the effects of CAP2 deletion on the formation and size of focal adhesions. Cell adhesion contributes substantially to the maintenance of tissue structure, the promotion of cell migration, and the transduction of information about the microenvironment of the cell. Focal adhesions are large macromolecular assemblies through which both mechanical force and regulatory signals are transmitted (Chen *et al.*, 2003). They are organized at the basal surface of cells and physically connect the extracellular matrix to the cytoskeleton and have long been speculated to mediate cell

migration. Vinculin is an essential and highly conserved cell adhesion protein found at both focal adhesions and adherens junctions where it couples integrins or cadherins to the actin cytoskeleton. It is involved in controlling cell shape, motility, and cell survival, and also plays a role in force transduction (Shen *et al.*, 2011). Moreover, expression of vinculin lacking the carboxyl terminus that bundles actin filaments in vinculin knock-out murine embryonic fibroblasts affects the number of focal adhesions formed, cell spreading as well as cellular stiffening in response to mechanical force (Shen *et al.*, 2011).

To visualize focal adhesions we used mAbs specific for vinculin and stained cells 12 h post trypsinization. Immunofluorescence analysis revealed that *Cap2<sup>gt/gt</sup>* cells had more focal adhesions than WT (Fig. 3.17 A, B) (Focal adhesions per cell, WT,  $72 \pm 28$ , *Cap2<sup>gt/gt</sup>*,  $102 \pm 30$ ,  $p = 0.00000000947434$ ). To evaluate the development of focal adhesions upon seeding, we stained the WT and mutant fibroblasts at several time points for vinculin. We found that WT and mutant fibroblasts attached to the substratum and adhesion increased progressively as revealed by vinculin staining. Interestingly, we observed that at 40 minutes post seeding mutant fibroblasts were flatter and started to develop focal adhesions, whereas for WT this process occurred at 90 minutes. Mutant fibroblasts exhibited at every time point a larger area of spreading on the substratum than WT (Fig. 3.17 C).

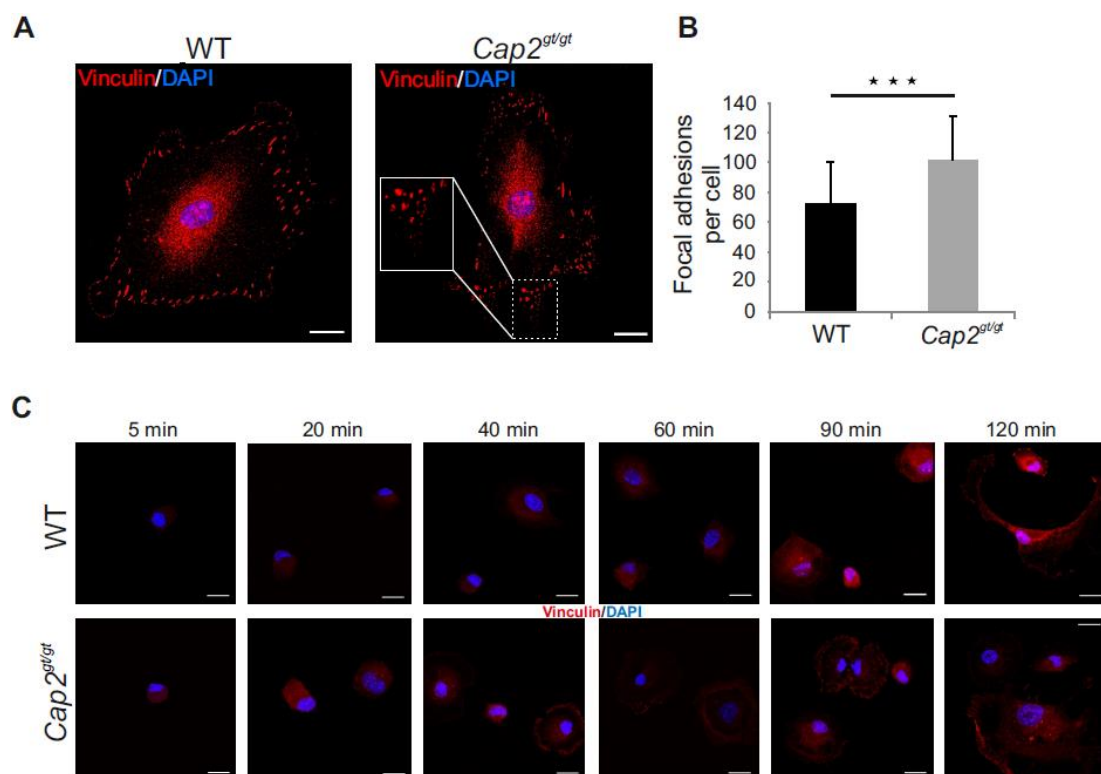


**Figure 3.17: Formation of focal adhesions in control and *Cap2<sup>gt/gt</sup>* primary fibroblasts.** A) Fibroblasts were trypsinized and plated and focal adhesion formation was assessed after 12 h by staining with mAb specific for vinculin; DAPI stained the nuclei. B) Quantification of focal adhesions per cell. Graph shows increased number of focal adhesions in *Cap2<sup>gt/gt</sup>* fibroblasts compared to WT (3 independent experiments;  $p \ll 0.001$ ;  $n = 40$  cells per cell type). C) Vinculin staining of WT and *Cap2<sup>gt/gt</sup>* fibroblasts showed that mutant cells were faster in adherence upon seeding compared to WT. Scale bar, 20  $\mu\text{m}$ .

#### 3.6.4 G-/F-actin ratio is altered in *Cap2<sup>gt/gt</sup>* fibroblasts

We next studied the F-actin distribution during progressive attachment. We observed that mutant fibroblasts were faster in spreading and in rearrangement of the F-actin cytoskeleton visualized through FITC-phalloidin (Fig. 3.18 A). We excluded that this was due to a reduction of the total actin content in mutant fibroblasts as in western blot analysis we did not observe a change in the total actin content in mutant fibroblasts when compared with WT fibroblasts (Fig. 3.18 B). The G/F-actin ratio at the cellular level is very crucial for actin dynamics and since CAP2 is a G-actin regulating protein, we performed G/F actin determination and found an increased F-actin content in mutant fibroblasts when compared to WT (Fig. 3.18 C) (G/F actin ratio, WT, 1, *Cap2<sup>gt/gt</sup>*,  $0.807026 \pm 0.097046$ ,  $p = 0.000459$ ). This points at a differential actin regulation upon loss of CAP2. Thus, ablation of CAP2 results in increased focal adhesion, rapid development of focal adhesions, rapid rearrangement of the F-actin cytoskeleton and increased F-actin content whereas the total actin content was unaltered.

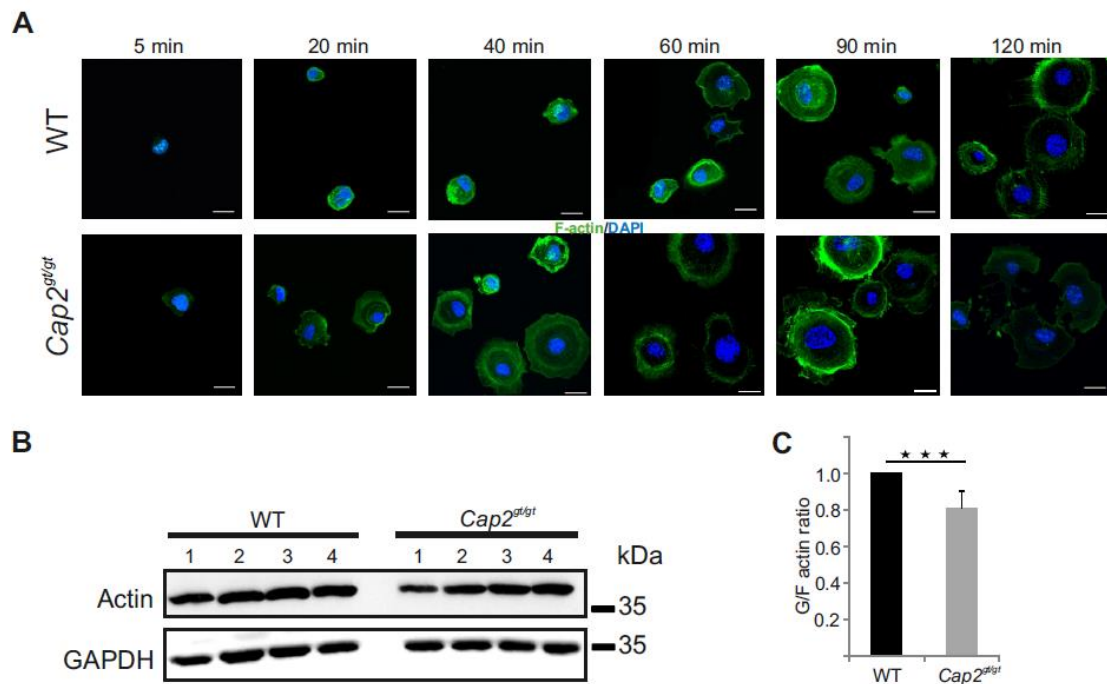


**Figure 3.18:** A) F-actin organization is altered in mutant cells as visualized by phalloidin staining at different time points after seeding. Scale bar, 20  $\mu$ m. B) Total actin content was determined using anti-actin antibodies. Total actin remains unaltered in *Cap2<sup>gt/gt</sup>* fibroblasts compared to WT (n=4). C) Quantification of G/F actin level in cultured primary fibroblasts showing significant increase in F-actin levels (n= 4 experiments). Scale bar, 20  $\mu$ m; \*\*\*p< 0.001.

### 3.6.5 Recovery of the actin cytoskeleton is faster in mutant fibroblasts

To study the dynamics of the actin cytoskeleton in CAP2 deficient cells we followed F-actin reorganization after disruption by latrunculin B. Latrunculin B binds monomeric actin with 1:1 stoichiometry and can be used to block actin polymerization both in vitro and in cells and is 10 to 100-fold more potent than cytochalasin (Wakatsuki *et al.*, 2001). However, latrunculin B is gradually inactivated by serum so that induced changes are transient in the continued presence of the compound. Untreated cells have an intact actin cytoskeleton, and stress fibers extend throughout the cells. WT and mutant primary fibroblasts were treated with latrunculin B at a concentration of 2.5  $\mu$ M for 30 minutes which led to complete disruption of the F-actin network (Fig. 3.19 A). Thereafter, we performed latrunculin B washout and allowed the cells to recover in normal media. We observed a faster reformation of F-actin in mutant cells and the cortical cytoskeleton was seen already at the 10 minutes time point of post recovery. For WT control fibroblast this stage was observed at 30 minutes post recovery. However, we noted a disturbed development of actin stress fibers in mutant fibroblast when compared to WT control cells. Additionally we noticed more

extended protrusions with increased cell-surface contacts (Fig. 3.19 B) (% of cells with extended protrusions, 10 min, WT  $23 \pm 1.414$ , *Cap2*<sup>gt/gt</sup>  $41 \pm 1.414$ , 20 min, WT  $30 \pm 1.414$ , *Cap2*<sup>gt/gt</sup>  $43 \pm 1.767$ , 10 min,  $p = 0.006116$ ; 20 min,  $p = 0.044144$ ). This was reminiscent of the observation that mutant fibroblasts had formed increased focal adhesions as visualized with vinculin staining (Fig. 3.17 A, B). It clearly indicates an alteration and deregulation of the actin cytoskeleton upon latrunculin B washout. This part of work was done with Atul Kumar.

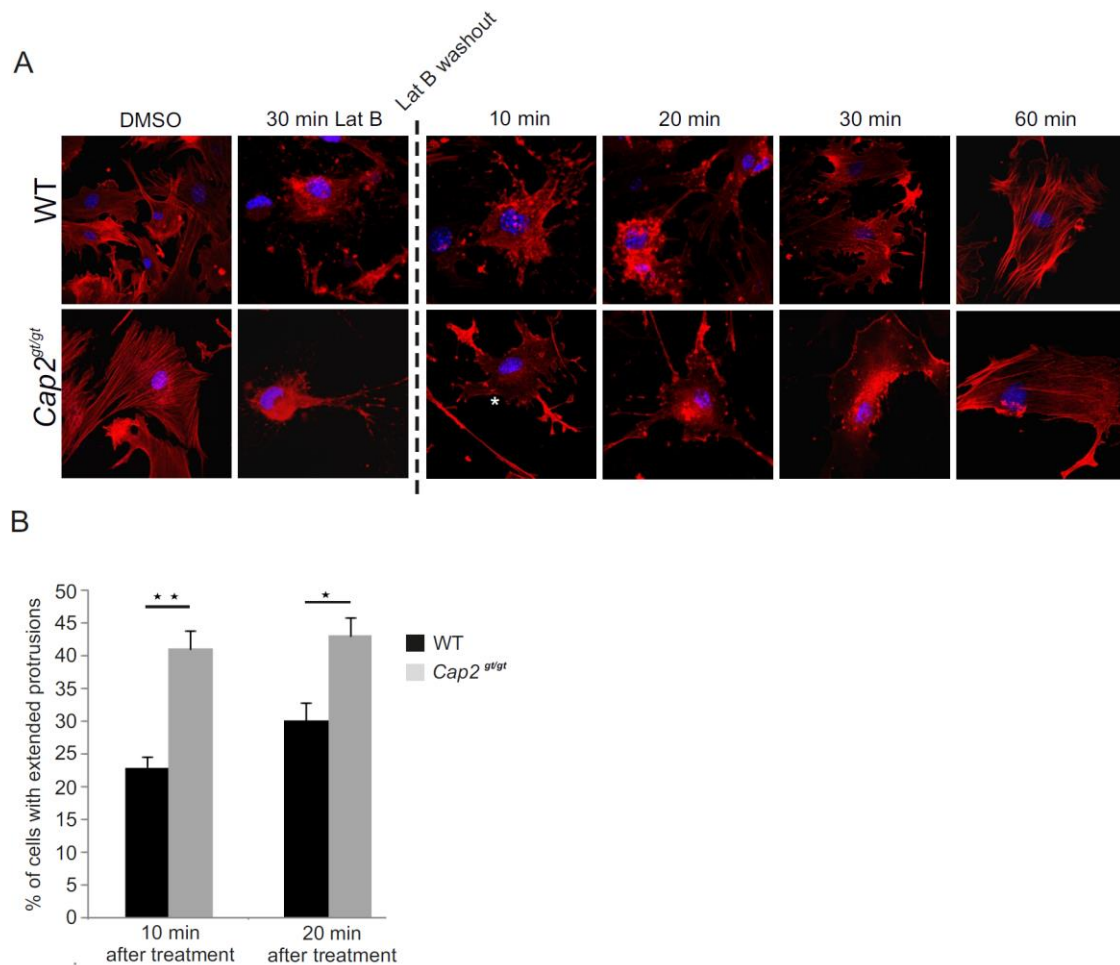


**Figure 3.19: Reformation of the actin cytoskeleton upon disruption with latrunculin B is altered in *Cap2*<sup>gt/gt</sup> fibroblasts.** A) WT and mutant fibroblasts were treated with latrunculin B (Lat B, 2.5  $\mu$ M) for 30 minutes. After washed out they were analyzed at different time points. F-actin was visualized by TRITC-phalloidin, nuclei were stained with DAPI. B) Quantification of the cells that developed long protrusions with increased cell surface contacts upon drug treatment and subsequent washout in mutant and WT fibroblasts. Significant increase was observed in mutant fibroblasts. \* $p < 0.05$ , \*\* $p < 0.01$ .

### 3.7 Identification of CAP2 interacting partners

To further analyse the CAP2 function, we tried to identify interacting partners of CAP2. N-CAP2 and C-CAP2 domains were produced as GST fusion proteins in *E. coli* (Fig. 3.20 A) and purified by single-step batch binding to glutathione-Sepharose 4B beads. The quality and quantity of the purified fusion proteins were assessed by Coomassie blue staining (Fig. 3.20 B), and pull down assays were performed using lysates from PAM212 cells and lysates from cardiac muscle. Bound proteins were eluted by boiling, resolved by SDS-PAGE and detected with Coomassie Blue staining. After 3 repetitions the bands were sent for LC-MS (mass spectrometry). Identified proteins are shown in Table 3.3.

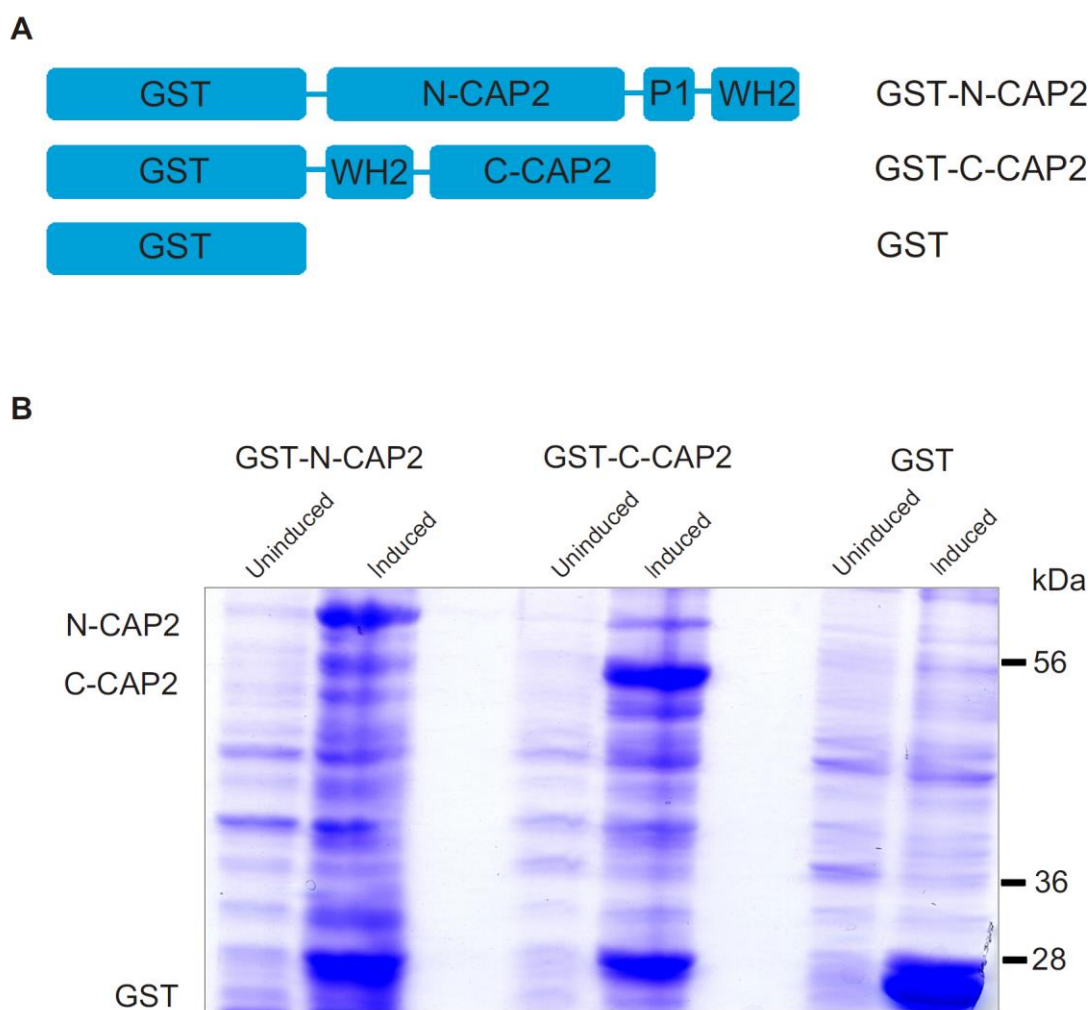


**Figure 3.20:** A) Schematic representation of CAP2 polypeptides fused to GST that were used in pull down experiments. B) The GST fusion proteins were produced in *E. coli* after induction with IPTG. Proteins of whole cell lysates were resolved by SDS-PAGE (x% acrylamide) and stained with Coomassie Blue. GST-N-CAP2 uninduced; GST-N-CAP2 induced sample; GST-C-CAP2 uninduced; GST-C-CAP2 induced sample; GST uninduced; GST induced sample. GST-fusion protein induction was with 0.75 mM IPTG.

**Table 3.3:** Proteins identified after pull down experiments using GST-N-CAP2 or GST-C-CAP2 as a bait and Pam212 cells extract or mouse cardiac muscle extract.

Pam212 cells		Cardiac muscle extract
N-CAP2	CAP2	CAP2
	Myosin 9	Carnitine O-palmitoyltransferase 1, muscle isoform
	Keratin ,Type I cytoskeletal 10	Trifunctional enzyme subunit alpha, mitochondrial
	Keratin ,Type I cytoskeletal 15	NADH- ubiquinone oxidoreductase 75 kDa subunit , mitochondrial
	Keratin ,Type II cytoskeletal 73	Long-chain-fatty-acid-CoA ligase 1
	Keratin ,Type II cytoskeletal 1	78 kDa glucose-regulated protein
	Keratin ,Type II cytoskeletal 8	Keratin ,Type I cytoskeletal 10
	Keratin ,Type II cytoskeletal 6A	Zinc transporter 1
	Zinc transporter 1	
	Loss of heterozygosity 12 chromosomal region 1 protein homolog	
	Pre-mRNA-processing-splicing factor 8	
C-CAP2	CAP2	CAP2
	Keratin ,Type II cytoskeletal 1	Myosin 6
	Keratin ,Type I cytoskeletal 10	Keratin ,Type II cytoskeletal 1
	Keratin ,Type II cytoskeletal 8	Keratin ,Type II cytoskeletal 8

Keratin ,Type II cytoskeletal 79	Cullin-associated NEDD8-dissociated protein 2
Keratin ,Type II cytoskeletal 6A	Heterogeneous nuclear ribonucleoprotein U
Myb-binding protein 1A	Keratin ,Type I cytoskeletal 10
Keratin ,Type II cytoskeletal 2 oral	Keratin ,Type II cytoskeletal 5
Zinc transporter 1	Keratin ,Type II cytoskeletal 79
Loss of heterozygosity 12 chromosomal region 1 protein homolog	Heat shock-related 70 kDa protein 2
UPF0415 protein C7orf25 homolog	Zinc transporter 1
Serine/threonine-protein kinase PLK4	Pyruvate carboxylase, mitochondrial
ATP synthase lipid-binding protein, mitochondrial	Proline-rich membrane anchor 1
U3 small nucleolar RNA-associated protein 6 homolog	Aldehyde dehydrogenase, mitochondrial precursor
	Loss of heterozygosity 12 chromosomal region 1 protein homolog
	Arf-GAP with SH3 domain, ANK repeat and PH domain protein 2
	Matrin 3
	Prostate tumor overexpressed gene 1 protein homolog
	Ubiquitin fusion degradation protein 1 homolog
	Uncharacterized protein KIAA0564 homolog
	Keratin ,Type II cytoskeletal 2 epidermal
	Keratin ,Type II cytoskeletal 6A
	Myosin 7
	Sarcoplasmic/endoplasmic reticulum ATPase 2
	UPF0415 protein C7orf25 homolog



ATP synthase lipid-binding protein, mitochondrial

U3 small nucleolar RNA-associated protein 6 homolog

The identified proteins that were pulled down can be categorized in 5 groups: intermediate filaments (keratins), splicing factors (Pre-mRNA-processing-splicing factor 8, U3 small nucleolar RNA-associated protein 6 homolog), motor proteins (myosins), heat shock proteins (Hsp70), membrane associated enzymes (Sarcoplasmic/endoplasmic reticulum ATPase2, ATP synthase, long-chain-fatty-acid-CoA ligase 1, Carnitine O-palmitoyltransferase 1, muscle isoform).

It is known that CAP1 has a role in apoptosis through translocating to mitochondria during early stages of apoptosis (Wang *et al.*, 2008). To test whether this is also the case for CAP2, we focused our studies on the interaction between CAP2 and the mitochondrial enzyme Carnitine O-palmitoyltransferase 1 (CPT1). CPT1 is a mitochondrial enzyme responsible for the formation of acyl carnitines by catalyzing the transfer of the acyl group of a long-chain fatty acyl-CoA from coenzyme A to l-carnitine. CPT1B is a key enzyme in the regulation of skeletal muscle mitochondrial  $\beta$ -oxidation of long-chain fatty acids. This enzyme is associated with the outer mitochondrial membrane and is required for the transport of long-chain fatty acyl-CoAs from the cytoplasm into mitochondria (McGarry *et al.*, 1978, Ramsay *et al.*, 2001). Its inhibition results in the accumulation of long-chain fatty acids (Dhe-Paganon *et al.*, 2002).

### 3.7.1 CAP2 interacts with CPT1B

In pull down experiments Carnitine O-palmitoyltransferase 1 (CPT1B) was identified when GST tagged N-CAP2 immobilized on glutathione-Sepharose 4B was incubated with cardiac tissue lysate (Table 3.3). CPT1B FL was cloned into pCMV-3Tag Flag-6 and transfected in COS-7 cells (Fig 3.21 B). GST-N-CAP2 was bound to glutathione Sepharose beads and then incubated overnight with lysates from COS-7 transfected with FLAG-tagged CPT1B. The pull-down complex was washed and the bound protein was analysed on polyacrylamide SDS gels and western blots which were probed with anti-Flag antibodies (Sigma). That verified that CPT1B interacts with CAP2. Ponceau staining was used for checking equal loading (Fig. 3.21 C). In

addition, we also performed immunofluorescence analysis which revealed colocalization of GFP tagged CAP2 with Flag tagged CPT1B (Fig. 3.21 A).

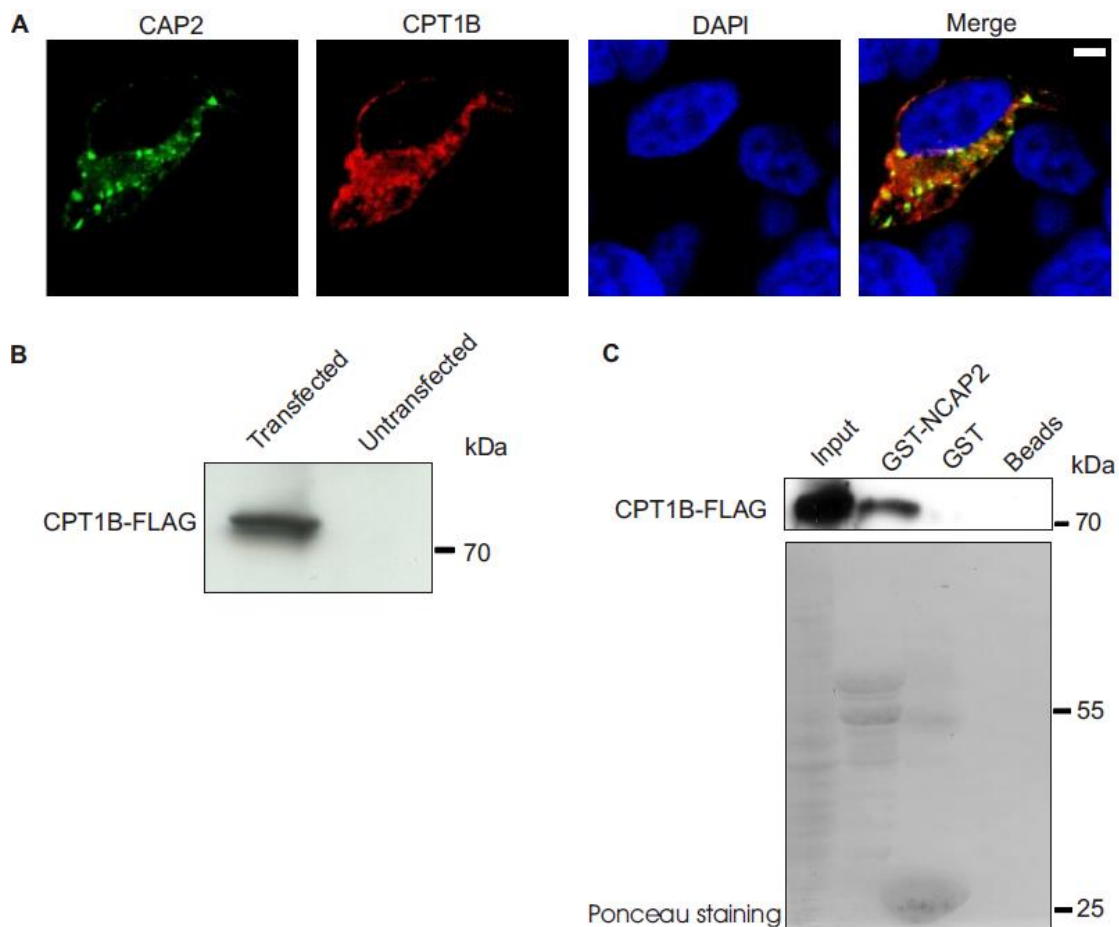


**Figure 3.21: CAP2 interacts with CPT1B.** A) Co-localization of GFP-CAP2 and FLAG-CPT1B. HEK293 cells were co-transfected with GFP-CAP2 and FLAG-CPT1B and analysed after 24 h. Immunofluorescence was performed with anti-FLAG antibodies and Alexa 568 conjugated secondary antibodies and DAPI. Scale bar, 4  $\mu$ m. B) Homogenates of COS7 cells and COS7 cells transfected with Flag tagged CPT1B were separated by SDS PAGE (10% acrylamide). The blot was probed with polyclonal antibodies against FLAG (1:500) followed by chemiluminescence. C) GST and GST-N-CAP2 proteins were expressed in *E. coli* BL21 and immobilized on glutathione-Sepharose 4B. The beads were then incubated with COS7 whole cell extracts expressing FLAG-tagged CPT1B and the pulled down protein was identified by western blot analysis using anti-Flag antibodies, Ponceau staining showed the expression of GST-N-CAP2 and GST proteins that were used in the pull down experiment.

### 3.8 CAP in cancer

It has been reported previously that CAP1 is overexpressed in pancreatic cancers (Yamasaki *et al.*, 2009) and CAP2 is highly upregulated in hepatocellular carcinoma, which is associated with chronic liver disease (Shibata *et al.*, 2006). In addition, at the

RNA level CAP2 is highly upregulated in bladder, colon, thyroid and kidney tumor (Peche *et al.*, 2007).

Here we studied CAP1 and CAP2 abundance at the protein level in breast, stomach and kidney tumor. Patient samples were obtained from the Institute for Pathology, Medical Faculty, University of Cologne. Equal amount of tissue was lysed in tissue lysis buffer. Proteins were separated by SDS PAGE and western blot analysis was performed using CAP1 and CAP2 specific antibodies. We observed that CAP1 is upregulated in breast and kidney cancer (Fig. 3.22 A) and CAP2 is upregulated in breast cancer (Fig. 3.22 B). Ponceau staining confirmed equal loading.

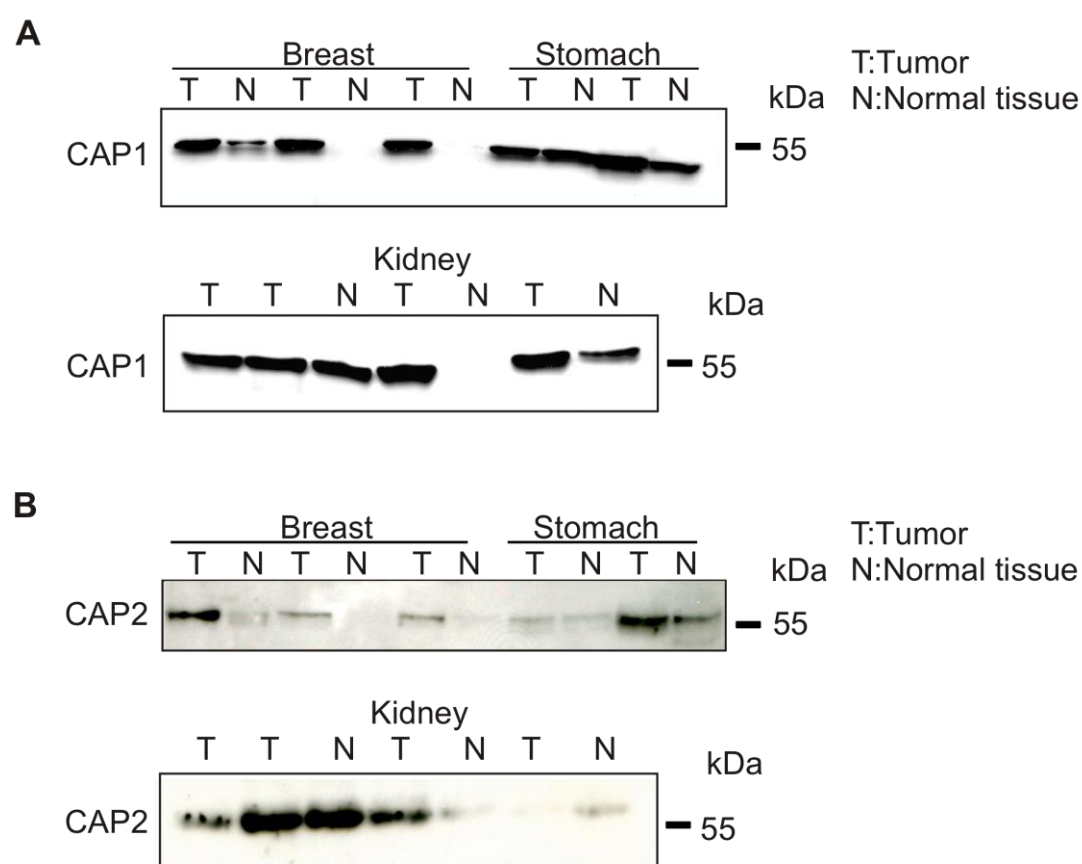


**Figure 3.22:** Proteins from cancer and normal tissue lysates were separated by SDS PAGE (10% acrylamide) and the blots were incubated with polyclonal CAP1 (A) and polyclonal CAP2 specific antibodies (B), respectively. T: Tumor, N: Normal tissue.

## 4. Discussion

All cells can respond to environmental signals by a redistribution of the actin cytoskeleton. Rearrangement of the actin cytoskeleton is critical for fundamental cell biological events like division, growth, and locomotion. Modulation of actin filament turnover and treadmilling play a pivotal role in these highly dynamic processes. The actin cytoskeletal dynamics involve a plethora of actin-binding proteins. These include regulatory proteins for nucleation, depolymerization, severing, capping and sequestration that can explain the basic mechanism of persistent actin filament turnover within cells. The cycling between actin polymerization and depolymerization is influenced by the concentration of G-actin in the cell, which fluctuates between 50 and 200  $\mu\text{M}$ . Paradoxically, once the concentration of G-actin rises above 0.1  $\mu\text{M}$ , which is considered as the critical concentration, polymerization into F-actin occurs and proceeds until the G-actin concentration once again reaches 0.1  $\mu\text{M}$ . (Carlier and Pantaloni, 1997). Actin sequestering factors can either enhance polymerization or disassemble F-actin (Hubberstey and Mottillo, 2002). Examples of G-actin binding proteins include Wiskott-Aldrich syndrome protein (WASp) (Zigmond, 2000),  $\beta$ -thymosins (Carlier and Pantaloni, 1994), profilin (Sohn and Goldschmidt-Clermont, 1994) and cyclase-associated proteins (CAPs).

### 4.1 CAP2 in the cardiovascular system and in skeletal muscle

A role for CAP2 in the cardiovascular system was also revealed in zebrafish. The zebrafish CAP2 sequence is 60% identical to human CAP2 and shares 77 % homology in the C-terminal actin-binding domain, and 58% in the N-terminal cyclase-binding domain. CAP2 expression was observed during zebrafish development and was preferentially expressed in the skeletal muscle and heart. The role of CAP2 was further investigated by using knockdown using two different morpholinos against CAP2 that resulted in a short-body morphant zebrafish phenotype with pericardial edema. Pericardial effusion ("fluid around the heart") is an abnormal accumulation of fluid in the pericardial cavity. Because of the limited amount of space in the pericardial cavity, fluid accumulation leads to an increased intrapericardial pressure which can negatively affect heart function (Effendi *et al.*, 2013).

The heart relies on a complex network of cardiomyocytes, endothelial, vascular smooth muscle cells, fibroblasts and immune cells to maintain appropriate function. Gap junctions electrochemically coordinate the contraction of individual cardiomyocytes, and their connection to the extracellular matrix (ECM) transduces force and coordinates the overall contraction of the heart.

Dilated cardiomyopathy is characterized by structural abnormalities that affect myocardial activation and mechanical contraction (Katz, 1990). We found a drastic reduction in the basal heart rate in the mutant mice that might point towards a pathological involvement of sinus node function. CAP2 expression at high levels in all major sites of the heart points to a general role of CAP2 in the physiology of the cardiac system. Young *Cap2<sup>8t/8t</sup>* mice exhibit DCM, thinning of ventricular wall, atrial dilation, and structural cardiac defects. Later on, with ageing, the whole heart is severely affected, leading to the dilation of all four chamber of the heart.

The sarcomere consists of the Z-disc, A-bands, and M-line. Organization of each of these structures is essential for proper functioning of the sarcomere and their perturbation can lead to malfunctioning of cardiac tissue. The M-band proteins myomesin and C-protein crosslink the thick filament system (myosins) and the M-band part of titin, the component of the elastic filaments. Thus, the impairment of the M-band structure and its consequence on overall sarcomere organization could be a key event during development of dilated cardiomyopathy. We study a further M-band protein, CAP2 (Peche *et al.*, 2007) and show that its ablation leads to ventricular DCM clearly indicating its necessity at the M-band and its effect on sarcomere organization. CAP2 is present in the relevant area of the sarcomere to regulate filament formation (Peche *et al.*, 2007) and our data show that lack of CAP2 leads to a disarray of the sarcomere, presumably due to the loss of its G-actin sequestering and filament-fragmenting activity. Interestingly, CAP2 deficiency reduces the cooperativity of calcium-regulated force development in right ventricular myofibrils, which might indicate that impaired cooperative activation of the regulatory troponin-tropomyosin units on the actin filament is a primary dysfunction associated with the development of DCM in CAP2-deficient mice. CAP2 might be one of the important genes that could be indispensable for physiological heart functioning in humans, an issue that must be addressed further. Our studies demonstrate that CAP2 is essential for physiological functioning of the cardiac system and a deficiency leads to DCM and various cardiac defects (Peche *et al.*, 2013).

Given the complexity of the coordinated efforts of the many proteins that exist in the basic functional unit of the cardiomyocyte that regulates muscle contraction, dysfunction occurs when these interactions are disrupted (Harvey and Leinwand, 2011). Failing hearts of the *Cap2<sup>gt/gt</sup>* mice are characterized by reduced contractile properties caused by impaired  $\text{Ca}^{2+}$  cycling between the sarcoplasm and sarcoplasmic reticulum (SR). Sarcoplasmic/endoplasmic reticulum  $\text{Ca}^{2+}$  ATPase 2a (SERCA2a) mediates  $\text{Ca}^{2+}$  reuptake into the SR in cardiomyocytes. Of note, the expression level and/or activity of SERCA2a, translating to the quantity of SR  $\text{Ca}^{2+}$  uptake is significantly reduced in failing hearts (Park and Oh, 2013). In our pull down experiments we identified the sarcoplasmic/endoplasmic reticulum ATPase 2 as an interacting partner of CAP2 which is (Table 3). Further investigation to decipher the role of CAP2 in  $\text{Ca}^{2+}$  regulation is required.

A significant contributing factor to cardiovascular and diseases can be sarcopenia, the age-related and progressive loss of skeletal muscle mass and function (Lang *et al.*, 2010). Cardiac and skeletal muscles critically depend on mitochondrial energy metabolism for their normal function. Mice in which the apoptosis-inducing factor (*Aif*) has been inactivated specifically in cardiac and skeletal muscle exhibit impaired activity and protein expression of respiratory chain complex I. Mutant animals develop severe dilated cardiomyopathy, heart failure, and skeletal muscle atrophy (Joza *et al.*, 2005). Sarcopenia is associated with increased apoptosis, autophagy, and proteolysis (Marzetti *et al.*, 2009). Ablation of CAP2 increased these degradative processes, which presumably disrupted muscle integrity and muscle mass. *Cap2<sup>gt/gt</sup>* mice also showed more cardiac muscle fibrosis than WT mice during aging. During aging, there is increased collagen deposition and fibrosis (Goldspink *et al.*, 1994). Fibrosis is supposedly driven by the repeated bouts of muscle fiber degeneration and ensuing inflammation, such as in Duchenne muscular dystrophy (McDouall *et al.*, 1990).

*Cap2<sup>gt/gt</sup>* mice had increased adipose fat tissue and decreased skeletal mass. In addition, CPT1B, which is a key enzyme in the regulation of the mitochondrial  $\beta$ -oxidation (Miljkovic *et al.*, 2009), was identified as an interacting partner of CAP2. Possible upregulation or downregulation of CPTIB in the *Cap2<sup>gt/gt</sup>* mice may contribute to impair long-chain fatty acid metabolism and predispose to the observed increased skeletal muscle fat infiltration. Further investigation is underway.

For the mechanism through which CAP2 might regulate actin dynamics in muscle, we propose a model based on our findings that CAP2 is essential for physiological functioning of the cardiac system and a deficiency leads to DCM and various cardiac defects. The sarcomere is the core structure responsible for active mechanical heart function. Cyclic interactions occur between the cross-bridges of the myosin filaments and the actin filaments. The forces generated by these cyclic interactions provide the molecular basis for cardiac pressure. (Fig. 4.1, Peche *et al.*, 2013) Ablation of CAP2 leads to disarray of the sarcomere since CAP2 binds to G-actin through its WH2 domain, prevents polymerization and also severs F-actin, thereby affecting filament stability, that are essential activities for the structural integrity of the sarcomere (Peche *et al.*, 2013).

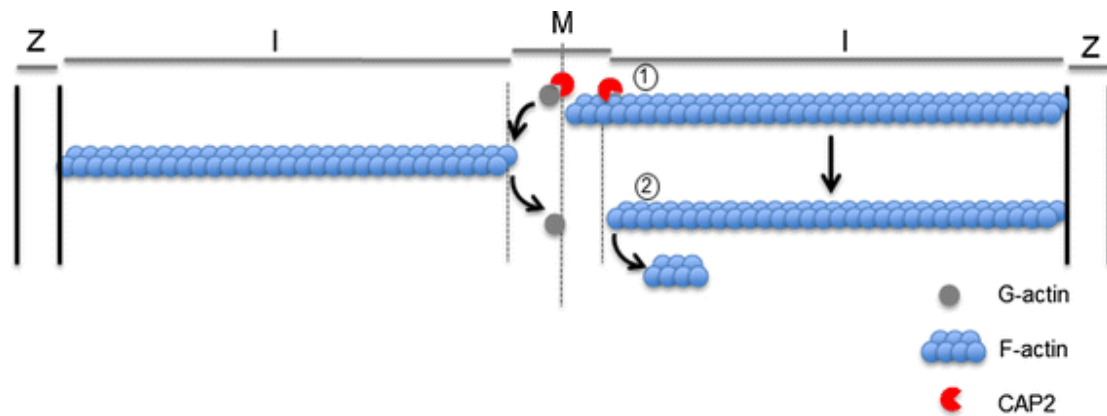


**Figure 4.1: Model illustrating CAP2 function in cardiac muscle.** CAP2 localizes to the M-band and adjacent regions of the sarcomere. Upon formation of F-actin in the sarcomere (1), the length of the filament is maintained through severing activity of CAP2 through its WH2 domain (2). Moreover, through its G-actin sequestering activity, which resides in the WH2 domain, it also maintains the pool of G-actin in the sarcomere. I, I-band; M, M-line; Z, Z-band.

#### 4.2 Role of CAP2 in wound healing

All living organisms have developed a variety of mechanisms for healing wounds in order to cope with constant physical and chemical stresses of their environment. A rapid wound repair response is absolutely necessary for survival from or a single cell to the whole organism. If a delay in the repair of the cell membrane occurs, the cell will die due to the loss of cytoplasm and the influx of extracellular molecules. At a bigger scale, rapid wound repair is necessary to maintain homeostasis, avoid infection, and maintain tissue function. Defects in injury repairs can lead to the death of an organism. The wound repair responses in single cells and tissues are alike: upon injury the wound is rapidly sealed, the wound area is reconstituted, and the damaged

area is then remodeled in order to restore normal function (Abreu-Blanco *et al.*, 2012). More detailed, the fundamental stages during cutaneous wound healing are acute inflammation, re-epithelialization and contraction of the wounded area facilitated by collagen deposition. Pivotal role in these processes have inflammatory cells concerning the immune response and fibroblasts and keratinocytes, which are responsible for rebuilding and repairing the wound (Martin, 1997). The multistage process of cutaneous wound repair is precisely orchestrated by the cell cytoskeleton, composed by actin, myosin and microtubule networks. The contractile actomyosin array initiates the repair process and the microtubules serve to traffic membrane and other components to the wound (Abreu-Blanco *et al.*, 2012). Adhesion signaling can activate Rho family GTPases including Cdc42 and Rac, which then stimulate cell migration by the formation of protrusions like filopodia and lamellipodia (Mitra *et al.*, 2005; Price *et al.*, 1998; Legate *et al.*, 2009). In detail, the actin filaments of the cell cytoskeleton upon stimuli generate the mechanical forces that are necessary for cell adhesion, contraction and motility that underpin tissue repair. These highly dynamic processes include infiltration of inflammatory cells, lamellipodial crawling of keratinocytes during wound re-epithelialization, and migration of fibroblasts followed by the deposition and remodelling of the ECM and dermal contraction at the wound site (Sun *et al.*, 1999, Jacinto *et al.*, 2001, Cowin *et al.*, 2003).

Up to date, many actin-remodelling proteins have been reported to play a crucial role in the wound healing process. For instance, gelsolin family proteins that regulate actin filaments by severing pre-existing filaments and/or capping the filament ends (Liu and Yin, 1998; Goshima *et al.*, 1999). After severing, they remain attached to the 'barbed' ends of the broken filament, thereby preventing annealing or addition of actin monomers. Gelsolin can also serve as a scavenger after tissue repair by removing any actin that is exposed to extracellular spaces or released into the circulation (Lee *et al.*, 2004). The family consists of gelsolin, Flightless I (FliI), adseverin, CapG, villin, advillin, protovillin and supervillin. Till now little is known about the exact mechanism with which the actin-remodelling proteins of the gelsolin family contribute to the wound repair process. In adult skin, gelsolin is expressed primarily in suprabasal keratinocytes and dermal fibroblasts and appears to be reduced in keratinocytes at the leading edge of migrating epidermis in suction blister wounds (Kubler and Watt, 1993).



Studies with gelsolin knockout mice, which exhibit normal embryonic development and longevity, indicate that gelsolin is required for rapid motile responses in cell types involved in hemostasis, inflammation, and wound healing. In detail, upon tail cutting platelet shape changes are decreased causing prolonged bleeding times. In addition, neutrophil migration *in vivo* into peritoneal exudates and *in vitro* is delayed. Moreover, analysis of skin fibroblasts showed that absence of gelsolin caused a variety of motility and actin-related defects including excessive stress fibres, slower migration, increased contractility *in vitro* and an inability to sever and remodel actin filaments (Witke *et al.*, 1995).

Another actin severing protein of the gelsolin family, flightless I (FliI), which is highly conserved between mouse and human also plays a role in wound repair (Claudianos and Campbell, 1995). In the fly, *fliI* null mutations are embryonic lethal. Furthermore, FliI is found in actin protrusions such as filopodia, suggesting a role in actin remodeling. The depolymerisation and repolymerisation of actin that occurs at membrane ruffles and which contributes to cell locomotion may be mediated by the actin-severing ability of FliI (Cowin 2006; Davy *et al.*, 2000; 2001). In addition, PI 3-kinase and members of the small GTPase family, Ras, Cdc 42 and RhoA colocalize with FliI in migrating Swiss 3T3 fibroblasts. In migrating serum-stimulated fibroblasts FliI specifically colocalizes with tubulin and actin-based structures connected with migration (Ben-Ze'ev, 1997; Kaibuchi *et al.*, 1999; Davy *et al.*, 2000; 2001). Concerning the localization, FliI and gelsolin are differentially expressed in the epidermis. FliI is present in foetal and adult mouse skin. It is highly expressed in the proliferative basal and differentiating suprabasal keratinocytes and present in dermal fibroblasts (Cowin 2006). Its expression in skin appears to overlap with the expression of gelsolin but interestingly gelsolin is primarily expressed in the differentiating suprabasal cells (Kubler and Watt, 1993).

Similar to the presence of CAP2 in all living layers of the epidermis (stratum basale, stratum spinosum, stratum granulosum) (Fig. 3.7 A) gelsolin and FliI are also localized in these subbasal layers. Since proliferative basal cells are the cells that repopulate and repair the epidermis in response to injury this suggests a vital role for FliI and CAP2 in wound repair particularly for re-epithelialization, matrix synthesis and wound contraction. Using *FliI* transgenic and knockout mice and *in vitro* models of wound repair, previous reports demonstrate that FliI is a crucial mediator of wound healing and that it provides a mechanistic link between cytoskeletal remodelling in

response to injury and induction of TGF- $\beta$ 1 expression. What is more, it may be possible to manipulate levels of such actin cytoskeletal proteins to promote healing via foetal wound repair mechanisms and thereby reduce scar formation (Cowin, 2006).

We found expression of CAP2 in human wounds in the hyperproliferative epidermis suggesting a functional role in the normal wound healing process. Here we described further functions of CAP2 and showed that it is important in the wound healing process and that its ablation impaired the normal wound healing. Within three to five days after injury, macrophages are the most prominent cells in the healing tissue. Depletion of macrophages during the inflammatory phase resulted in significant delay of wound repair in a mouse model (Lucas *et al.*, 2010; DiPietro and Polverini, 1993; Eming *et al.*, 2007). During the early and short inflammatory phase macrophages exert pro-inflammatory functions like antigen-presenting, phagocytosis and the production of inflammatory cytokines and growth factors that facilitate the wound healing process. We found that macrophage infiltration was delayed in wounds of CAP2 deficient mice. This might result in overall delays in the following steps of re-epithelialization and wound closure. Macrophage infiltration at the wound site is a complex and highly orchestrated event. It is regulated by gradients of different chemotactic factors, including growth factors, proinflammatory cytokines and chemokines (Frank *et al.*, 2000; Wetzler *et al.*, 2000; Eming *et al.*, 2007). The major source of these chemoattractants includes platelets trapped in the fibrin clot at the wound surface and hyperproliferative keratinocytes at the wound edge. Macrophages play an important role in the healing process synthesizing potent growth factors like TGF- $\beta$ , TGF- $\alpha$ , basic fibroblast growth factor, platelet derived growth factor and vascular endothelial growth factor which promote cell proliferation and synthesis of extracellular matrix by resident skin cells. Actin binding proteins Filamin A and drebrin were shown to be involved as modulator of chemokines (Jiménez-Baranda *et al.*, 2007, Pérez-Martínez *et al.*, 2010) and CAP mutants of *D. discoideum* had altered chemotactic signalling (Noegel *et al.*, 2004). The observed wound closure delay in mutant mice coupled with earlier data from various studies in CAP mutants in *D. discoideum* points at a possible role of CAP2 in chemokine release and/or chemokine sensing by numerous receptors and its absence results in delayed macrophage infiltration and thus delay in wound healing.

The localization of cofilin and CAP1 to mitochondria during apoptosis provides a direct link between apoptosis and the actin cytoskeleton (Wang *et al.*, 2008; Gourlay and Ayscough, 2006). We observed an increase in apoptosis and a decrease in proliferation at day 3 and day 7 post wounding in the CAP2 deficient mice. Similar to CAP1 and cofilin this may also be mediated by a translocation of CAP2 to mitochondria which needs to be studied further.

Fibroblasts regulate the turnover of ECM under normal conditions. In injured tissues, fibroblasts differentiate into myofibroblasts which contract and participate in healing by reducing the size of the wound and secreting ECM proteins. This differentiation of fibroblasts to myofibroblasts is a key event in connective tissue wound healing (Li and Wang, 2011). At day 10 which is the phase when myofibroblasts contribute to the wound healing process *Cap2<sup>gt/gt</sup>* mice showed a significant delay. Loss of CAP2 delayed or altered myofibroblast differentiation as indicated by reduced levels of  $\alpha$ -SMA from day 7 onward. CAP2 is abundant at actin rich structures and regulates actin filaments to ascertain cell polarity, motility and morphogenesis (Peché *et al.*, 2007; Bertling *et al.*, 2004). The phenotypic effect at the single cell level was also evident when we observed different cellular properties of fibroblasts isolated from mutant mice. The altered focal adhesions and F-actin content may contribute to the differentiation process, which were addressed further by fixation at time different points after seeding and calculation of the G/F actin level in cultured cells respectively.

In general, our data and reports for CAP1 indicate that the CAP family of proteins plays an essential role in healing processes post injury. CAP1 was differentially regulated in sciatic nerve crush (SNC). In normal sciatic nerve the expression level of CAP1 was lower but upon injury it was highly expressed during the different stages of recovery. It was highest at day 5 post SNC, and slowly decreased through a 4 weeks span (Zhu *et al.*, 2014). When we quantified the CAP2 intensity per unit area in human wounds we observed a significant increase in CAP2 expression at day 5 post injury which emphasizes the role of CAP2 in the healing process.

*Cap2<sup>gt/gt</sup>* fibroblasts develop extended filopodia and more focal adhesions and show reduced velocity in comparison to control cells. Consistent with our observations, in HCC cell lines CAP2 silencing resulted in a defect in lamellipodium formation and decreased cell motility (Effendi *et al.*, 2013). The abnormal filopodia formation in *Cap2<sup>gt/gt</sup>* may lead to the altered velocity. Multiple cellular processes like

embryogenesis and wound healing require cells to sense and respond to environmental cues such as mechanical forces (Janmey and McCulloch, 2007; Parsons *et al.*, 2010; Geiger *et al.*, 2009). These forces can be transmitted across the cell membrane in both directions. To this aim, actin cytoskeleton couples transmembrane receptors (integrin or cadherin), through points of cell adhesion consisting of cell-cell (adherens junctions) contacts and multiple protein complexes (vinculin, talin, zyxin, FAK and paxilin) that connect the cytoskeleton of a cell to extracellular matrix (focal adhesions) (Geiger *et al.*, 2001; 2009). Vinculin is a highly abundant and conserved cytoskeletal protein that is found in both focal adhesions and adherent junctions and plays a key role in regulating cell morphology, cell motility, and force transduction (Parsons *et al.*, 2010, Ziegler *et al.*, 2006). Furthermore, vinculin also possesses tumor suppressor properties as vinculin KO cells are less adherent, have a rounded morphology, reduced lamellipodial stability, increased motility, and are resistant to apoptosis and anoikis (Xu *et al.*, 1998; Coll *et al.*, 1995; Subauste *et al.*, 2004). What is more, vinculin knock-out (KO) mouse embryos fail to survive beyond day E10 with extensive defects in myocardial and endocardial structures (Xu *et al.*, 1998). Consistent with the importance in the embryonic development and role in muscle structure, vinculin heterozygous mice are predisposed to stress-induced cardiomyopathy (Zemljic-Harpf *et al.*, 2004).

Since focal adhesions play an important role in cell spreading and cell attachment and are important for stability and subsequent movement of a cell in a 3D environment, we investigated the formation of focal adhesions in mutant fibroblasts. We observed a higher number of focal adhesions in mutant fibroblasts, which may contribute to the delay in wound closure. In contrast, the increased cell spreading area and focal contacts in *Cap2<sup>gt/gt</sup>* were however not paralleled by increased amounts of vinculin but might be achieved by its redistribution, due to a lack of connection between focal adhesion and cell motility. Previous studies suggested that the mean size of focal adhesions robustly and precisely predicts cell speed independently of focal adhesion surface density and molecular composition. More precisely, MEF speed steadily increases with focal adhesion size until a threshold value of  $\sim 0.7$  (corresponding to  $\sim 2.6 \mu\text{m}^2$ ) in normalized focal adhesion size beyond which cell speed declines. However, whether a subset or all focal adhesion-specific proteins need to cluster into focal adhesion complexes in order to mediate cell migration is unknown, i.e., whether any change in the clustering of focal adhesion proteins induced by a change in

expression/activation of a known or yet unidentified regulator of focal adhesions or biophysical/biochemical changes in the microenvironment necessarily can predict a change in cell migration is unknown (Kim and Wirtz, 2012). During reepithelialization cellular movement is a critical parameter and reduced cell velocity may contribute to the delay in wound healing. Moreover, latrunculin B washout experiment revealed a function of CAP2 in the organization of the actin cytoskeleton, which is important for cell migration. Knockdown of CAP1 in Schwann cells led to reduced migration and motility (Zhu *et al.*, 2014). In TE1 cells (human esophageal cancer cells), knockdown of CAP1 leads to reduced cell motility and migration. Interestingly, CAP1 expression was negatively associated with E-cadherin and knockdown of CAP1 in TE1 cells resulted in decreased vimentin and F-actin levels (Li *et al.*, 2013). Similar mechanisms could exist in migrating cells at the migrating tongue and also in dermal fibroblasts, which upon CAP2 ablation resulted in altered wound healing in the mutant mice.

Thus, depletion of CAP2 leads to an increase in focal adhesion in resting (Fig. 4.2 A) and in migrating cells (Fig. 4.2. B, C). In CAP2 knockout, cell motility is affected either by stabilization of focal adhesions and/or disruption of cell polarity (Fig. 4.2 B, C). A dense meshwork of peripheral actin filaments with less stress fibers may lead to reduced cell motility (Fig. 4.2 B) accounting for the altered wound healing response and contraction *in vivo*. In conclusion, CAP2 is an important regulator of wound healing and ablation of which leads to reduced cellular migration, increased focal adhesions and slow macrophage infiltration. Additionally, regulation of the actin cytoskeleton by CAP2 is a crucial event during wound healing, deletion of which leads to altered wound contraction.

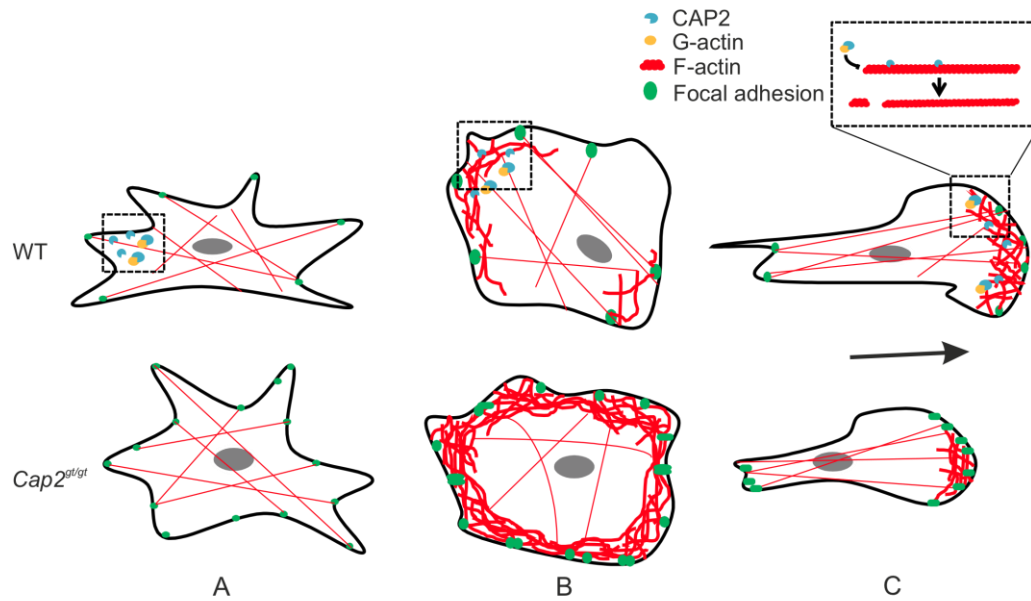


**Figure 4.2: Model illustrating cellular functions of CAP2.** Ablation of CAP2 leads to cytoskeleton defects. CAP2 sequesters G-actin and also severs F-actin filaments. Increased F-actin content in cells lacking CAP2 and altered reorganization of cortical actin cytoskeleton in mutant cells are the consequences. Depletion of CAP2 leads to an increase in focal adhesion in resting (A) and in migrating cells (B, C). In CAP2 knockout, cell motility is affected either by stabilization of focal adhesions and/or disruption of cell polarity (B, C). A dense meshwork of peripheral actin filaments with less stress fibers may lead to reduced cell motility (B) accounting for altered wound healing response and contraction *in vivo*.

## Summary

Cyclase-associated proteins (CAPs) are evolutionary conserved proteins, essential for normal actin organization by binding to G-actin and regulating actin filament dynamics. Loss of CAP results in defects in cell morphology, migration, endocytosis and development. Higher eukaryotes have two homologs of CAP, CAP1 and CAP2, which are closely related. CAP1 shows a broad tissue distribution, whereas CAP2 is significantly expressed only in brain, heart and skeletal muscle, and skin. To identify the *in vivo* function of CAP2 we generated mice in which the *Cap2* gene was inactivated by a gene-trap approach. Mutant mice showed a decrease in body weight and had a decreased survival rate. We analyzed skeletal muscle, heart and skin phenotypes. Knockout mice developed a severe cardiac defect marked by dilated cardiomyopathy (DCM) associated with drastic reduction in basal heart rate and prolongations in atrial and ventricular conduction times. In muscle, CAP2 is an essential component of the M-line in the sarcomere and its ablation leads to disarrayed sarcomeric organization.

In human skin, CAP2 is present in all living layers of the epidermis localizing to the nuclei and the cell periphery. We performed *in vivo* wound healing experiments in WT and in mice lacking CAP2 and observed delayed wound repair in knockout mice. In addition, knockout mice showed decreased macrophage infiltration, slower neovascularization and increase in apoptosis. Furthermore, fibroblasts which were isolated from mice lacking CAP2 showed reduced velocity, developed long filopodia and increased focal adhesions, something that can be attributed to the effect of CAP2 on G-/F-actin ratio.

Taken together, our studies so far show that CAP2 has roles in cardiac physiology, cell migration and wound healing.

## Zusammenfassung

Zyklase-assoziierte Proteine (CAP) sind evolutionär hoch konservierte Proteine, die durch die Bindung an G-Aktin die Dynamik der Aktinfilamente regulieren. Verlust von CAP führt zu Defekten in Zellentwicklung, -morphologie, -migration sowie Endozytose. Höhere Eukaryoten weisen zwei CAP-Isoformen auf, CAP1 und CAP2. CAP1 ist ubiquitär, während CAP2 ausschließlich im Gehirn, Herz, Skelettmuskulatur und in der Haut exprimiert wird.

Um die *in vivo* Funktion von CAP2 zu untersuchen, wurde ein Mausmodell entwickelt, in dem das *Cap2* Gen mit Hilfe der sog. "gene trap"-Methode inaktiviert wurde. Die Mutanten wiesen geringeres Körpergewicht sowie geringere Lebenserwartung auf. Des Weiteren wurden Skelettmuskulatur-, Herz- und Hautphänotypen untersucht. Die Knockoutmäuse entwickelten schwere Herzfehler, die sich durch dilatative Kardiomyopathie definierten. Ferner zeigten sie eine reduzierte Basalfrequenz sowie verlängerte Atrium- und Ventrikelkonduktionszeiten. Im Muskel stellt CAP2 eine essentielle Komponente der M-Bande im Sarkomer) dar, deren Organisation bei fehlendem CAP2 beeinträchtigt ist.

In humaner Haut ist CAP2 in allen epidermalen Schichten vorzufinden und ist in den Zellen sowohl im Kern als auch an der Zellperipherielokalisiert. Wundheilungsexperimente an CAP2-Knockoutmäusen führten zur verzögerten Wundschließung im Vergleich zu Wildtypmäusen. Zudem wurden verringerte Makrophageninfiltration, langsamere Neovaskularisation und erhöhte Apoptose in Knockoutwunden beobachtet. Primäre Fibroblasten aus der CAP2-Knockouthaut zeigten außerdem eine reduzierte Migrationsgeschwindigkeit, bildeten lange Filopodien und vermehrt Fokaladhäsionen, was wahrscheinlich auf den Effekt von CAP2 auf das G/F-Aktinverhältnis zurückzuführen ist.

Zusammengefasst zeigen die oben genannten Befunde, dass CAP2 eine Rolle in der Herzphysiologie, Zellmigration und Wundheilung spielt.



## Bibliography

Abreu-Blanco, M. T., Watts, J. J., Verboon, J. M., Parkhurst, S. M. (2012) Cytoskeleton responses in wound repair. *Cell. Mol. Life Sci.* **69**, 2469-2483

Alberts, B., Johnson, A., Walter, P., Lewis, J., Raff, M. (2007) *Molecular Biology of the Cell*, 5<sup>th</sup> Edition

Almine, J. F., Wise, S. G., Weiss, A. S. (2012) Elastin signaling in wound repair. *Birth Defects Res. C Embryo Today* **96**, 248-57

Balcer, H. I., Goodman, A. L., Rodal, A. A., Smith, E., Kugler, J., Heuser, J. E., Goode, B. L. (2003) Coordinated regulation of actin filament turnover by a high-molecular-weight Srv2/CAP complex, cofilin, profilin, and Aip1. *Curr. Biol.* **13**, 2159-2169

Barrero, R. A., Umeda, M., Yamamura, S., Uchimiya, H. (2002) Arabidopsis CAP regulates the actin cytoskeleton necessary for plant cell elongation and division. *Plant Cell* **14**, 149-163

Baum, B., Li, W., Perrimon, N. (2000) A cyclase-associated protein regulates actin and cell polarity during *Drosophila* oogenesis and in yeast. *Curr. Biol.* **10**, 964-973

Baum, C. L., Arpey, C. J. (2005) Normal cutaneous wound healing: clinical correlation with cellular and molecular events. *Dermatol. Surg.* **31**, 674-686

Ben-Ze'ev, A. (1997) Cytoskeletal and adhesion proteins as tumor suppressors. *Curr. Opin. Cell Biol.* **9**, 99-108

Benlali, A., Draskovic, I., Hazelett, D. J., Treisman, J. E. (2000) act up controls actin polymerization to alter cell shape and restrict Hedgehog signaling in the *Drosophila* eye disc. *Cell* **101**, 271-281

Bertling, E., Hotulainen, P., Mattila, P. K., Matilainen, T., Salminen, M., Lappalainen, P. (2004) Cyclase-associated protein 1 (CAP1) promotes cofilin-induced actin dynamics in mammalian nonmuscle cells. *Mol. Biol. Cell* **15**, 2324-2334

Blumbach, K., Zweers, M. C., Brunner, G., Peters, A. S., Schmitz, M., Schulz, J. N., Schild, A., Denton, C. P., Sakai, T., Fässler, R., Krieg, T., Eckes, B. (2010) Defective granulation tissue formation in mice with specific ablation of integrin-linked kinase in fibroblasts - role of TGFbeta1 levels and RhoA activity. *J. Cell Sci.* **123**, 3872-3883

Broughton, G. II, Janis, J. E., Attinger, C. E. (2006) Wound healing: an overview. *Plast. Reconstr. Surg.* **117**, (7 Suppl): 1e-S-32e-S

Brown, D. L., Kao, W. W., Greenhalgh, D. G. (1997) Apoptosis down-regulates inflammation under the advancing epithelial wound edge: delayed patterns in diabetes and improvement with topical growth factors. *Surgery* **121**, 372-380

Bugyi, B., and Carlier, M. F. (2010) Control of actin filament treadmilling in cell

motility. *Annu. Rev. Biophys.* **39**, 449-470

Carrier, M. F., and Pantaloni, D. (1994) Actin assembly in response to extracellular signals: role of capping proteins, thymosin beta 4 and profilin. *Semin. Cell Biol.* **5**, 183-191

Carrier, M. F., and Pantaloni, D. (1997) Control of actin dynamics in cell motility. *J. Mol. Biol.* **269**, 459-467

Chen, C. S., Alonso, J. L., Ostuni, E., Whitesides, G. M., Ingber, D. E. (2003) Cell shape provides global control of focal adhesion assembly. *Biochem. Biophys. Res. Commun.* **307**, 355-361

Chereau, D., Kerff, F., Graceffa, P., Grabarek, Z., Langsetmo, K., Dominguez, R. (2005) Actin-bound structures of Wiskott-Aldrich syndrome protein (WASP)-homology domain 2 and the implications for filament assembly. *Proc. Natl. Acad. Sci.* **102**, 16644-16649

Chhabra, E. S., Higgs, H. N. (2007) The many faces of actin: matching assembly factors with cellular structures. *Nat. Cell Biol.* **9**, 1110-1121

Christoforou, N., Miller, R. A., Hill, C. M., Jie, C. C., Mccallion, A. S., Gearhart, J. D. (2008) Mouse ES cell-derived cardiac precursor cells are multipotent and facilitate identification of novel cardiac genes. *J. Clin. Invest.* **118**, 894-903

Claudianos, C., and Campbell, H. D. The novel flightless-I gene brings together two gene families, actin-binding proteins related to gelsolin and leucinerich- repeat proteins involved in Ras signal transduction. *Mol. Biol. Evol.* **12**, 405-414

Coll, J. L., Ben-Ze'ev, A., Ezzell, R. M., Rodríguez Fernández, J. L., Baribault, H., Oshima, R. G., Adamson, E. D. (1995) Targeted disruption of vinculin genes in F9 and embryonic stem cells changes cell morphology, adhesion, and locomotion. *Proc. Natl. Acad. Sci.* **92**, 9161-9165

Cory, G. O., and Ridley, A. J. (2002) Cell motility: braking WAVES. *Nature* **418**, 732-733

Cowin, A. J., Hatzirodos, N., Teusner, J. T., Belford, D. A. (2003) Differential effect of wounding on actin and its associated proteins, paxillin and gelsolin, in fetal skin explants. *J. Invest. Dermatol.* **120**, 1118-1129

Cowin, A. J. (2006) Role of the actin cytoskeleton in wound healing and scar formation. *Primary Intention* **14**, 39-42

Davy, D. A., Ball, E. E., Matthaei, K. I., Campbell, H. D., Crouch, M. F. (2000) The flightless I protein localizes to actin-based structures during embryonic development. *Immunol. Cell Biol.* **78**, 423-429

Davy, D. A., Campbell, H. D., Fountain, S., de Jong, D., Crouch, M. F. (2001) The flightless I protein colocalizes with actin- and microtubule-based structures in motile

Swiss 3T3 fibroblasts: evidence for the involvement of PI 3-kinase and Ras-related small GTPases. *J. Cell Sci.* **114**, 549-562

Dhe-Paganon, S., Duda, S., Iwamoto, M., Chi, Y. I., Shoelson, S. E. (2002) Crystal structure of the HNF4  $\alpha$  ligand binding domain in complex with endogenous fatty acid ligand. *J. Biol. Chem.* **277**, 37973-37976

DiPietro, L. A., and Polverini, P. J. (1993) Role of the macrophage in the positive and negative regulation of wound neovascularisation. *Am. J. Pathol.* **143**, 678-684

Dos Remedios, C. G., Chhabra, D., Kekic, M., Dedova, I. V., Tsubakihara, M., Berry, D. A., Nosworthy, N. J. (2003) Actin binding proteins: regulation of cytoskeletal microfilaments. *Physiol. Rev.* **83**, 433-473

Ducka, A. M., Joel, P., Popowicz, G. M., Trybus, K. M., Schleicher, M., Noegel, A. A., Huber, R., Holak, T. A., Sitar, T. (2010) Structures of actin-bound Wiskott-Aldrich syndrome protein homology 2 (WH2) domains of Spire and the implication for filament nucleation. *Proc. Natl. Acad. Sci.* **107**, 11757-11762

Effendi, K., Yamazaki, K., Mori, T., Masugi, Y., Makino, S., Sakamoto, M. (2013) Involvement of hepatocellular carcinoma biomarker, cyclase-associated protein 2 in zebrafish body development and cancer progression. *Exp. Cell Res.* **319**, 35-44.

Egozi, E. I., Ferreira, A. M., Burns, A. L., Gamelli, R. L., Dipietro, L. A. (2003) Mast cells modulate the inflammatory but not the proliferative response in healing wounds. *Wound Repair Regen.* **11**, 46-54

Eichinger, L., Noegel, A. A., Schleicher, M. (1991) Domain structure in actin-binding proteins: Expression and functional characterization of truncated severin. *J. Cell Biol.* **112**, 665-676

Eming, S. A., Krieg, T., Davidson, J. M. (2007) Inflammation in wound repair: molecular and cellular mechanisms. *J. Invest. Dermatol.* **127**, 514-525

Etienne-Manneville, S., and Hall, A. (2002) Rho GTPases in cell biology. *Nature* **420**, 629-635

Fedor-Chaiken, M., Deschenes, R. J., Broach, J. R. (1990) SRV2, a gene required for RAS activation of adenylate cyclase in yeast. *Cell* **61**, 329-340

Field, J., Xu, H. P., Michaeli, T., Ballester, R., Sass, P., Wigler, M., Colicelli, J. (1990) Mutations of the adenylyl cyclase gene that block RAS function in *Saccharomyces cerevisiae*. *Science* **247**, 464-467

Fischer, D., Clemen, C. S., Olive, M., Ferrer, I., Goudeau, B., Roth, U., Badorf, P., Wattjes, M. P., Lutterbey, G., Kral, T., van der Ven, P. F., Fürst, D. O., Vicart, P., Goldfarb, L. G., Moza, M., Carpen, O., Reichelt, J., Schröder, R. (2006) Different early pathogenesis in myotilinopathy compared to primary desminopathy. *Neuromuscul. Disord.* **16**, 361-367

- Frank, S., Kämpfer, H., Wetzler, C., Stallmeyer, B., Pfeilschifter, J. (2000) Large induction of the chemotactic cytokine RANTES during cutaneous wound repair: a regulatory role for nitric oxide in keratinocyte-derived RANTES expression. *Biochem. J.* **347**, 265-273
- Freeman, N. L., Chen, Z., Horenstein, J., Weber, A., Field, J. (1995) An actin monomer binding activity localizes to the carboxyl-terminal half of the *Saccharomyces cerevisiae* cyclase-associated protein. *J. Biol. Chem.* **270**, 5680-5685
- Freeman, N. L., and Field, J. (2000) Mammalian homolog of the yeast cyclase associated protein, CAP/Srv2p, regulates actin filament assembly. *Cell Motil. Cytoskeleton* **45**, 106-120
- Geiger, B., Bershadsky, A., Pankov, R., Yamada, K. M. (2001) Transmembrane crosstalk between the extracellular matrix-cytoskeleton crosstalk. *Nat. Rev. Mol. Cell Biol.* **2**, 793-805
- Geiger, B., Spatz, J. P., Bershadsky, A. D. (2009) Environmental sensing through focal adhesions. *Nat. Rev. Mol. Cell Biol.* **10**, 21-33
- Gerst, J. E., Ferguson, K., Vojtek, A., Wigler, M., Field, J. (1991) CAP is a bifunctional component of the *Saccharomyces cerevisiae* adenylyl cyclase complex. *Mol. Cell. Biol.* **11**, 1248-1257
- Gieselmann, R., and Mann, K. (1992) ASP-56, a new actin sequestering protein from pig platelets with homology to CAP, an adenylate cyclase-associated protein from yeast. *FEBS Lett.* **298**, 149-153
- Goldspink, G., Fernandes, K., Williams, P. E., Wells, D. J. (1994) Age-related changes in collagen gene expression in the muscles of mdx dystrophic and normal mice. *Neuromuscul. Disord.* **4**, 183-191
- Goshima, M., Kariya, K., Yamawaki-Kataoka, Y., Okada, T., Shibatohe, M., Shima, F., Fujimoto, E., Kataoka, T. (1999) Characterization of a novel Rasbinding protein Ce-FLI-1 comprising leucine-rich repeats and gelsolin-like domains. *Biochem. Biophys. Res. Commun.* **257**, 111-116
- Gottwald, U., Brokamp, R., Karakesisoglou, I., Schleicher, M., Noegel, A. A. (1996) Identification of a cyclase-associated protein (CAP) homologue in *Dictyostelium discoideum* and characterization of its interaction with actin. *Mol. Biol. Cell* **7**, 261-272
- Greenhalgh, D. G. (1998) The role of apoptosis in wound healing. *Int. J. Biochem. Cell Biol.* **30**, 1019-1030
- Grinnell, F. (1982) Fibronectin and wound healing. *Am. J. Dermatopathol.* **4**, 185-188
- Gurtner, G. C., Werner, S., Barrandon, Y., Longaker, M. T. (2008) Wound repair and regeneration. *Nature* **453**, 314-321

Hartmann, H., Schleicher, M., Noegel, A. A. (1990) Heterodimeric capping proteins constitute a highly conserved group of actin-binding proteins. *Dev. Genet.* **11**, 5-6

Harvey, P. A., and Leinwand, L. A. (2011) The cell biology of disease: cellular mechanisms of cardiomyopathy. *J. Cell Biol.* **194**, 355-365.

Haus, U., Hartmann, H., Trommler, P., Noegel, A. A., Schleicher, M. (1991) F-actin capping by cap32/34 requires heterodimeric conformation and can be inhibited with PIP<sub>2</sub>. *Biochem. Biophys. Res. Commun.* **181**, 833-839

Herman, I. M. (1993) Actin isoforms. *Curr. Opin. Cell Biol.* **5**, 48-55

Hinz, B., Celetta, G., Tomasek, J. J., Gabbiani, G., Chaponnier, C. (2001) Alpha-smooth muscle actin expression upregulates fibroblast contractile activity. *Mol. Biol. Cell* **12**, 2730-2741

Hinz, B., and Gabbiani, G. (2003) Mechanisms of force generation and transmission by myofibroblasts. *Curr. Opin. Biotechnol.* **14**, 538-546

Hinz, B. (2007) Formation and function of the myofibroblast during tissue repair. *J. Invest. Dermatol.* **127**, 526-537

Hliscs, M., Sattler, J. M., Tempel, W., Artz, J. D., Dong, A., Hui, R., Matuschewski, K., Schüler, H. (2010) Structure and function of a G-actin sequestering protein with a vital role in malaria oocyst development inside the mosquito vector. *J. Biol. Chem.* **285**, 11572-11583

Hubberstey, A. V., and Mottillo, E. P. (2002) Cyclase-associated proteins: Capacity for linking signal transduction and actin polymerization. *FASEB J.* **16**, 487-499

Isola, J., Helin, H., Kallioniemi, O. P. (1990) Immunoelectron-microscopic localization of a proliferation-associated antigen Ki-67 in MCF-7 cells. *Histochem. J.* **22**, 498-506

Jacinto, A., Martinez-Arias, A., Martin, P. (2001) Mechanisms of epithelial fusion and repair. *Nat. Cell Biol.* **3**, 117-123

Janmey, P. A., and McCulloch, C. A. (2007) Cell mechanics: integrating cell responses to mechanical stimuli. *Annu. Rev. Biomed. Eng.* **9**, 1-34

Jefferies, J. L., and Towbin, J. A. (2010) Dilated cardiomyopathy. *Lancet* **375**, 752-762

Jiménez-Baranda, S., Gómez-Moutón, C., Rojas, A., Martínez-Prats, L., Mira, E., Ana Lacalle, R., Valencia, A., Dimitrov, D. S., Viola, A., Delgado, R., Martínez-A., C., Mañes, S. (2007) Filamin-A regulates actin-dependent clustering of HIV receptors. *Nat. Cell Biol.* **9**, 838-846

Joza, N., Oudit, G. Y., Brown, D., Bénit, P., Kassiri, Z., Vahsen, N., Benoit, L., Patel, M. M., Nowikovsky, K., Vassault, A., Backx, P. H., Wada, T., Kroemer, G., Rustin, P., Penninger, J. M. (2005) Muscle-specific loss of apoptosis-inducing factor leads to

mitochondrial dysfunction, skeletal muscle atrophy, and dilated cardiomyopathy. *Mol. Cell. Biol.* **25**, 10261-10272

Kaibuchi, K., Kuroda, S., Amano, M. (1999) Regulation of the cytoskeleton and cell adhesion by the Rho family GTPases in mammalian cells. *Ann. Rev. Biochem.* **68**, 459-486

Katz, A. M. (1990) Cardiomyopathy of overload. A major determinant of prognosis in congestive heart failure. *N. Engl. J. Med.* **322**, 100-110

Kim, D. H., and Wirtz, D. (2013) Focal adhesion size uniquely predicts cell migration. *FASEB J.* **27**, 1351-1361

Krafts, K. P. (2010) Tissue repair: The hidden drama. *Organogenesis* **6**, 225-233

Kubler, M. D., and Watt, F. M. (1993) Changes in the distribution of actin-associated proteins during epidermal wound healing. *J. Invest. Dermatol.* **100**, 785-789

Lang, T., Streeper, T., Cawthon, P., Baldwin, K., Taaffe, D. R., Harris, T. B. (2010) Sarcopenia: etiology, clinical consequences, intervention, and assessment. *Osteoporos. Int.* **21**, 543-559

Lauffenburger, D. A., and Horwitz, A. F. (1996) Cell migration: a physically integrated molecular process. *Cell* **84**, 359-369

Lee, Y. H., Campbell, H. D., Stallcup, M. R. (2004) Developmentally essential protein flightless I is a nuclear receptor coactivator with actin binding activity. *Mol. Cell. Biol.* **24**, 2103-2117

Legate, K. R., Wickström, S. A., Fässler, R. (2009) Genetic and cell biological analysis of integrin outside-in signaling. *Genes Dev.* **23**, 397-418

Lehman, W., Craig, R., Vibert, P. (1994) Ca<sup>2+</sup>-induced tropomyosin movement in Limulus thin filaments revealed by three-dimensional reconstruction. *Nature* **368**, 65-67

Levenson, S. M., Geever, E. F., Crowley, L. V., Oates, J. F. 3<sup>rd</sup>, Berard, C. W., Rosen, H. (1965) The healing of rat skin wounds. *Ann. Surg.* **161**, 293-308

Li, B., and Wang, J. H. (2011) Fibroblasts and myofibroblasts in wound healing: force generation and measurement. *J. Tissue Viability* **20**, 108-120

Li, M., Yang, X., Shi, H., Ren, H., Chen, X., Zhang, S., Zhu, J., Zhang, J. (2013) Downregulated expression of the cyclase-associated protein 1 (CAP1) reduces migration in esophageal squamous cell carcinoma. *Jpn. J. Clin. Oncol.* **43**, 856-864

Littlefield, R. S., and Fowler, V. M. (2008) Thin filament length regulation in striated muscle sarcomeres: pointed-end dynamics go beyond a nebulin ruler. *Semin. Cell Dev. Biol.* **19**, 511-519

Liu, Y. T., and Yin, H. L. (1998) Identification of the binding partners for flightless I,

a novel protein bridging the leucine-rich repeat and the gelsolin superfamilies. *J. Biol. Chem.* **273**, 7920-7927

Lovvorn, H. N. III, Cheung, D. T., Nimni, M. E., Perelman, N., Estes, J. M., Adzick, N. S. (1999) Relative distribution and crosslinking of collagen distinguish fetal from adult sheep wound repair. *J. Pediatr. Surg.* **34**, 218–223

Lucas, T., Waisman, A., Ranjan, R., Roes, J., Krieg, T., Müller, W., Roers, A., Eming, S. A. (2010) Differential roles of macrophages in diverse phases of skin repair. *J. Immunol.* **184**, 3964-3977

Mahdavian Delavary, B., van der Veer, W. M., van Egmond, M., Niessen, F. B., Beelen, R. H. (2011) Macrophages in skin injury and repair. *Immunobiology* **216**, 753-762

Mann, D. L., Urabe, Y., Kent, R. L., Vinciguerra, S., Cooper, G. IV. (1991) Cellular versus myocardial basis for the contractile dysfunction of hypertrophied myocardium. *Circ. Res.* **68**, 402–415

Martin, P. (1997) Wound healing-aiming for perfect skin regeneration. *Science* **276**, 75-81

Martin, P., and Leibovich, S. J. (2005) Inflammatory cells during wound repair: the good, the bad and the ugly. *Trends Cell Biol.* **15**, 599-607

Marzetti, E., Lees, H. A., Wohlgemuth, S. E., Leeuwenburgh, C. (2009) Sarcopenia of aging: Underlying cellular mechanisms and protection by calorie restriction. *Biofactors* **35**, 28–35

Mattila, P. K., Quintero-Monzon, O., Kugler, J., Moseley, J. B., Almo, S. C., Lappalainen, P., Goode, B. L. (2004) A high-affinity interaction with ADP-actin monomers underlies the mechanism and in vivo function of Srv2/cyclase-associated protein. *Mol. Biol. Cell.* **15**, 5158-5171

Mattila, P. K., and Lappalainen, P. (2008) Filopodia: molecular architecture and cellular functions. *Nat. Rev. Mol. Cell Biol.* **9**, 446-454

McDouall, R. M., Dunn, M. J., Dubowitz, V. (1990) Nature of the mononuclear infiltrate and the mechanism of muscle damage in juvenile dermatomyositis and Duchenne muscular dystrophy. *J. Neurol. Sci.* **99**, 199–217

McGarry, J. D., Leatherman, G. F., Foster, D. W. (1978) Carnitine palmitoyltransferase I. The site of inhibition of hepatic fatty acid oxidation by malonyl-CoA. *J. Biol. Chem.* **253**, 4128–4136

Metcalf, A. D., and Ferguson, M. W. (2007) Bioengineering skin using mechanisms of regeneration and repair. *Biomaterials* **28**, 5100-5113

Midwood, K. S., Williams, L. V., Schwarzbauer, J. E. (2004) Tissue repair and the dynamics of the extracellular matrix. *Int. J. Biochem. Cell Biol.* **36**, 1031-1037

- Miljkovic, I., Yerges, L. M., Li, H., Gordon, C. L., Goodpaster, B. H., Kuller, L. H., Nestlerode, C. S., Bunker, C. H., Wheeler, V. W., Zmuda, J. M. (2009) Association of the CPT1B gene with skeletal muscle fat infiltration in Afro-Caribbean men. *Obesity (Silver Spring)* **17**, 1396-1401
- Mitchell, J. J., Woodcock-Mitchell, J. L., Perry, L., Zhao, J., Low, R. B., Baldor, L., Absher, P. M. (1993) In vitro expression of the alpha-smooth muscle actin isoform by rat lung mesenchymal cells: regulation by culture condition and transforming growth factor-beta. *Am. J. Respir. Cell Mol. Biol.* **9**, 10-18
- Mitra, S. K., Hanson, D. A., Schlaepfer, D. D. (2005) Focal adhesion kinase: in command and control of cell motility. *Nat. Rev. Mol. Cell Biol.* **6**, 56-68
- Moriyama, K., and Yahara, I. (2002) Human CAP1 is a key factor in the recycling of cofilin and actin for rapid actin turnover. *J. Cell Sci.* **115**, 1591-1601
- Nagamoto, T., Eguchi, G., Beebe, D. C. (2000) Alpha-smooth muscle actin expression in cultured lens epithelial cells. *Invest. Ophthalmol. Vis. Sci.* **41**, 1122-1129
- Nagasaki, A., Kanada, M., Uyeda, T. Q. (2009) Cell adhesion molecules regulate contractile ring-independent cytokinesis in *Dictyostelium discoideum*. *Cell Res.* **19**, 236-246
- Noegel, A. A., Witke, W., Schleicher, M. (1987) Calcium-sensitive non-muscle alpha-actinin contains EF-hand structures and highly conserved regions. *FEBS Lett.* **221**, 391-396
- Noegel, A. A., Blau-Wasser, R., Sultana, H., Müller, R., Israel, L., Schleicher, M., Patel, H., Weijer, C. J. (2004) The cyclase-associated protein CAP as regulator of cell polarity and cAMP signaling in *Dictyostelium*. *Mol. Biol. Cell* **15**, 934-945
- Nomura, K., Ono, K., Ono, S. (2012) CAS-1, a *C. elegans* cyclase-associated protein, is required for sarcomeric actin assembly in striated muscle. *J. Cell Sci.* **125**, 4077-4089
- Nomura, K., and Ono, S. (2013) ATP-dependent regulation of actin monomer-filament equilibrium by cyclase-associated protein and ADF/cofilin. *Biochem. J.* **453**, 249-259
- Nowak, D., Popow-Woźniak, A., Raźnikiewicz, L., Malicka-Błaszkiwicz, M. (2009) [Actin in the wound healing process]. *Postepy Biochem.* **55**, 138-144
- Park, W. J., and Oh, J. G. (2013) SERCA2a: a prime target for modulation of cardiac contractility during heart failure. *BMB Rep.* **46**, 237-243
- Parsons, J. T., Horwitz, A. R., Schwartz, M. A. (2010) Cell adhesion: integrating cytoskeletal dynamics and cellular tension. *Nat. Rev. Mol. Cell Biol.* **11**, 633-643
- Peche, V., Shekar, S., Leichter, M., Korte, H., Schröder, R., Schleicher, M., Holak, T. A., Clemen, C. S., Ramanath, Y., Pfitzer, G., Karakesisoglou, I., Noegel, A. A. (2007)



CAP2, cyclase-associated protein 2, is a dual compartment protein. *Cell. Mol. Life Sci.* **64**, 2702–2715

Peche, V. S., Holak, T. A., Burgute, B. D., Kosmas, K., Kale, S. P., Wunderlich, F. T., Elhamine, F., Stehle, R., Pfitzer, G., Nohroudi, K., Addicks, K., Stöckigt, F., Schrickel, J. W., Gallinger, J., Schleicher, M., Noegel, A. A. (2013) Ablation of cyclase-associated protein 2 (CAP2) leads to cardiomyopathy. *Cell. Mol. Life Sci.* **70**, 527-543

Pérez-Martínez, M., Gordón-Alonso, M., Cabrero, J. R., Barrero-Villar, M., Rey, M., Mittelbrunn, M., Lamana, A., Morlino, G., Calabia, C., Yamazaki, H., Shirao, T., Vázquez, J., González-Amaro, R., Veiga, E., Sánchez-Madrid, F. (2010) F-actin-binding protein drebrin regulates CXCR4 recruitment to the immune synapse. *J. Cell Sci.* **123**, 1160-1170

Peters, R.A. (1930) Surface structure in the integration of cell activity. *Trans. Faraday Soc.* **26**, 797–809

Pollard, T. D., and Borisy, G. G. (2003) Cellular motility driven by assembly and disassembly of actin filaments. *Cell* **112**, 453-465

Price, L. S., Leng, J., Schwartz, M. A., Bokoch, G. M. (1998) Activation of Rac and Cdc42 by integrins mediates cell spreading. *Mol. Biol. Cell* **9**, 1863-1871

Quintero-Monzon, O., Jonasson, E. M., Bertling, E., Talarico, L., Chaudhry, F., Sihvo, M., Lappalainen, P., Goode, B. L. (2009) Reconstitution and dissection of the 600-kDa Srv2/CAP complex: roles for oligomerization and cofilin-actin binding in driving actin turnover. *J. Biol. Chem.* **284**, 10923-10934

Ramsay, R. R., Gandour, R. D., van der Leij, F. R. (2001) Molecular enzymology of carnitine transfer and transport. *Biochim. Biophys. Acta* **1546**, 21-43

Rashmi, R. N., Eckes, B., Glockner, G., Groth, M., Neumann, S., Gloy, J., Sellin, L., Walz, G., Schneider, M., Karakesisoglou, I., Eichinger, L., Noegel, A. A. (2012) The nuclear envelope protein Nesprin-2 has roles in cell proliferation and differentiation during wound healing. *Nucleus* **3**, 172-186

Ridley, A. J., Schwartz, M. A., Burridge, K., Firtel, R. A., Ginsberg, M. H., Borisy, G., Parsons, J. T., Horwitz, A. R. (2003) Cell migration: integrating signals from front to back. *Science* **302**, 1704-1709

Ryall, J. G., Schertzer, J. D., Lynch, G. S. (2008) Cellular and molecular mechanisms underlying age-related skeletal muscle wasting and weakness. *Biogerontology* **9**, 213–228

Schafer, M., and Werner, S. (2008) Cancer as an overhealing wound: an old hypothesis revisited. *Nat. Rev. Mol. Cell Biol.* **9**, 628-638

Schaper, J., Froede, R., Hein, S., Buck, A., Hashizume, H., Speiser, B., Friedl, A., Bleese, N. (1991) Impairment of the myocardial ultrastructure and changes of the cytoskeleton in dilated cardiomyopathy. *Circulation* **83**, 504–514

Seeley, R. R., Stephens, T. D., Tate, P. (2005) Essentials of anatomy and physiology 5<sup>th</sup> Edition

Shen, K., Tolbert, C. E., Guilluy, C., Swaminathan, V. S., Berginski, M. E., BurrIDGE, K., Superfine, R., Campbell, S. L. (2011) The vinculin C-terminal hairpin mediates F-actin bundle formation, focal adhesion, and cell mechanical properties. *J. Biol. Chem.* **286**, 45103-45115

Shibata, R., Mori, T., Du, W., Chuma, M., Gotoh, M., Shimazu, M., Ueda, M., Hirohashi, S., Sakamoto, M. (2006) Overexpression of cyclase-associated protein 2 in multistage hepatocarcinogenesis. *Clin. Cancer Res.* **12**, 5363-5368

Singer, A. J., and Clark, R. A. (1999) Cutaneous wound healing. *N. Engl. J. Med.* **341**, 738–746

Skwarek-Maruszewska, A., Hotulainen, P., Mattila, P. K., Lappalainen, P. (2009) Contractility-dependent actin dynamics in cardiomyocyte sarcomeres. *J. Cell Sci.* **122**, 2119–2126

Smola, H., Thiekotter, G., Fusenig, N. E. (1993) Mutual induction of growth factor gene expression by epidermal-dermal cell interaction. *J. Cell Biol.* **122**, 417–429

Sohn, R. H., and Goldschmidt-Clermont, P. J. (1994) Profilin: at the crossroads of signal transduction and the actin cytoskeleton. *Bioessays* **16**, 465-472

Stossel, T. P., Condeelis, J., Cooley, L., Hartwig, J. H., Noegel, A., Schleicher, M., Shapiro, S. S. (2001) Filamins as integrators of cell mechanics and signalling. *Nat. Rev. Mol. Cell Biol.* **2**, 138-145

Subauste, M. C., Pertz, O., Adamson, E. D., Turner, C. E., Junger, S., Hahn, K. M. (2004) Vinculin modulation of paxillin-FAK interactions regulates ERK to control survival and motility. *J. Cell Biol.* **165**, 371-381

Sun, H. Q., Yamamoto, M., Mejillano, M., Yin, H. L. (1999) Gelsolin, a multifunctional actin regulatory protein. *J. Biol. Chem.* **274**, 33179-33182

Sussman, M. A., Welch, S., Cambon, N., Klevitsky, R., Hewett, T. E., Price, R., Witt, S. A., Kimball, T. R. (1998) Myofibril degeneration caused by tropomodulin overexpression leads to dilated cardio-myopathy in juvenile mice. *J. Clin. Invest.* **101**, 51–61

Tamura, N., Ogawa, Y., Chusho, H., Nakamura, K., Nakao, K., Suda, M., Kasahara, M., Hashimoto, R., Katsuura, G., Mukoyama, M., Itoh, H., Saito, Y., Tanaka, I., Otani, H., Katsuki, M. (2000) Cardiac fibrosis in mice lacking brain natriuretic peptide. *Proc. Natl. Acad. Sci.* **97**, 4239–4244

- Taranum, S., Vaylann, E., Meinke, P., Abraham, S., Yang, L., Neumann, S., Karakesisoglou, I., Wehnert, M., Noegel, A. A. (2012) LINC complex alterations in DMD and EDMD/CMT fibroblasts. *Eur. J. Cell Biol.* **91**, 614-628
- Tomasek, J., Gabbiani, G., Hinz, B., Chaponnier, C., Brown, R. A. (2002) Myofibroblasts and mechano-regulation of connective tissue remodelling. *Nat. Rev. Mol. Cell Biol.* **3**, 349–363
- Tonnesen, M. G., Feng, X., Clark, R. A. (2000) Angiogenesis in wound healing. *J. Investig. Dermatol. Symp. Proc.* **5**, 40-46
- Trott, A. (1988) Mechanisms of surface soft tissue trauma. *Ann. Emerg. Med.* **17**, 1279–1283
- Verheijen, R., Kuijpers, H. J., van Driel, R., Beck, J. L., van Dierendonck, J. H., Brakenhoff, G. J., Ramaekers, F. C. (1989) Ki-67 detects a nuclear matrix-associated proliferation-related antigen. II. Localization in mitotic cells and association with chromosomes. *J. Cell Sci.* **92**, 531-540
- Vojtek, A., Haarer, B., Field, J., Gerst, J., Pollard, T. D., Brown, S., Wigler, M. (1991) Evidence for a functional link between profilin and CAP in the yeast *S. cerevisiae*. *Cell* **66**, 497-505
- Wakatsuki, T., Schwab, B., Thompson, N. C., Elson, E. L. (2001) Effects of cytochalasin D and latrunculin B on mechanical properties of cells. *J. Cell Sci.* **114**, 1025-1036
- Wang, C., Zhou, G. L., Vedantam, S., Li, P., Field, J. (2008) Mitochondrial shuttling of CAP1 promotes actin- and cofilin-dependent apoptosis. *J. Cell Sci.* **121**, 2913-2920
- Welch, M. D., and Mullins, R. D. (2002) Cellular control of actin nucleation. *Annu. Rev. Cell Dev. Biol.* **18**, 247-288
- Werner, S., Krieg, T., Smola, H. (2007) Keratinocyte-fibroblast interactions in wound healing. *J. Invest. Dermatol.* **127**, 998–1008
- Wetzler, C., Kampfer, H., Stallmeyer, B., Pfeilschifter, J., Frank, S. (2000) Large and sustained induction of chemokines during impaired wound healing in the genetically diabetic mouse: prolonged persistence of neutrophils and macrophages during the late phase of repair. *J. Invest. Dermatol.* **115**, 245–53
- Wills, Z., Emerson, M., Rusch, J., Bikoff, J., Baum, B., Perrimon, N., Van Vactor, D. (2002) A *Drosophila* homolog of cyclase-associated proteins collaborates with the Abl tyrosine kinase to control midline axon pathfinding. *Neuron* **36**, 611-622
- Witke, W., Sharpe, A. H., Hartwig, J. H., Azuma, T., Stossel, T. P., Kwiatkowski, D. J. (1995) Hemostatic, inflammatory, and fibroblast responses are blunted in mice lacking gelsolin. *Cell* **81**, 41-51

Xu, W., Baribault, H., Adamson, E. D. (1998) Vinculin knockout results in heart and brain defects during embryonic development. *Development* **125**, 327-337

Yamashiro, S., Gokhin, D. S., Kimura, S., Nowak, R. B., Fowler, V. M. (2012) *Cytoskeleton (Hoboken)* **69**, 337-370

Yamazaki, K., Takamura, M., Masugi, Y., Mori, T., Du, W., Hibi, T., Hiraoka, N., Ohta, T., Ohki, M., Hirohashi, S., Sakamoto, M. (2009) Adenylate cyclase-associated protein 1 overexpressed in pancreatic cancers is involved in cancer cell motility. *Lab. Invest.* **89**, 425-432

Zelicof, A., Gatica, J., Gerst, J. E (1993) Molecular cloning and characterization of a rat homolog of CAP, the adenyl cyclase-associated protein from *Saccharomyces cerevisiae*. *J. Biol. Chem.* **268**, 13448-13453

Zemljic-Harperf, A. E., Ponrartana, S., Avalos, R. T., Jordan, M. C., Roos, K. P., Dalton, N. D., Phan, V. Q., Adamson, E. D., Ross, R. S. (2004) Heterozygous inactivation of the vinculin gene predisposes to stress-induced cardiomyopathy. *Am. J. Pathol.* **165**, 1033-1044

Zhou, G. L., Zhang, H., Field, J. (2014) Mammalian CAP (Cyclase-associated protein) in the world of cell migration: Roles in actin filament dynamics and beyond. *Cell Adh. Migr.* **8**, 55-59

Zhu, X., Yao, L., Guo, A., Li, A., Sun, H., Wang, N., Liu, H., Duan, Z., Cao, J. (2014) CAP1 was associated with actin and involved in Schwann cell differentiation and motility after sciatic nerve injury. *J. Mol. Histol.* **45**, 337-348

Ziegler, W. H., Liddington, R. C., Critchley, D. R. (2006) The structure and regulation of vinculin. *Trends Cell Biol.* **16**, 453-460

Zigmond, S. H. (2000) How WASP regulates actin polymerization. *J. Cell Biol.* **150**, 117-120

## **Erklärung**

Ich versichere, dass ich die von mir vorgelegte Dissertation selbständig angefertigt, die benutzten Quellen und Hilfsmittel vollständig angegeben und die Stellen der Arbeit - einschließlich Tabellen und Abbildungen -, die anderen Werke im Wortlaut oder dem Sinn nach entnommen sind, in jedem Einzelfall als Entlehnung kenntlich gemacht habe; dass diese Dissertation noch keiner anderen Fakultät oder Universität zur Prüfung vorgelegen hat; dass sie - abgesehen von unten angegebenen beantragten Teilpublikationen - noch nicht veröffentlicht ist, sowie, dass ich eine Veröffentlichung vor Abschluss des Promotionsverfahrens nicht vornehmen werde. Die Bestimmungen dieser Promotionsordnung sind mir bekannt. Die von mir vorgelegte Dissertation ist von Herr Dr. Vivek Peche betreut worden.

Köln, den

Kosmas Kosmas

## Curriculum Vitae

### Personal information

Name: Kosmas Kosmas  
Address: Deutzer Ring 5, Et-Zi: 19-07,  
50679, Cologne, Germany  
Email: kosmaskosmas555@yahoo.gr  
Date of birth: 29/06/1987  
Place of birth: Ioannina, Greece

Nationality: Greek

### Academic Qualifications

High School: 3<sup>rd</sup> High school of Ioannina, Greece  
(2002-2005)

University studies: Ptychio from the Department of Molecular Biology  
(2005-2009) and Genetics, Health Sciences – School, Democritus  
University of Thrace, Alexandroupoli, Greece

Diploma thesis: Investigations on the Protein Arginine Methyl  
(2009) Transferase 8 (PRMT8) and its potential interaction  
with another member of the PRMT family, PRMT2.  
Diploma thesis was done under the supervision of Dr.  
Frank O. Fackelmayer, FORTH, Institute of Molecular  
Biology and Biotechnology, Biomedical Research  
Division, Ioannina, Greece.

Post graduation studies: Mathematics and Natural Science Faculty,  
(2010-2014) University of Cologne, Germany  
Doctoral work was done under the supervision of  
Dr. Vivek Peche in the Institute for Biochemistry I,  
Medical Faculty, University of Cologne, Germany,  
with the support of IGSDHD.

### Publications

Peche V. S., Holak T. A., Burgute B. D., **Kosmas K.**, Kale S. P., Wunderlich F. T., Elhamine F., Stehle R., Pfitzer G., Nohroudi K., Addicks K., Stöckigt F., Schrickel J. W., Gallinger J., Schleicher M., Noegel A. A. (2013) Ablation of cyclase-associated protein 2 (CAP2) leads to cardiomyopathy. *Cell. Mol. Life Sci.* **70**, 527-5.

**Kosmas K.**, Eskandarnaz A., Khorsandi A. B., Kumar A., Ranjan R., Eming S. A., Noegel A. A., Peche V. S. (2015) CAP2 is a regulator of the actin cytoskeleton and its absence changes infiltration of inflammatory cells and contraction in wounds. *Eur. J. Cell Biol.* **94**, 32-45.

## Lebenslauf

### Persönliche Informationen

Name: Kosmas Kosmas  
Adresse: Deutzer Ring 5, Et-Zi: 19-07,  
50679, Köln, Deutschland  
Email: kosmaskosmas555@yahoo.gr  
Geburtsdatum: 29/06/1987  
Geburtsort: Ioannina, Griechenland  
Nationalität: Griechisch

### Akademische Qualifikationen

Schule: 3. High School in Ioannina, Griechenland  
(2002-2005)  
Studium: Ptychio von der Abteilung für Molekulare Biologie  
(2005-2009) und Genetik, Gesundheitswissenschaften - Schule,  
Demokritus-Universität Thrakien, Alexandroupolis,  
Griechenland  
Diplomarbeit: “Untersuchung des Proteins Arginin-Methyl-  
(2009) 8 Transferase (PRMT8) und seiner möglichen  
Interaktion mit einem weiteren Mitglied der PRMT  
Familie, PRMT2. ”  
Die Diplomarbeit wurde unter der Aufsicht von Dr.  
Frank O. Fackelmayer, FORTH, Institut für Molekulare  
Biologie und Biotechnologie, Biomedizinische  
Forschungsabteilung, Ioannina, Griechenland  
durchgeführt.  
Promotionsstudium: Mathematisch-Naturwissenschaftlichen Fakultät ,  
(2010-2014) Universität zu Köln, Deutschland  
Die Doktorarbeit wurde unter der Aufsicht von Dr.  
Vivek Peche im Institut für Biochemie I , Medizinische  
Fakultät , Universität zu Köln, Deutschland, mit  
Unterstützung von IGSDHD, durchgeführt.

### Publikationen

Peche V. S., Holak T. A, Burgute B. D., **Kosmas K.**, Kale S. P., Wunderlich F. T., Elhamine F., Stehle R., Pfitzer G., Nohroudi K., Addicks K., Stöckigt F., Schrickel J. W., Gallinger J., Schleicher M., Noegel A. A. (2013) Ablation of cyclase-associated protein 2 (CAP2) leads to cardiomyopathy. *Cell. Mol. Life Sci.* **70**, 527-543.



**Kosmas K.**, Eskandarnaz A., Khorsandi A. B., Kumar A., Ranjan R., Eming S. A., Noegel A. A., Peche V. S. (2015) CAP2 is a regulator of the actin cytoskeleton and its absence changes infiltration of inflammatory cells and contraction in wounds. *Eur. J. Cell Biol.* **94**, 32-45.

